Search to Recover:

Simulating the Site Formation Process of the 1733 Fleet

By

Sean Cox

December 2019

Director of Thesis: Dr. Charles Ewen

Major Department: Program in Maritime Studies, Department of History

Archaeological surveys and interpretive efforts rely upon personal observations and second-hand sources— historical documentation, oral histories, and eye-witness accounts—for information about shipwreck events. These sources frequently lack quantifiable certainty. The proposed methodology uses recent wind and ocean current data from the Florida Keys as inputs to simulate shipwreck debris from the site of *La Capitana el Rubi*, flagship of the 1733 Spanish Treasure Fleet. The results of the simulation demonstrate that the shipwrecked vessel's scatter pattern is consistent with the location's mean ambient environmental conditions and is likely consistent with conditions on site during the summer and fall of 1733, when Spanish shipwreck salvors worked to recover material from the sunken fleet. The simulation results demonstrate shipwreck materials likely drifted further from the site than archaeological investigations have previously documented and rule out the 1733 hurricane as the primary cause of the present scatter pattern.

Search to Recover:

Simulating the Site Formation Process of the 1733 Fleet

A Thesis

Presented to the Faculty of the Department of History

East Carolina University

In Partial Fulfillment of the Requirements of the Degree:

Master of Arts in Maritime Studies

By

Sean Cox

December 2019

SEARCH TO RECOVER:

Simulating the Site Formation Process of the 1733 Fleet

by

Sean Cox

APPROVED BY:

DIRECTOR OF
THESIS: _____
(Dr. Charles Ewen, Ph.D.)

COMMITTEE MEMBER: _____
(Dr. Nathan Richards, Ph.D.)

COMMITTEE MEMBER: _____
(Dr. Sangwoo Sung, Ph.D.)

DEAN OF THE
GRADUATE SCHOOL: _____
(Dr. Paul Gemperline, Ph.D.)

DEDICATION PAGE

This degree marks the end of another adventure the author has been fortunate to pursue. John, Cheryl, and Brittany Cox have always and continue to show boundless patience and steadfast love. This thesis is dedicated in recognition of their lives of service to their friends, communities, and country.

ACKNOWLEDGEMENTS

This work would not have been possible without the support of Drs. Charles Ewen and Sangwoo Sung. Dr. Ewen was instrumental in helping formulate these ideas into the written word, while Dr. Sung's advice on coding the Python simulation enabled me to grow as a thinker, researcher, and scientist. I am indebted to both men. Special thanks also go to Kristina Fricker, who illustrated sections and helped to format much of this work, and Yoonji Jung, who improved the clarity of the original site maps. Finally, Gregg Parrish provided support and advice as I learned to code, enabling a much cleaner final product.

Thanks to all of you.

Table of Contents

List of Tables

List of Figures

Chapter 1: Introduction

1.1: Purpose

Spain's *Flota de Indias* was among the most formative cultural processes of European colonial powers in the New World. For more than two centuries, the seasonal convoy patterned the lives of millions in the Americas and Europe, as Spain initiated the diplomatic, economic, and ecological changes necessary to transfer wealth from its colonies to Seville. Conceived in 1556 by Pedro Menéndez de Avilés, in response to naval threats to Spain's New World interests, it was by Royal Decree on 10 July 1561, that the annual launch of two fleets from the Guadalquivir River was formally institutionalized (Salmoral 1985; Aliaga 2015). For the next two hundred years, ships of these fleets departed Spain each spring, traversing to Spanish holdings in western Africa to take on slaves and cargo, before proceeding to exchange goods in the Americas. The fleet would reassemble in Havana in July, and return with wealth from *Nueva España* comprising gold, silver, silk, and porcelain.

The fleet sailed from Europe on the equatorial "Trade Winds" and returned on the "Prevailing Westerlies" of the northern latitudes (Salmoral 1985; Aliaga 2015). As such, the fleet's July return voyage from the Havana necessitated routing through the Straits of Florida, north to the Carolinas, before turning east to cross the Atlantic. Twice during the eighteenth century the *Flota de Indias* met with catastrophic losses along the coast of Florida—in 1715 and 1733.

The sites of these shipwrecks have been impacted by repeat human intervention. The Spanish shipwreck survivors were the first to salvage material from the shipwrecks, and soon after, salvors dispatched by colonial authorities began more destructive salvage

efforts (Benson 2002: Appendix 1). Within six months of the wrecking event, word of the disaster had spread throughout Europe and even the Spanish expressed concern that other salvors would be first on the sites, so it is probable to expect that others may have made the attempt (Benson 2002: Appendix 1). Then, in the 20th century, archaeologists and treasure hunters took their turn in mining the shipwrecks for data and valuables (Smith and Dunbar 1977; Benson 2002; McKinnon 2006). Due to these impacts, the approach taken in this thesis is to simulate archaeological remains from the 1733 flotilla with search and rescue methods. The key inputs utilized in operations research are applied to simulate environmental conditions on the site of *La Capitana el Rubi*, in order to examine shipwreck site formation processes.

The winds of the Florida region demonstrate remarkable predictability, not only such that they could be relied upon by Spanish sailors, but also as an aid to archaeologists seeking to understand the material drift trajectory from of the region's shipwreck sites. This thesis uses wind data collected by the National Oceanographic and Atmospheric Administration (NOAA) (National Data Buoy Center [NDBC] 1971) as the core input for a leeway field simulation developed in the Python (van Rossum 2001). NOAA's time series data on the region's wind patterns allow for mathematical analysis of wind behavior in 10-minute intervals (NDBC 1971), which enables modeling of key environmental conditions. The ocean simulator developed for this study examines shipwreck scatter in the context of the ambient conditions in the Florida Keys for the months of July and October. The aim in modeling these conditions is to interpret the sites with reduced spatial and temporal uncertainty and explore the value that quantifiable environmental data can bring to unquantifiable cultural factors affecting shipwreck site

formation. This computerized support enables users to visualize the shipwreck context, identifying probable drift trajectories for material that floats away from the shipwreck sites, and enabling comparison with scatter patterns that would likely result from pre-wreck cultural transforms, such as disaster response efforts, or post-wreck interventions, like salvage. Such simulation enables archaeologists to integrate environmental and cultural considerations into the interpretation of the 1733 fleet.

The Python programming language is used to visualize drift trajectories and support discussion of various site formation patterns related to the disaster response and the historical salvage efforts (Schiffer 1987:22). Given that computerized models have already been successfully applied to problems of locating missing archaeological remains and identifying previously un- or mis-identified remains, it is prudent to verify the effectiveness of these methods and the variables that make them successful. This study adds to the small body (Fernández-Montblanc et al. 2016) of mathematical modeling research in maritime archaeology by assessing the viability of this approach in material prospection at scattered sites and testing the utility of probabilistic frameworks for interpretation.

1.2: Research Questions

The aim of this thesis is to visualize the link between environmental and cultural transformations that affect a shipwreck site formation processes (Schiffer 1987; Ward et al. 1999; Gibbs 2006). The central hypothesis underpinning this study is that identifying patterns among non-cultural transforms improves the interpretation of cultural ones, such

as disaster response efforts and salvage operations contemporary to the wrecking event. This will be accomplished through the following research questions:

- What interpretive outcomes result from simulating short term time-series physical processes of site formation?
- How do explanatory models of environmental processes help archaeologists interpret shipwreck remains?
- Can shipwreck scatter patterns be modeled in isolation of archaeological data? Does the comparison of a model's results and real-world observations lead to empirical interpretation of a shipwreck event?

To address the research questions above, this thesis will review the following:

- Use of mathematical modeling in maritime archaeological survey
- The theory of site formation processes as a means of interpreting a wreck site
- History of the 1733 fleet and salvage efforts at *La Capitana El Rubi*

1.3: Background

The 1733 *Flota de Indias* embarked for Spain from Havana on 13 July of the year that bears its name, under the command of Rodrigo de Torres (Scott-Ireton and Mattick 2006b:22 and 2006c:8). The fleet comprised four armed galleons, 18 merchant vessels, and an unknown number of smaller ships, but just a day after its departure, it was overtaken by a hurricane that sank most of the ships along an 80-mile stretch of the Florida Keys (Benson 2002: Appendix 1). In the aftermath, Spanish colonial authorities conducted rescue and salvage operations. Some ships were refloated, but many of the

wrecked vessels were charted and became the sites of salvage activity for many years (Scott-Ireton and Mattick 2006a:5, 2006b:28-29, 2006c:6-7). From the 1733 fleet, 13 ships comprising 14 sites were investigated archaeologically between 1977 and 2005 (Smith and Dunbar 1977; Smith et al. 1990; Benson 2002; McKinnon 2006). These vessels were subsequently placed on the National Register of Historic Places: (from northeast to southwest) *Populo*, *Infante*, *San Jose*, *El Rubi*, *Chaves*, *Tres Puentes*, *Herrera*, *San Pedro*, *El Terri*, *San Francisco*, *Almiranta*, *Angustias*, and *Sueco de Arizon* (Scott-Ireton and Mattick 2006a, 2006b, 2006c).

Prior to the archaeological investigations, the sites were popular with American treasure hunters. Figures like Carl Ward and Bob Weller (2001:9-15) dove the sites in the 1960s and 70s, and their tales were among many that flavored the treasure-hunting culture of the contemporary Florida Keys. The negative effects of their treasure hunting activities are also a lasting legacy (Price 2015), though before them, the Spanish colonial authorities had conducted salvage operations to recover cargo, cannons, and in some cases, the ships themselves (Scott-Ireton and Mattick 2006a, 2006b, 2006c). The Spanish records (Benson 2002: Appendix 1) tell a tale of a failed attempt by the fleet to escape a deadly storm, efforts by survivors to reach the relative safety of land, and rescue and salvage work by colonial administrators. These records give clues to the forensic context, indicating some ships were burned to the water line to provide divers access to the contents of their hulls, but that whenever possible, vessels were disassembled (Benson 2002: Appendix 1). The disaster response and salvage efforts exposed archaeological material to the elements in ways that are potentially distinct from naturally occurring scatter patterns, and these may have accelerated the natural disintegration of the ships.

However, it is probable that disaster response or salvage activity introduced new archaeological material to the sites or moved archaeological material in detectable ways (Scott-Ireton and Mattick 2006a, 2006b, 2006c).

The use of statistical approaches for drift modeling was pioneered by Bob Ballard and John Piña Craven (Craven 2001), who applied statistical inference in the search effort for a lost hydrogen bomb in Palomares, Spain, in 1966, and in the location and recovery of the USS *Scorpion*, which sank near the Azores in 1968. Similar techniques were also applied to help locate Air France Flight 447, which disappeared mid-flight in 2009 (Stone 2014). Currently, robust Bayesian search and survey models are used by the Coast Guard and the National Park Service in search and rescue operations (Allen 2015), and the Bureau of Land Management has used weighted models to anticipate the locations of underwater paleolithic settlement remains along US coastlines (Judge and Sebastian 1988:413). However, despite decades of gains in computational power and mathematical techniques that enable empirical modeling of conditions at underwater archaeological sites, these methods are not utilized as the baseline for the development of archaeological survey plans. As a result, underwater surveys rely upon outdated approaches that underestimate the scope of shipwreck scatter and encourage interpretations that deviate from the probable boundaries imposed by the physical context.

To discern details about cultural impacts at the site that of the 1733 shipwrecks—impacts that result from both contemporary and 18th century salvage efforts—the simulation discussed below first analyzes the NDBC's 30-plus-year longitudinal wind data set. These data are then analyzed using a frequentist approach to identify the most likely conditions during Spain's salvage efforts in October 1733. The model creates

virtual objects and simulates their drift trajectories from these conditions. Finally, the output from the simulation is considered alongside material and documentary evidence, to infer the potential impacts of Spanish colonial and contemporary salvage from the material remains, as documented by Smith and Dunbar (1977), Smith et al. 1990, Benson (2002), and McKinnon (2006).

1.4: The Sites

From the 21 ships that are known to have wrecked in the 1733 storm (Benson 2002: Appendix 1) there are 13 archaeological sites, which extend from northeast to southwest along the Florida Keys (Smith et al. 1990:12). The shipwrecks all sit atop the shallow reef, from the northern-most *Populo*, off Elliot Key, to *Sueco del Arizon*, located south of Marathon (Figure 1). Spanish eye-witness accounts indicate the 1733 storm exhibited a northerly wind, one typical at the start of a hurricane or tropical storm and may have been centered north of the fleet. Meanwhile, the prevailing conditions in the area include an easterly wind and the Florida Current, which travels northeast through the Strait of Florida.

These strikingly divergent weather patterns enable researchers to simulate conditions such that the empirical cause of shipwreck scatter and material transport can be analyzed. These sites and the successive periods of human impact upon them have not yet been subject to a computerized site formation study. Their shared geography and the similar conditions of the vessels' loss offer a uniquely cohesive data set for a simulation of this kind. Data recovered about *La Capitana el Rubi* (Smith and Dunbar 1977; Benson 2002; McKinnon 2006) provide an opportunity for researchers to probabilistically model

the ship's maritime site formation process and quantifiably interpret natural and cultural factors influencing its scatter.

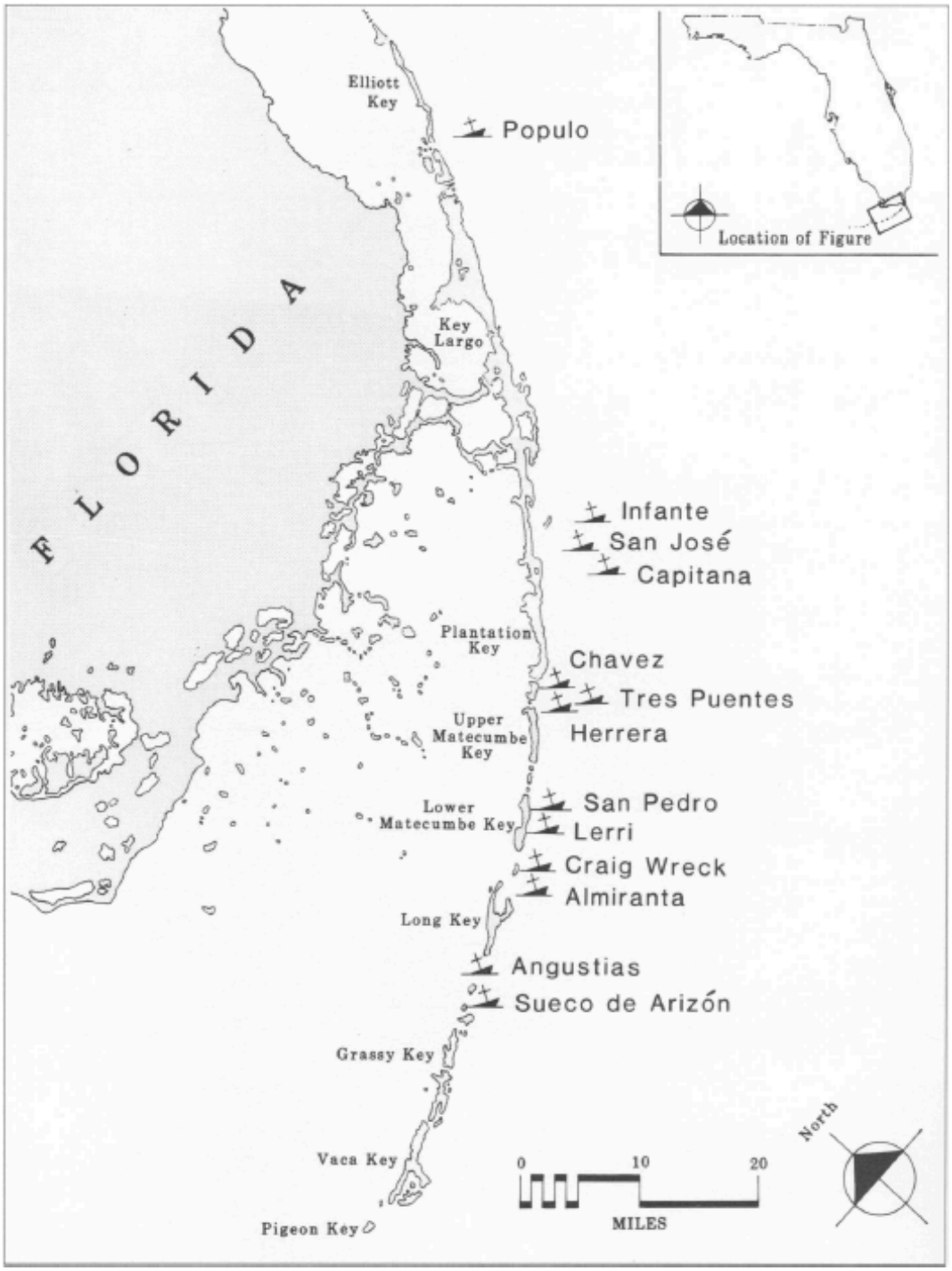

Figure 1: Map indicating known sites of the 1733 fleet (Smith et al. 1990:12).

1.5: Simulating Site Formation Processes

The study of site formation processes, as proposed by Muckelroy (1976) advocates the use of statistical tools to interrogate shipwreck scatter via distribution mapping, an approach he asserts reveals relationships among artifacts and their context at the wrecking site. Muckelroy extended this work to a descriptive framework that outlines the natural processes that break down shipwreck sites, focusing on the interaction of material culture with the wrecking environment (Figure 2). Muckelroy's approach treats the component site formation processes as singular depositional events.

Ward et al. (1999 and 2003) and Gibbs (2006) build upon Muckelroy's framework (Figures 2) to include more discrete consideration of the component processes of shipwreck dispersion. They define the physical mechanisms involved and expand the site formation process in temporal terms. The resulting framework (Figure 3), which Ward et al. term a "process-based model," positions the shipwreck site in the context of the entropic physical, biological, and chemical mechanisms that break down the material remains of a site, freeing them to scatter (Ward et al. 1999:563-569). In a computerized simulation of great power, each of these processes could be reproduced to analyze the total breakdown of a shipwreck, to the extent even of offering predictive certainty about its ultimate decay. Such a robust model is far beyond the aim of this thesis, which instead applies a simpler process-based approach to simulate the shipwreck scatter pattern and examine it in light of planning and interpretive purposes. This follows from Banning (2002:vi), who asserted, "Quantitative evaluation of a survey design and its results allows us to make realistic assessments... about the places where targets probably will and will

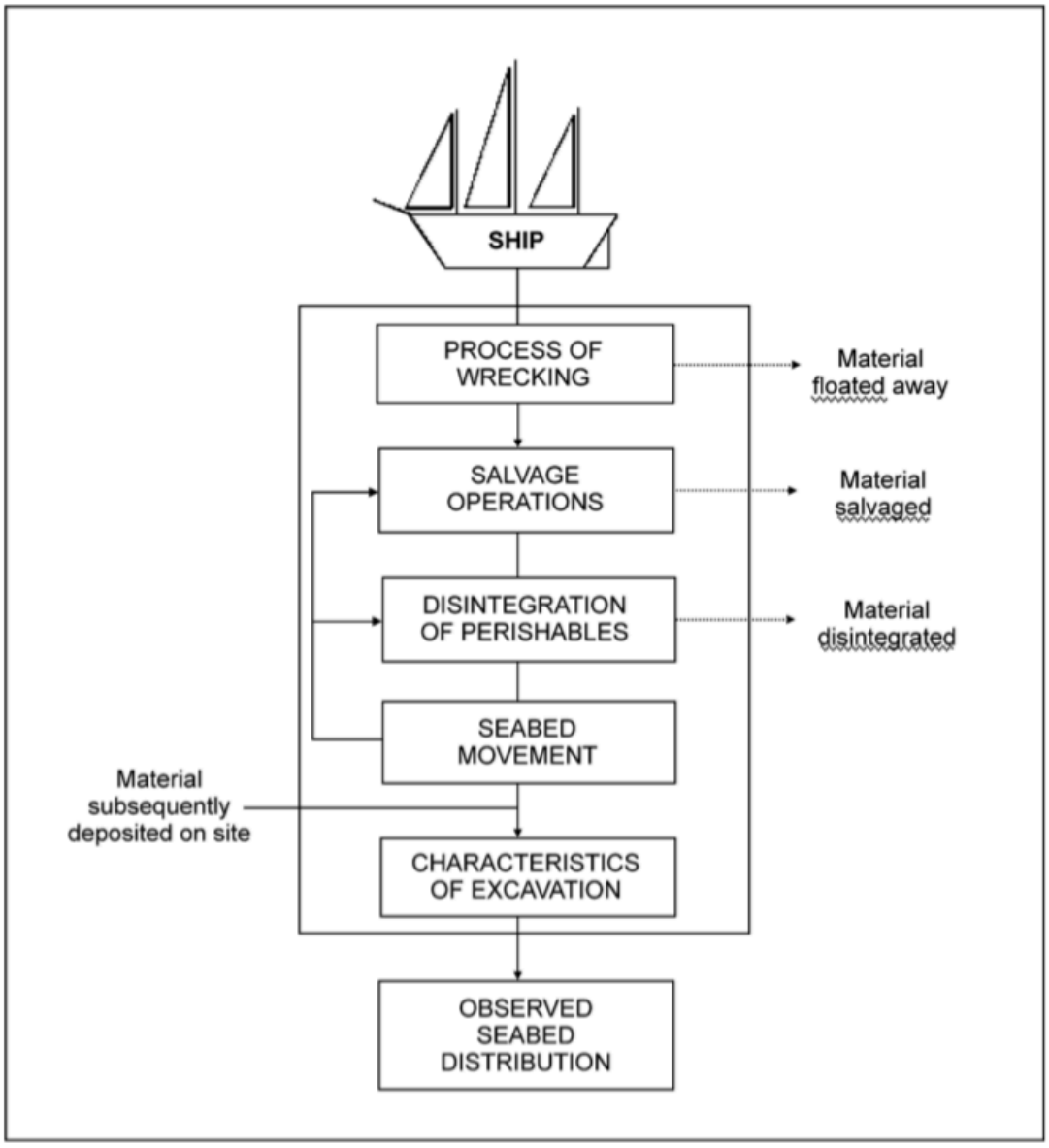

Figure 2: Flow chart to indicate development of a wreck site (Muckelroy 1976:282)

not occur in as yet unsurveyed regions". In this case, the already surveyed region of *LaCapitana el Rubi* serves as a comparative study to establish the accuracy of the leeway field simulation method and focus the site's reinterpretation on possible explanations that are congruous with its results.

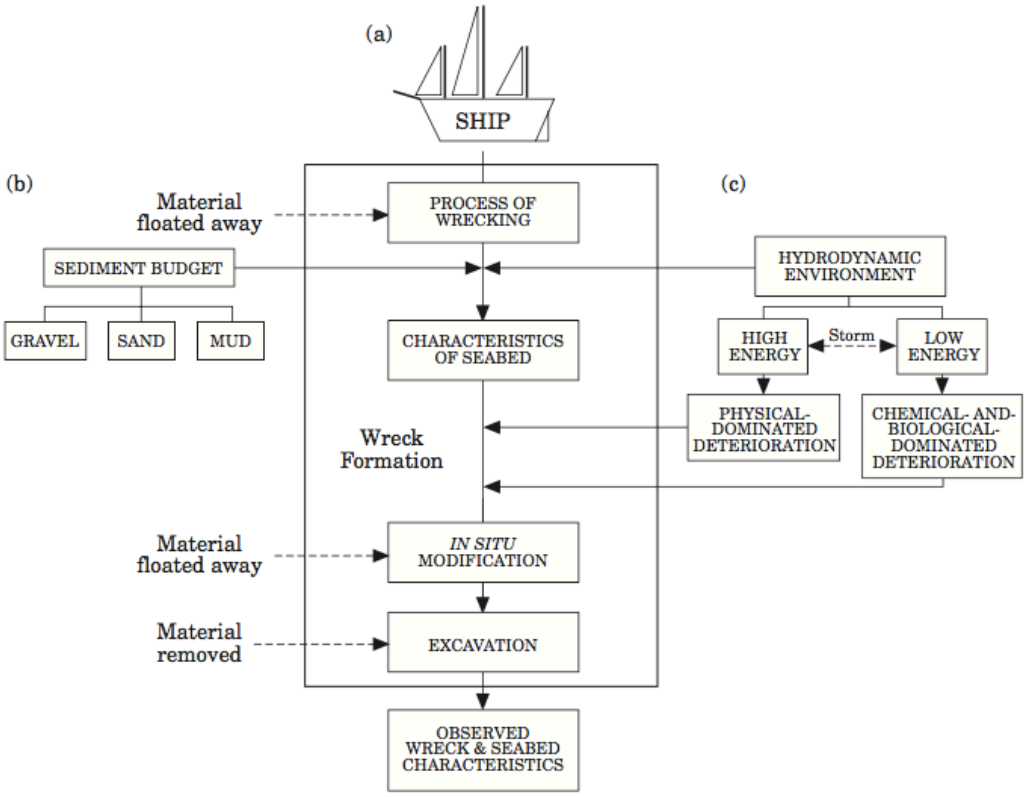

Figure 3: The Ward et al. (1999:564) site formation process model.

The psychologist John Leach (1994) makes a critical examination of disasters and finds they comprise five stages (Table 1): 1. Pre-impact stage; 2. Impact stage; 3. Recoil stage; 4. Rescue stage; and 5. Post-trauma stage. Martin Gibbs (2006) seeks to integrate these stages into a site formation framework, introducing a cultural element to the environmental processes driving ship decomposition. Gibbs links stages of a wrecking disaster to human behaviors, such as jettisoning material before sinking, or salvaging cargo after the ship has sunk (Figure 3). Gibbs offers a robust interpretive framework for examining site formation processes, incorporating disaster response efforts and salvage activities into the process-based approach of Ward et al. (1999), such that the environmental and cultural considerations are juxtaposed for complete understanding of a shipwrecking event.

Table 1: Leach's responses to shipwreck crises (1994), in Gibbs (2006:9).

Pre-impact Threat phase	**Long-term** Collection of information on potential threats. Decisions to take/avoid routes, develop sailing instructions and seasonal restrictions Design or modification of vessels and equipage suitable to overcome potential threat Selection or training of crew **Short-term** Changes to course, increased awareness for lookouts, preparation or stowage of equipment	**Pre-depositional.** If strategies to avoid impact are successful, this may result in there being no archaeological evidence. Where archaeological remains do exist, these may exhibit evidence of Pre-impact strategies to diminish or negate risk.
Pre-impact Warning phase	Radical changes to course or attempts to slow, stop or turn, including dropping anchor. Jettisoning of some items. Running ashore to avoid catastrophic impact. Pre-impact abandonment possible but unlikely. Possible intervention by external sources.	**Pre-depositional.** Effective Pre-impact behaviours may result in no arch evidence, or a debris trail of jettisoned items, but no wreck. Disposition of wreck and presence/absence of materials may be indicative of pre-impact awareness, preparedness and response.
Impact	Strategies and actions dependent upon the nature of Impact (catastrophic v. low-intensity). **Decision to remain aboard** Club-hauling (use of anchors) to pull off, or driving over obstacle. Jettisoning heavy items or cutting away masts in order to re-float or save the structure. Patching leaks until repairs can be made. **Decision to abandon a vessel** Lowering of the ship's boats or lifeboats, securing a line to shore, removal of people. Rapid selection and removal of primarily survival-oriented materials ('Crisis Salvage'). Initial post-disaster survivor landing site.	**Depositional** If Impact is negated, the vessel may be recovered, resulting in no archaeological remains or jettisoned materials only. If unsuccessful, site may include ship's structure, cargo and human fatalities.' Crisis Salvage'—absence of primarily survival-oriented materials, including boats from the wreck-site, or evidence of the same at land sites (easily accessible contents and cargo, fixtures and fittings). Discard of human remains resulting from post-impact mortality.
Recoil	Establishment of survivor camp Establishment of authority structure and possible re-organization of population. Organization of subsistence and rescue strategy. Further selection and removal of materials ('Survivor Salvage'), assuming that a return to the vessel is possible. Limited by available labour and equipment. Repair and re-floating.	**Post-depositional** Establishment of survivor camp. Site structure reflecting survival strategies. 'Survivor Salvage' (cargo, fixtures, minor structural) materials absent from wreck site or located within land site. Adaptation of materials and foraging behaviour. Evidence of human fatalities may indicate unsuccessful strategies. Possible removal of vessel.
Rescue and Post-Disaster	Complete abandonment of wreck and contents. Salvage depends upon accessibility of sites and benefits versus cost, effort and time required. **Opportunistic salvage**: short duration and intensity, resulting in focus on particular types of material. Legal rights to salvage unlikely. **Systematic salvage**: over an extended period with access to increased equipment and labour, including recovery of all or part of the cargo, fixtures/fittings, minor and major structure, or complete recovery. Legal owner or agents of the wreck and materials.	**Post-depositional** Establishment of salvage camp for storage of salvaged materials and habitation of salvage crew. Evidence of removal or non-removal of materials from wreck and land sites. Removal of vessel. Removal of cargo and fittings, through to 'Breaking' and removal of minor and major structural elements, leaving only residual elements.

Ward et al. (1999) and Gibbs (2006) are working to extend upon the site formation processes proposed by Schiffer (1987), who postulated specific processes that would transform an archaeological site, even as it decayed. Schiffer asserts that site scatter patterns cannot be assumed to lend themselves to intuitive interpretations of the human behavior or organization that created them, and that this is true regardless of the quantity of physical evidence involved. However, Schiffer (1987:10) provides the hopeful avenue that Gibbs (2006) combines with the approach of Ward et al. (1999): "Because formation processes themselves exhibit patterning, the distortions can be rectified by using appropriate analytic and inferential tools built upon our knowledge of the laws governing these processes". In the context of maritime archaeological scatter, isolating the effects of winds and waves upon remains can be crucial to understanding behavior on sites, but it is only recently that sufficient data has become available to model these effects empirically. To augment Gibbs theoretical framework for cultural transformations of shipwreck sites, this study deploys a simulation of the physical environment to examine the effects of the prevailing environmental conditions and their possible contribution to the scatter pattern of *La Rubi*.

Gibbs is explicit that his approach involves distinguishing between non-cultural transformation processes and cultural ones in the archaeological record, and that doing so involves probabilistic analysis. "By employing a consistent framework in examining shipwreck events, we can more effectively extract and synthesize information from the different data-sets, compare and contrast between sites, and consider the probable processes at less-documented sites" (Gibbs 2006:4). However, he does not identify empirical data that could inform the framework he proposes. Instead, he explains

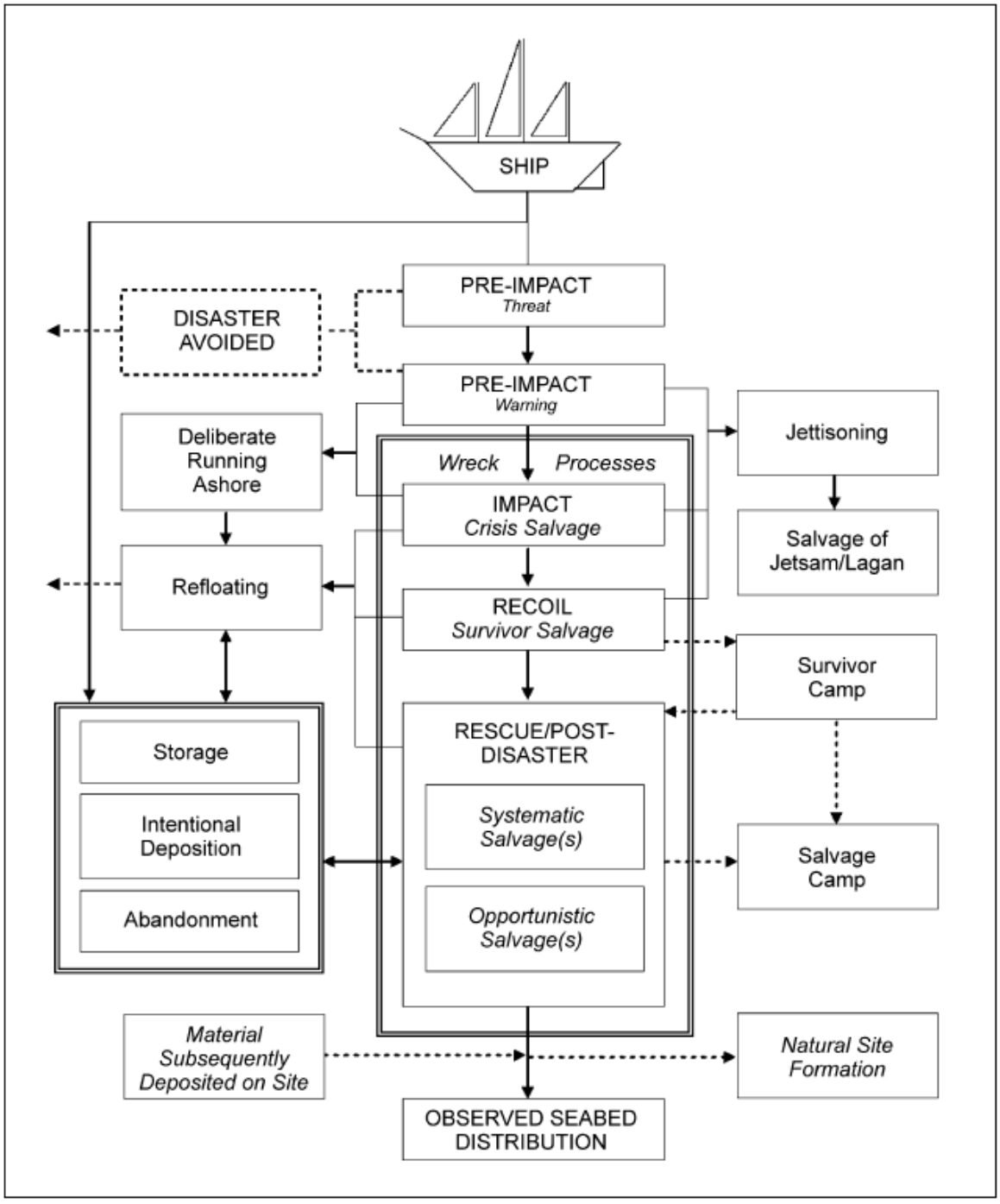

Figure 4: Gibbs (2006) disaster response framework for site-formation processes

(2006:18), "This framework means that the sometimes fragmentary oral, documentary and archaeological data-sets can be critically evaluated and synthesized into a logical sequence, while identifying ambiguities requiring further attention".

Although he presents the logical organization of fragmentary data as an advantage of his framework, Gibbs is also highlighting a core weakness of this approach—results likely cannot be reproduced by other archaeologists, because of the proposed over-reliance on interpreting possible shipwreck scenarios from ambiguous or unreliable human sources (Puddifoot 2018). However, he establishes the importance of cultural behavior in shipwreck site formation processes and regards documentation of this behavior as the main means of accessing their interpretation from the archaeological record. This thesis takes another approach. By identifying specific physical conditions affecting sites, it is hypothesized that human behaviors that affect shipwrecks can be revealed deductively as the probable explanations for the observable scatter patterns. Put another way: visualizing the environmental context of shipwreck decay enables the elimination of spurious interpretations, while lending credibility to others.

In the context of the 1733 shipwreck sites, the weather patterns for the storm (Figure 5) and ambient conditions (Figure 6) diverge considerably, making these sites particularly useful for a site-formation study of this kind. The survivors' reports from the 1733 *Flota de Indias* indicate that the hurricane struck the fleet on the evening of 14 July 1733 (Benson 2002: Appendix 1), exhibiting a strong northerly wind. The storm then passed over the ships in

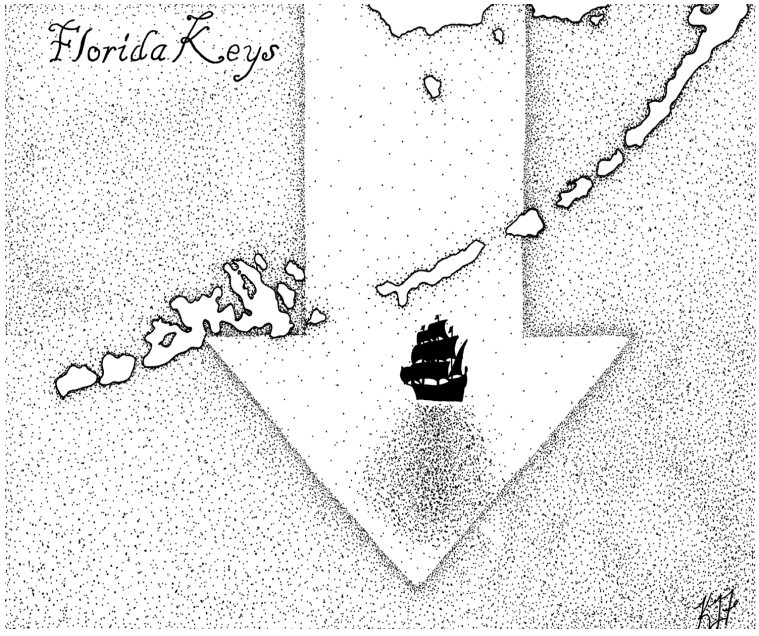

Figure 5: Illustration of shipwreck material drift trajectory during the 1733 hurricane (Fricker 2018)

approximately 35 hours, grounding most of the vessels on the shallow near shore rock ledge to the south and east of the Florida Keys. Figure 5 illustrates the storm's dominant winds and associated material scatter pattern that might be expected for the duration of the event. Given the influence winds have on sea surface currents (Ren et al. 2018), the northerly forcing winds from the storm passing over the shipwrecks likely altered the surface currents of the region as well, blowing material to the south. While the extent of the drift for these sites and this event has not been investigated, current oceanographic research suggests the wind would has the most pronounced effect of the geophysical forces acting on the material (Breivik et al. 2011; Fernández-Montblanc et al. 2016).

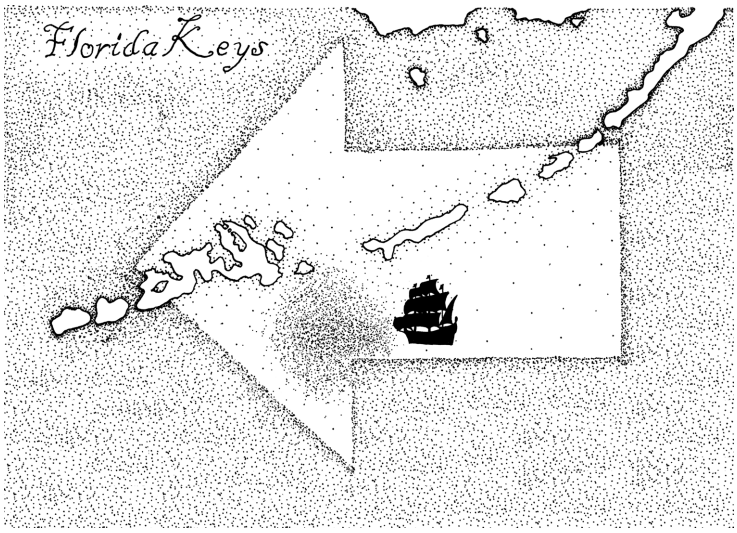

Figure 6: Illustration of ambient conditions and drift trajectory (Fricker 2018)

While tropical storms and hurricanes are not uncommon for the region, they exhibit patterns that are distinct from the ambient conditions in the Florida Keys. NOAA NDBC (1971) data indicates the prevailing trade wind of the region is an easterly that, in many cases, is nearly perpendicular to the storm scenario illustrated in Figure 5. A typical day, like that displayed in Figure 6, would have characterized the drift trajectory of material separating from the wreck during the salvage operations in 1733 (and possibly any such later operations). Given the known locations of the ballast piles, it is possible to extrapolate whether the material was scattered from the wreck site during the storm, or

during the salvage efforts, using a computerized simulation of geophysical forces and drift trajectories.

1.6: Computing Shipwreck Scatter

Computerized modeling has been applied in archaeology since the 1960s, part of the Processual or 'New Archeology' approach to determining where sites were located and, in some cases, why (Verhagen and Whitley 2012:50). Advances in processing power and the integration of computational methods with visualization enable contemporary archaeologists to conduct robust analyses with greater ease than their predecessors. Banning (2002:45-46) advocates for the application of mathematical modeling in the interpretation of maritime cultural heritage, and such techniques were applied with limited success in the search for the *BonHomme Richard* (Melissa Ryan and Peter Guth, personal communication 2017) and the *Fougueux* (Fernández-Montblanc et al. 2016).

The computerized model applied to the 1733 shipwrecks here builds upon the work of Fernández-Montblanc et al. (2016), which was highly dependent upon historical documentation of the *Fougueux* and the way it broke up and dispersed. For the purpose of this study, the location of the ballast pile is the only prior condition to the simulation, as the historical documentation does not tell archaeologists where or how material disbursed during salvage operations was scattered. For this reason, a probability estimation is applied to enable researchers to achieve some quantifiable certainty of the context through which the remains can be interpreted.

To accomplish this, NOAA wind and current data (NDBC 1971) from the 1980s and 1990s are utilized as forcing inputs for the simulation. Mean and mode directions are

extracted from each 10-minute interval of the July datasets and applied to objects of variable size, generating a point cloud of probable drift trajectories and extents. The simulation is run for an ambient scenario, simulating the drift trajectories of 10 virtual objects during 30 three-day wind and ocean current scenarios that reflect Florida Keys weather conditions during October. The output is used to create a visually comprehensible heat map that displays the density of shipwreck scatter around the starting coordinate. The map provides both spatial and temporal representations of the conditions compelling material to drift away from the site after wrecking. The resulting dispersion field is then visualized in a Python mapping package. This representation can be compared to data in the archaeological record and serve as a quantifiable starting point for discussing whether the material was discarded into the water during the storm, or during the salvage evacuation of the wrecked vessels. This approach builds specifically upon Gibbs' (2006:18) assertion that, "The disaster-response model proposed here hopefully provides an extended structure for understanding cultural actions before, during and after the wreck event, as well as allowing them to be integrated with the natural processes," by relying on environmental data to reveal the context for the specific cultural process of shipwreck salvage. Figure 7 models the interaction of input data, simulation, and the visualized output.

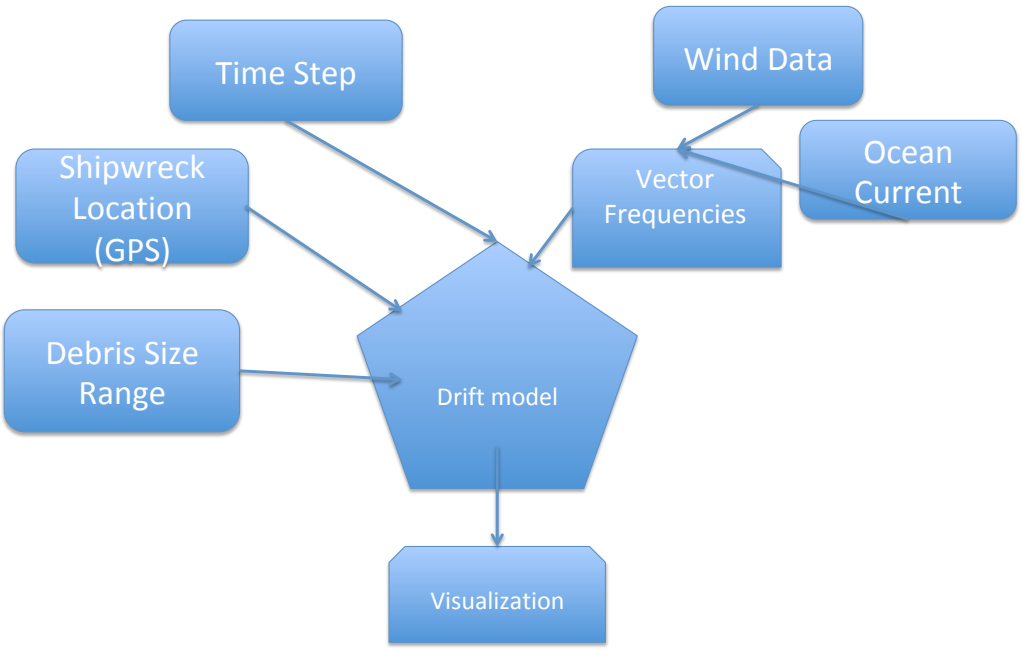

Figure 7: Framework for drift trajectory simulation

The aim of this thesis is to discuss the activities of human beings in the past, by visually plotting known remains of their activity into the geophysical context of natural processes. The endeavor is to ascertain which objects on the seabed were likely deposited as a result of human decision making, rather than environmental conditions. The sentiment was expressed clearly by Mark Gillings (2012:601):

> That despite over a decade and a half of research, effective dialogue within archaeology between Geographic Information System (GIS) (on one hand) and experiential theory (on the other) remains elusive is nothing short of remarkable. The present discussion seeks to not only explore the reasons behind this impasse but to suggest that perhaps the time for dialogue has passed and rather than building bridges, researchers in

> archaeological GIS should instead begin to build their own theoretical frameworks.

Thus, this study aims to contribute to archaeological surveys through the application of pre-survey forensic models that reduce costs and increase the likelihood of locating scattered remains associated with known shipwrecks. The completed simulations can bring mathematical certainty to the interpretation of specific wrecking events, with consideration given to linking scattered remains among known sites, and examining remains that fall outside of expected patterns, as possible evidence of salvage activity. Finally, these results are considered alongside documentary evidence, for the purposes of comparing the accounts of Spanish salvors with extant remains on sites from the fleet, offering comparison to this cultural transform process.

Chapter 2: History

This account of the history of the 1733 Spanish treasure flotilla relies heavily on primary resources translated from Spanish by Jack Haskins (Benson 2002: Appendix 1). The documents comprise administrative records issued by the *Consejo de Indias*, the Royal and Supreme Council of the Indies, which administered the Spanish government's overseas holdings. The stories relayed here are derived from the archive's *Indiferente General* holdings, documentation "of a general nature" not considered specific to any of the 14 administrative regions of the colonial empire (Stony Brook University Libraries *Archivo General de Indias* 2018). As result, this chapter is limited to the perspectives of the prominent merchants and administrators of Spain's Caribbean empire. In these documents, the imperial apparatus is most concerned with the ships and treasure that were damaged, and the value of the goods recovered. The fates of few passengers and crew are reported, and there is no mention of African peoples, who were surely on board as slaves early in the journey, and possibly as passengers. These omissions leave contemporary scholars with an incomplete picture of events surrounding the 1733 hurricane and position the narrative of the fleet's loss in terms of wealth and power, rather than memorializing the greater number of un-named individuals who conducted the work of sailing, protecting, and salvaging the fleet.

2.1: Logistics for the 1733 Fleet

A letter (Benson 2002: Appendix 1), written in Cadiz, offers some administrative detail of the 1733 fleet. The notice is dated 4 August 1732, and names the ships, owners, and captains, who are expected to carry out the voyage. Four ships of the crown set sail

with 16 vessels owned by Spanish merchants. In the archival documents, the vessels are referred to by their roles in the fleet, names, and nicknames, interchangeably. *El Rubi Segundo* was the flagship (*La Capitana*), accompanied by *El Indiano* as the secondary command vessel (*Almiranta*). A supply ship (*Refuerzo*), *Nuestra Senora de Balvaneda* (*El Infante)*, and smaller cargo vessel (*Pinque*), named *El Populo*, supported the galleons. These four vessels carried the king's treasurers and property managers, who were to oversee the accounting of the various riches acquired on the voyage. The letter also names 16 privately owned ships (*particulares*) that were accompanying the fleet. The names and titles of the men on these vessels gives no indication they played a specific role in the flotilla's operation, though some ships did carry government officials and mail. The letter is interesting more for what it lacks, than for its content, as there is no timetable, no list of destinations, nor an expected arrival date for the fleet (Benson 2002: Appendix 1).

The flotilla sailed under the command of Don Rodrigo de Torres y Morales, who was accompanied on board *La Capitana* by a king's Master of Silver, Don Balthesar de la Torre. Two other silver accountants accompanied *Almiranta* and *Refuerzo*, Don Bernadino de Maturana and Don Domingo de Lanz, respectively. The *Pinque* carried the fleet's quartermaster, Don Francisco Imbernón. Several family shipping business operators furnished vessels for and accompanied the flotilla. Don Joseph Sanchez de Madrid owned both the *Nuestra Senora De Las Angustias* and *San Raphael*. Don Joseph's son, Don Francisco Sanchez de Madrid, served as captain aboard *La Angustias*, but he is also listed as the owner of *El Gran Poder De Dios*. Don Jacinto de Arizon sailed with his ships, *Nuestra Senora Del Rosario*, *San Antonio*, and *San Vicente Ferrer*. His

son, Don Juan de Arizon, captained the *Rosario*. Two young members of the Arizon family also joined the voyage, Don Miguel de la Ranaga and Don Joseph Hoscarer. According to the 1732 missive Don Alonso Herrera Barragan, Royal Commissioner of the Navy, accompanied the voyage and attended to the administration of the fleet (Benson 2002: Appendix 1).

2.2: Administering A Treasure Fleet

The wealth involved and the logistical demands of maintaining a global commercial empire necessitated significant planning and oversight. Due to Spain's experience in the Mediterranean over the previous centuries, it was not unprepared for the transition to global maritime commerce. According to Tracy (1990:47), "By the 15th century, the peoples of the Iberian Peninsula… were well supplied technologically and administratively to pursue commercial opportunities outside the boundaries of Europe". Exploration and the founding of colonies characterized the early decades following Columbus's contact with the Americas. As New World plantations and trade colonies became viable, the nature of trade came to resemble a closed cycle: raw materials were exported from the colonies and developed into manufactured goods, which were sold back to the colonies or, on to other developing markets in the empire.

The practicalities of this closed system were reflected in the imperial legal apparatus.

> The colonies were organized to supply what Spain did not produce and to purchase manufactured goods and some agricultural products from Spain. Foreigners were legally excluded from direct trade with what the Spanish called the Indies; instead they had to deal through the port of Seville in the sixteenth and seventeenth centuries and through the port of Cadiz for much of the eighteenth century (Tracy 1990:76).

Over the course of the 16th century, the fleet system was refined to address the risks posed to the emerging global trade network.

The *Casa de la Contratación de las Indias* (Trade House of the Indies) maintained a monopoly over the flotilla's operations. It was a one-stop shop, created by Queen Isabella in 1503, administering maritime law, tax collection, exploration, and intelligence work for operations related to commerce with Spain's colonies, including the annual flotilla when it was developed by Pedro Menéndez de Avilés in 1561 (Salmoral 1985:5). The flotilla was the solution to the problem of securely moving vast wealth from all over the globe to a central location in the West Indies, before embarking to Seville. Initially, it was contrived as a system of defended waypoints for provisioning. These fortified colonies took on a life all their own, but their critical purpose to Spain over the ensuing two centuries was fleet safety and supply.

In addition to developing the flotilla concept, one of Menéndez's early accomplishments was identifying land and seascapes important to its operation. Spain had control over lands along the south and western edge of the Caribbean, and many of the Caribbean islands. The French, particularly in Florida, contested Spanish holdings in North America, while the English had fledgling Caribbean and North American colonies. The entire trade route spanned the Pacific, Central America, and the Gulf of Mexico, making in vulnerable in its early years. The Straight of Florida was a particularly exposed point on the route. In 1565 Menéndez secured this final portion of the route in a brutal attack on the French colony of La Caroline and the supply fleet of Jean Ribault, cementing Spanish control in eastern Florida just seven years after Philip II had

appointed him Captain General of the Indies Fleet (Aliaga 2015:10). As the trade route prospered, the colonies expanded, and by the 18th century, the treasure flotilla system was defining the lives of millions of people around the globe.

Seville was the main point of disembarkation and return for the fleet and the seat of the *Casa de Contratación*. Sixteenth century Seville was a nexus of global trade, a place where politics and commerce were deeply intertwined. It had not always been so, and the economic opening of the city to the wider world lured its aristocrats to shirk the stigma and xenophobia associated with trade, and themselves form mercantile enterprises (Pike 1965:440). One such family, the Alcázars, claimed their ancestors had helped drive the Muslims from the city in the 13th century. Aligned as they were to the liberation of the city, their aristocratic status was not a question. Still, by the 16th century, family members held both municipal posts and ran trading businesses with the Americas. "Francisco del Alcázar, the head of the family during the first half of the century, is a good example of this combination of office holding and trading... [he] eventually became the Mayor of Seville, and Treasurer of the Mint" (Pike 1965:443-444). The aristocrats were not the only people in Seville who valued the city's commercial status. According to Pike (1965:440), "The whole city lived under the spell of the fabulous American treasure that, 'at the arrival of the fleet was carried in carts pulled by four oxen along the streets from the Guadalquivir to the *Casa de Contratacion*'". Over the next two centuries, public access to the ostentatious wealth that accompanied the return of the treasure fleet liberalized, helping to define the Mercantile period and the development of a middle class, while shaping the Capitalist era yet to come.

> European economic expansions were located in coastal zones, with a few exceptions that confirm the rule… A further characteristic of this system was the predominant role of merchants and the prominent role of the precious metals (gold, silver, even copper). The conflicts among the metals were only brought to a partial end with the decisive development of credit toward the end of the 16th century (Braudel 2009:181).

Commercial trade flows throughout the period of the flotilla pair with the demographic story of Europe and the Americas. The initial stages of expansion increased contact between peoples and resulted in the spread of diseases that vastly reduced the Indigenous population of Spain's holdings in the Americas (Devans 1992). As colonies stabilized, there are indications that these populations did as well, and were then supplemented with Spanish immigrants and sub-Saharan African slaves. Population estimates for Spain range around 8 million to 8.5 million during the 1500-1600s (Phillips 1999). William Denevan's (1992: xxviii) estimates for the regional population of the Americas indicate that as many as 25.5 million Indigenous Americans occupied what would become Spanish territory in the Caribbean, Central America, and Mexico. As a result, by the 18th century, Spain's colonies societies were highly diversified, compared to their European counterparts.

Population figures are also more difficult to delineate by ethnic group during this period. Around 450,000 Spaniards had officially immigrated to the American colonies (Phillips 1999: 3), and approximately 3.5 million Africans had been brought to the Americas (Eltis 2013). Families and women played a notable role in driving permanent emigration from Spain. Meanwhile, the slave trade was also moving millions of Africans to the colonies. As a result, the population of the Spanish Main and the Caribbean began to recover and diversify in the latter 17th century.

> Women accounted for 5.6% of legal immigrants for 1493-1519, 6.3% for 1520-1539, 16.4% for 1540-1559, 28.5% (60% single) for 1560-1579, and 26% (59.5% single) for 1580-1600. Among legal emigrants from Andalusia in the seventeenth century, women accounted for 51%. In short, contrary to persistent assumptions, women and families played a continuing and important role in Spanish migration across the Atlantic (Phillips 1999:4).

The people on board the flotilla experienced a diverse colonial world, as compared to the Iberian Peninsula. South American and Caribbean ports were home to very mixed populations. Havana, whence the flotilla would return to Cadiz, was the third-most populated city in Spain's American colonies, and one-third of the black or mulatto population comprised freed former slaves (Murillo 2013; Bethell 1993:4). The influence of the African population is still felt today. Cuba's population shares 17% to 26% sub-Saharan African ancestry (Fortes-Lima et al. 2018). Spanish African ancestry is similarly around 20%, but from Northern Africa and mostly from the Ancient period (Botigue 2013:5).

Cuba would have seemed both exotic and familiar to initiates from mainland Spain. It was a space where Spanish culture was evolving alongside other European aesthetic influences (Smallwood 1975). The *Castillo de San Salvador de la Punta* and *Castillo De Los Tres Reyes Del Morro* guarded the southern and northern points at the entry to the port of Havana. Their neo-classical style is seen in fortifications throughout the Caribbean and was a reminder of institutional structures at home. The Jesuit *Catedral de La Habana* had been completed in 1704, in the Italian Baroque style (Gravette 2000:134). To its south, across a plaza, was the *Palacio de los Condes de Casa-Bayona* (the Palace of the Counts of House Bayona). Further south, the *Espiratu Santo* Chuch and

the *Convento de Santa Clara*, founded in 1632 and 1636, respectively. Espiratu Santo harkened to its Spanish-Moorish influence, with an arched doorway and patterned stone. Meanwhile, the first nuns of the convent were from Cartegena, Colombia, adding to the internationalism of the city. To the west 3.5 km, was the Santo Domingo Monastery, site of the University of Havana upon its founding in 1728 (Gravette 2000:144). These sites would, in just a half a century, inspire the Cuban *baroque* style (Kerr 2009: 25). In total, contemporary Havana is home to 144 buildings from the 16th and 17th centuries, and 197 survive from the 18th century (Gravette 2000:127). For early 18th century visitors from Spain, there would also have been much that was familiar.

Eighteenth century Cuban culture exhibited hierarchical structures reticent of mainland Spain. The aristocratic customs of Havana, for example, would have been familiar to the elite among the passengers and officers. Havana had a large population of urban plantation owners who, like their counterparts in Spain, only occasionally visited their holdings in the country (Bethell 1993:4). This rural/urban divide was not as common in other Spanish colonies, and uniquely situates Havana in cultural proximity to Spain, at the disembarkation point of the concluding leg of the treasure fleet's voyage. For all the foreign-ness of the colonies, Havana offered a taste of home before the long voyage to Cadiz.

2.3: Overseeing Trade

Carla Rahn Phillips (Tracy 1990) examined records of trade flows between the Iberian powers and the Americas, during the early modern period. Her analysis offers concrete insight into the scale of and changing trends in the flotilla trade. During the

period of 1566 to 1570, roughly 132 ships per year traversed the Atlantic to trade with the colonies, and roughly one-third to one-half traveled with the flotilla system (Tracy 1990:43) (Figure 8). In these early days, the average tonnage of known ships participating in trans-Atlantic trade was approximately 212 tons.

Sampling of Phillip's (1990) data set for the 1731-1735 period reveals significant changes—foremost, the use of fewer and larger ships (Figure 9). The average annual number of ships for this period slips to 36, while the tonnage rises by over 50%, to 362.8 (Tracy 1990:45). Total tonnage transported to the Spanish West Indies peaked during the 1606-1610 period, averaging 45,593.4 tons per year (Figure 10). This was nearly double the average annual tonnage of 27,985 shipped during 1566 to 1570, and roughly quadruple the 11,974 shipped during 1731 to 1735, despite the use of larger ships in the later period. These figures offer insight into the declining role of the flotilla operation in the conveyance of wealth throughout the empire and may be related to a decline in the role of precious metals exports from the Americas, which dropped from during the period from 1625 to 1725, before rebounding (Tracy 1990:238).

Spain's mariners' guild, the *Universidad de los Mareantes*, set regulations for ship and crew sizes, and saw to the training of Spanish seamen (Taylor 1922). No ship was to exceed 550 tons, but while the fleet sailed from Seville—for the first 142 years of the flotillas operation—crossing the bar at San Luca (Sanlúcar de Barrameda) presented such difficulty that, initially, the ships typically only ranged from 100 to 200 tons. Phillips' (Tracy 1990) observations on ship size in Fig 9 also indicate that the sizes of ships involved in the flotilla had grown significantly by 1733, following the move of the *Casa de Contratación* to the deeper harbor of Cadiz.

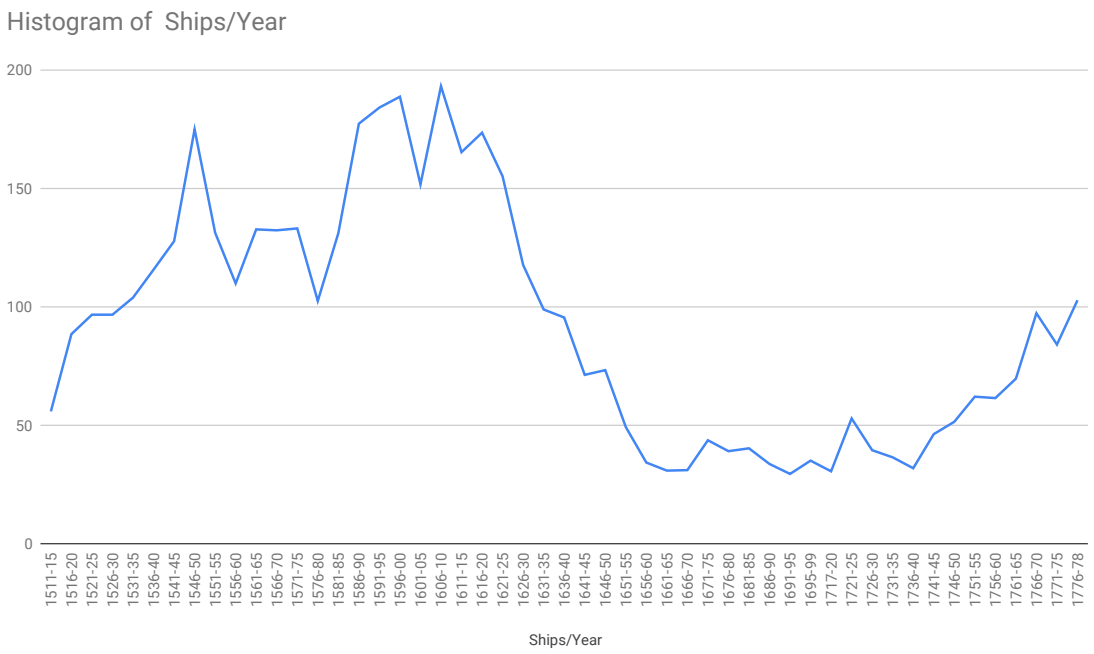

Figure 8: A histogram indicating the number of ships traveling between the Spanish Caribbean and Spain (Tracy 1990).

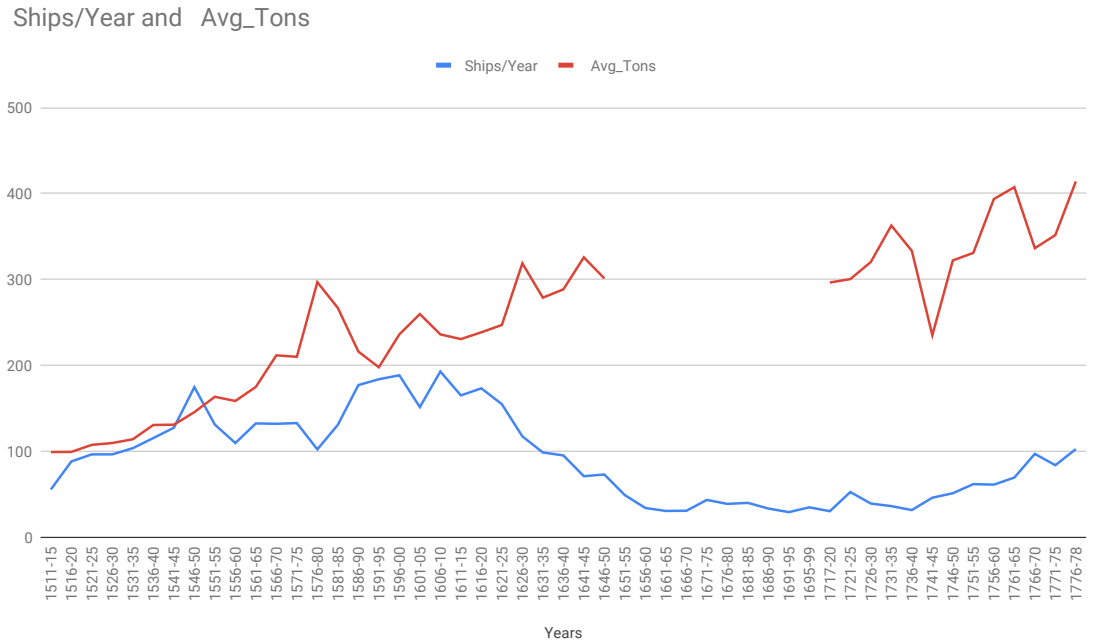

Figure 9: A histogram comparing the number of ships traveling between the Spanish Caribbean and Spain and the average tonnage of vessels (Tracy 1990). [Note: Missing data in primary record is the cause for the gap in the graph]

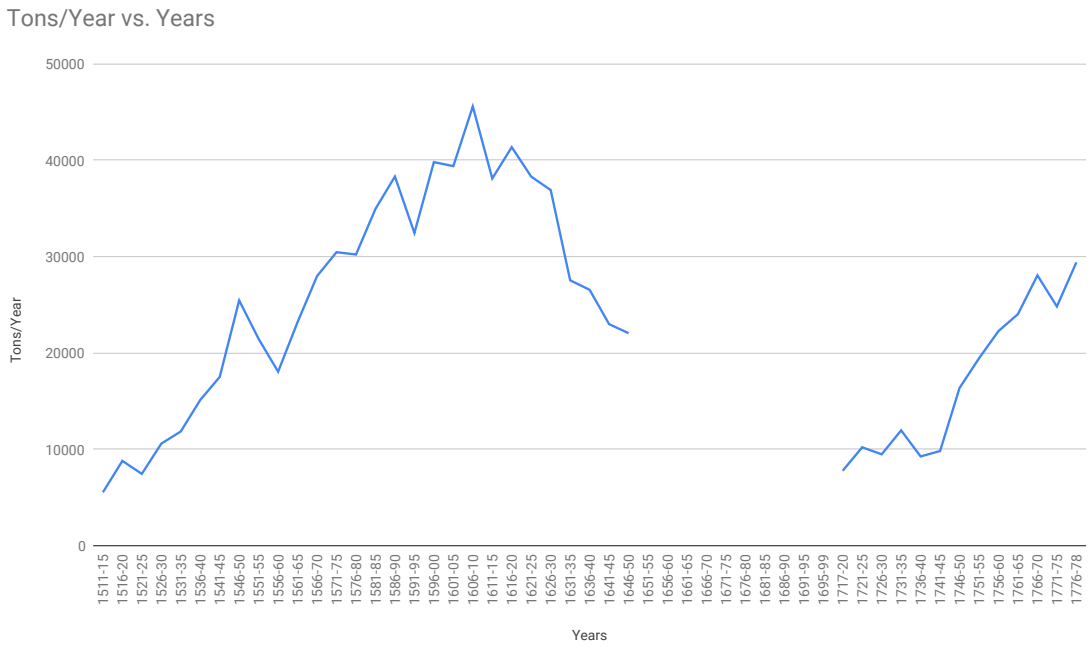

Figure 10: Total tonnage of cargo shipped to Spain from the Caribbean (Tracy 1990). [Note: Missing data in primary record is the cause for the gap in the graph]

In addition to dictating ship sizes, the guild also prescribed minimum crew standards for each vessel type participating in the flotilla:

Size of Ship	Mariners	Apprentices	Boys
100-170 Tons	18	8	2
170-220 "	28	12	4
220-320 "	35	15	5

(Taylor 1922:643)

In 1717, the *Casa de Contratación* relocated to Cadiz. The move enabled the crown to reduce the influence of Seville and its merchant guilds on the empire's global trade. It also served a practical purpose. Ships no longer needed to navigate the hazards associated with the Guadalquivir River, such as the seasonal sand bar at San Luca, as a departure from Cadiz cut out the leg from Seville to the Atlantic Ocean. Additionally, this

enabled the entire fleet to assemble before departure with the inclusion of its largest, 500-ton vessels.

By the time the Trading House was relocated, Spain's empire had been beleaguered by over a century of external and internal conflicts, and its European holdings had been partitioned under the terms of the Treaty of Utrecht in 1713 and Treaty of Rastatt in 1714. Philip, Duke of Anjou and King of Spain, renounced his claim to the French throne in 1712 to ensure that the succession of the monarchy was limited to his male line, before it could pass to any females in the family, helping to achieve a peace settlement. The treaties of Utrecht and Rastatt ended the War of Spanish Succession and saw Spanish power in Europe greatly reduced. Several of Spain's important European holdings were transferred to other powers: Gibraltar and Menorca to Great Britain; the Spanish Netherlands, Naples, Milan, and Sardinia to the Habsburgs in Austria; and Sicily and parts of Milan to the Dutchy of Savoy, which became a kingdom (Bromley 1970). Yet, Spain's colonial empire remained intact. Philip V would attempt to restore Spain's power in Europe, but the key to financing these operations remained the trade and treasure from the colonies

2.4: The Route

The 1733 fleet departed Cadiz in August 1732. The flotilla first sailed to the Canary Islands, and from there proceeded on a roughly 50-day journey across the Atlantic to the Lesser Antilles (Aliaga 2015). There were two component fleets at the start of each flotilla voyage. After arriving in Guadalupe, the fleets proceeded southwest, together, separating upon sighting Isla de Margarita, off the coast of modern-day Venezuela. Two

groups of ships would form, the *Tierra Firme* fleet, bound for Caracas, Maracaibo, Santa María, and Nombre de Dios (Taylor 1922:642). The fleet of *Nueva España* would head north to Puerto Rico, then west to Puerto Caballos in Honduras, via Hispaniola and Cuba, before finally sailing on to Veracruz, Mexico. The escorts would break from the second group in Havana, using it as a base for operations against pirates or other threats (Aliaga 2015:12-13).

Given a 2 August departure and allowing two weeks from Cadiz to Tenerife, and seven more to Guadalupe, the fleet of 1733 would have reached the Caribbean in early October 1732. Another week under sail could have put the *Nueva España* fleet in Mexico. Through the winter the fleets operated independently, delivering and loading goods intended for Spain. The fleets would reconvene in Havana in June, and from there return to Spain via the Straight of Florida, passing near Bermuda en route to the Azores.

Don Francisco de Vara y Valdez recounts the arrival of the lieutenant and notary of the *Senor San Joseph* (*El Africa*), Don Francisco Perez de Claras and Don Antonio Prieto, in Cadiz. The men explain that the flotilla departed Veracruz on 25 May and the ships arrived in Havana between 24 and 26 June. When it departed, the flota comprised 19 ships, five of which were ships of the crown: *El Rubi*, *El Gallo Indiano*, *El Infante*, *El Africa*, and *El Pinque Populo* (Indiferente General 1987-1733 Flota). In the letter, they recount the storm and survival/salvage efforts. Since *El Africa* survived the storm, it was able to sail on to Spain earlier than other vessels. Having departed from Key Largo on 24 July, it likely brought the first news of the hurricane to mainland Spain, arriving in September.

2.5: The Storm

The 1733 hurricane lasted more than two weeks and traveled from the Lesser Antilles, through the Bahamas, then across Cuba and the Florida Keys, before proceeding into the Gulf of Mexico. Such a storm track is not uncommon in the Western Atlantic, matching 20 hurricane events in the late-19th and 20th centuries for which there is meteorological data. The closest matching storm tracks include Hurricanes Donna (1960), Betsy (1965), Inez (1966), Andrew (1992), Georges (1998), and an unnamed 19th-century storm that began in July 1894 (Figure 11).

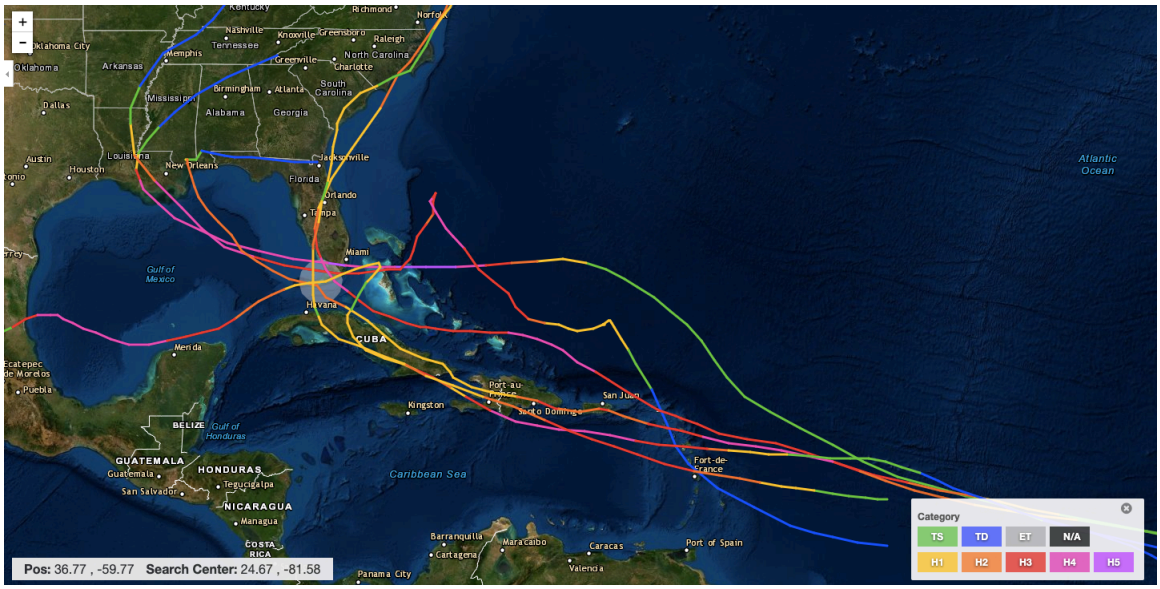

Figure 11: Storm tracks of Hurricanes Donna, Betsy, Inez, Andrew, Georges, and an unnamed 1894 storm (Office of Coastal Management 2019)

The 1733 storm came early in the hurricane season, hitting St. Lucia, Montserrat, and Nevis at around dawn on 30 June (Robertson 1733; Chenoweth 2006).

> We were taken napping and unprovided [*sic*]; and tho', for two or three days before we saw all the signs that are [here] believ'd to be the

> prognostics of a hurricane; yet being in the month of June, and no hurricane having been known with us in the memory of man, till after the 20th of July, no body suspected the least danger, till we were in it.
>
> - Rev. Robertson (1733:5-6)
> Nevis; 9 July 1733

In the 18th century, timing the hurricane months was based on tracking the moon cycle. Hurricane season begins, "as our way of reckoning has been hitherto, with the first full moon or change after the middle of July, and end[s] with the first full or change after the 10th of October" (Robertson 1733:13). The 1733 hurricane was an early storm, from the perspective of 18th-century Caribbean setters, and this made it more destructive to inhabitants and sailors alike. Robertson (1733:3) describes the storm as coming unexpectedly and from due east of the Lesser Antilles, before proceeding roughly northwest. In all, it appears to only have affected the southern Caribbean islands for approximately 24 hours but exhibited hurricane-forces from its first landfall (Robertson 1733:4-5; Chenoweth 2006: Table IV).

English accounts of the damage offer insight into the strength of the storm at this early stage. Roberston (1733:10) recounts that survivors on the island of St. Christopher reported the complete destruction of windmills and houses, while on Montserrat, 30 out of 36 windmills were "blown down to the ground, and the other six are much shatter'd, having left their veins and round-houses" (Roberston 1733:12). The hurricane winds in Montserrat were sufficient to move stone structures. "A cattle millhouse belonging to Mr. James Huffey, weighing at least 20,000 lb., was taken fairly in the air, carry'd some distance from its proper place, lodg'd in a piece of canes, and broke in ten thousand pieces by the force of the fall" (*Maryland Gazette* 1734).

Antigua was somehow spared the worst damage and was able to send ships to other islands relatively soon after the hurricane passed (Robertson 1733:13). However, reports from other ports north and west of the storm indicate the effects on shipping were considerable. News of the hurricane traveled throughout the colonies during late July and August 1733, and the *Boston Gazette* (1733) ran several accounts of the hurricane's effects on various islands, as details came in via letters and ships' captains. "Notwithstanding all the care, industry and pains to secure them [ships], it [the hurricane] proved fatal to almost every vessel then riding at anchor in Basseterre Road," on Nevis. The same paper (*Boston Gazette* 1733) later recounts the effects of the storm on other islands: 24 ships lost at St. Thomas and 13 ships sunk at Montserrat. *The Weekly Rehearsal* (1733) quotes a source the same week, saying "that above an hundred vessels have been destroyed at the several islands thereabouts [near St. Christopher's], and abundance of men lost".

The loss of the treasure flotilla is also noted in several English sources, starting in October. The 2 October 1733, edition of the *New England Weekly Journal* publishes excerpts from a 21 August letter of that year, which recounts the damage to the flotilla. "You will have heard before this of the dismal loss's that on the 19th inst. [August] we saw lost on the Florida shore 12 or 14 sail of vast large ships, which undoubtedly, in my opinion, must be the flota." The article continues, reporting 31 tents on the shore, made from sailcloth, and a two-tier, 50-gun sloop anchored within a mile of the camp and a shipwreck site, upon which sailors and salvors appeared to be working. "The wrecks all appeared to be as large as that afloat." An October 13 headline declares: "The flotilla are

lost, consisting of three men of war and 18 merchant men, upon the Cayo Largo, or Long Keys" (*Boston Weekly News Letter* 1734).

These stories of the hurricane's disastrous effects on English and Spanish colonies demonstrate the close ties among Caribbean islands of the two empires, and the inhabitants of the Caribbean were keenly aware of the hurricane's potential to spark a geopolitical crisis. Robertson sent his concerns to London, indicating that damage to the sugar trade on Nevis and Montserrat could compel colonists to migrate to more secure islands. In particular, he was concerned that such migration would leave the English colonies insufficiently policed and exposed to acquisition from other powers.

> I, with some gentlemen, would consider before it be too late, that the loss of the sugar trade would be to Great Britain, upon the general balance with a certain neighbouring power, what deserters are in a battle: a loss to the side they leave, and a gain to that they go to, which is double (Robertson 1733:30).

There may well have been a culture of opportunism among the European powers in the New World, leading to shared fears of lost advantage by the English and Spanish alike. Robertson's concerns, for example, are mirrored in the Spanish documentary record. However, the Spanish were more interested in the immediate recovery of the fleet, rather than leveraging the storm for an expansion into English settlements. Spain sought to recover as much salvage as possible from the sunken fleet, before English colonists could respond to news of its vulnerability. The governor of Havana specifically names the risk of English salvors visiting the wreck sites from New Providence, which was fewer than 170 nautical miles from the shipwrecks (Marques De Cavecas 1733, in Benson 2002).

2.6: Shipboard Experience

When the fleet departed Havana on 13 July 1733, there was no indication of a storm approaching the region. The weather was favorable for the start of the trans-Atlantic voyage, enabling the fleet to make good time toward the Florida Keys.

> On the 13th of July we sailed from the Port of Havana with good weather, and the following day, 14th; discovered the land of the Cayos de la Florida. At 9 that night the wind began rise out of the North, then it freshened to the point where we knew a hurricane was imminent. We found ourselves close to the expressed Cayos and the wind and seas were very strong making it impossible for the ships to govern themselves. Each hour it increased with major force. On the 15th signs were made for the Flota to head for Havana but we were unable to do so for the wind came around to the south without slacking it's force or the seas. At 10:30 of the night of this day we all grounded in the expressed Cayos, at a distance of 28 leagues on length, with this *Capitana* off the one called Cayo Largo 2 1/2 leagues from shore (Alonso de Herrera Barragan in Benson 2002: Appendix 1).

The hurricane had not diminished in intensity by the time it struck the treasure fleet, though compared to its pace in the Southern Caribbean, it appears it slowed slightly. Having passed the islands of the Lesser Antilles in roughly 18 to 24 hours (Robertson 1733), the hurricane's pace slowed as it approached the Florida Keys and was over the fleet for approximately 30 hours (Benson 2002: Appendix 1). As a result, the risks posed by wind and wave actions were made more complicated by the additional rainfall that inundated the ships. Many of the vessels sailed successfully through the first day of the storm and maneuvered the tacks necessary for their retreat to Havana. However, as Barragan notes, the flotilla struggled as the hurricane changed direction, likely moving to the southwest of the Florida Keys, such that the fleet was presented with a southern headwind on their retreat to Cuba. Many of the ships became inundated with water to

such an extent that, had they not grounded upon the reef, they would have been completely lost. *Capitana*, aboard which Barragan was grounded through much of the storm, lost two men in the hurricane. Meanwhile, *San Ignacio* and an unnamed fragata were "swallowed" by the ocean, lacking the protection offered by the reef's shallow waters (Benson 2002: Appendix 1). The people, ships, and cargo that survived did so as a direct result of grounding on the reef.

The surviving members of the crews undertook salvage efforts within days of wrecking. Barragan notes that the silver from *Capitana*, *Almiranta*, and *Infante*, was among the first items salvaged, and that quantities of indigo and cochineal were recovered from other vessels. Nine ships were dispatched from Havana with rations, supplies, troops, and divers, and by 12 August, Barragan (Benson 2002: Appendix 1) reports that much of the galleons' treasures had been recovered.

2.7: The Human Impact

By the 18th century, Spain had become so reliant upon its closed cycle of global trade routes, that it was financially and geopolitically exposed by the risks posed to the fleet. "Among the most destructive and disruptive events threatening the political and economic integrity of the Spanish Empire was the wrecking at sea of its treasure fleets that resulted from unexpected storms" (Carlos E. Marquez in Tarver 2016:116). The treasure fleet entangled the lives and fortunes of thousands of people. Jack Haskin's translation of Spanish archival material (Benson 2002: Appendix 1) provides valuable insight into the salvage operations and material recovered from the shipwrecks, discussed

in the 'Archaeology' chapter below. The documents also convey some of the human story of the flotilla, its destruction, and the effects its loss had on families back in Spain.

The documents from the *Indifferente General* portray the flotilla as a family business affair. The Spanish empire had been wealthy but had spent centuries waging expensive wars against the Ottoman Empire and Northern Europe. The nobility of Seville had grown significantly wealthier, due to their proximity to the *Casa de Contratación*, and the merchants of Cadiz gained a greater share of this prosperity when the *Casa* moved to their city in 1717. By 1733, the power of the Spanish monarchy had been significantly reduced in Europe, and it was facing significant internal corruption. Poorly paid officials were skimming off the top of the treasure fleet, in order to support their families. There was also money to be made in supplying the fleet and transporting goods, and in 1733 several merchants with shipping operations were training their sons to learn the family business, a business fraught with risk (Benson 2002: Appendix 1).

Even before the storm, the voyage took a considerable toll on participants. Just out of Veracruz, eight people in the convoy, including two children, as well as uncounted numbers of soldiers, sailors, and servants, all died from yellow fever, picked up while at port (Benson 2002: Appendix 1). Don Jacinto de Arizon owned at least three ships in the flotilla, when it departed. Another two are attributed to him in the folio of letters and depositions that Benson translated, though these may be a false positive for Don Juan de Arizon, ship or cargo master for one of the vessels, who may also be Jacinto's son. The letter does not note the ages of Don Miguel de la Ranaga and Don Joseph Hoscarer, just that they were of "tender age". The flotilla voyage had not yet faced the most dangerous catastrophe of the voyage, and it had already become the setting for a tragic family loss—

a family traded for fortune. Don Jacinto de Arizon was not the only father to lose a son on the journey. Don Geronimo de Ariscum also lost a child, but to the hurricane weeks later (Benson 2002: Appendix 1).

Although the Arizon and Ariscum families lost a great deal, there are harrowing individual survival stories in the documentation of the voyage as well. *Fragata de la Florida* is reported as complete loss, with only one man escaping. The unnamed survivor escaped to a survivor camp on Long Key by floating or swimming with a spar from the frigate. At the camp, he would have been among two other survivors who became key players in the initial rescue and salvage efforts. Don Juan Clemente Sanchez Duran was ordered to take a small armed launch and deliver letters to the Governor of Havana, among other officials, notifying them of the wrecking event and beseeching them for assistance and supplies (Benson 2002: Appendix 1).

The launch arrived on 25 July 1733. The author of the letters is unknown, but they summarize key details of the rescue and recovery work. Don Juan Feliz de Andrade was heading efforts to seek a rescue from Long Key, and dispatched Juan Clemente, a royal commerce official, in a launch to Havana. Juan Clemente sailed in small skiff or longboat with a jury-rigged sail, and conveyed letters and other royal officials, as well as some of the merchants who had survived. He then led colonial officials back to the survivor camps and shipwreck sites. In Havana, the governor placed Juan Clemente in charge of organizing the resupply for the survivor camps: “These Deputies are knowledgeable in the general needs of all the camps, such as how to best benefit the lives and work on these wrecked ships” (Benson 2002: Appendix 1).

The deliberate planning of colony spacing in the Spanish Caribbean enabled a swift response to the hurricane. Havana was close enough to the wrecking sites that it could be reached in roughly a day's sail. Marques De Cavecas, the Governor of Havana, recounts the arrival two other captains, who had also sailed from separate survivors' camps in launches: Don Francisco Sanchez de Madrid and Don Raymundo de Soto. De Soto conveyed a letter "from the Chief of the Flota asking me for arms, munitions, and all other things which I [Marques De Cavecas] had already provided in anticipation of his notice" (Benson 2002: Appendix 1). Don Joseph Sanchez de Madrid was the owner of the Angustias, which had been captained by his son, Maestre Don Francisco Sanchez de Madrid. The disarray of the wrecked flotilla represented risks to the immediate survivors of the storm, foreshadowed the potential ruin of several families' merchant enterprises, in addition to posing an existential threat to the operations of the Spanish Empire. The swift initiation of salvage operations was key to minimizing the losses to all parties involved.

2.8: Scattering a Shipwreck

Salvage operations on some of the shipwrecks began as early as four days after the storm. In Jack Haskins (Benson 2002) translation of Spanish archival correspondence, Alonso de Herrera Barragan names the *Capitana*, *Almiranta*, and *Infante*, as being the first ships to be salvaged. The historic record indicates that several ships were burned during this recovery effort (Smith and Dunbar 1977). In his book *Galleon Alley*, Robert Weller (2001) asserts that the Chaves was burned to the water line by Spanish salvors, and the archaeological report from the *Tres Puentes* site indicates the presence of burned wooded remains (Smith and Dunbar 1977b). Carbonized remains from the shipwrecks

would be expected to drift in a manner that reflects the probable environmental conditions during the salvage operations (a prevailing easterly or south-easterly wind, with a northeastern current). Sediment sampling from the sites should reflect this, with an increased content of carbon in sediment aligning with vectors associated with particle drift on a fair-weather day. Conversely, if a ship burned during the storm, the pattern of scattered carbon would travel along a completely different course—most probably the sum of the northerly wind and the northeastern current (NDBC 1971).

However, no sediment data has ever been gathered at the sites with the frequency and granularity that would be required to discern carbon traces from an 18th-century vessel. Archaeologists can rely upon other material remains and for the purposes of this study, a variety of wood types and shipwreck material shapes are examined to isolate likely directions of material drift. Provenience data for these remains is the most effective means by which this simulation's efficacy can be confirmed, and it offers the interpretive capacity to characterize shipwreck scatter as distinct from salvage scatter.

Emerging computational methods and advances in speed offer archaeologists an important opportunity to experiment with modeling techniques that have the power to influence archaeological interpretation. The applications are numerous. In this case, the historical accounts of the 1733 shipwreck and storm—and the wind data, course information, and disaster response descriptions they contain—provide unique parameters that can be computationally modeled with contemporary tools. The underlying theory behind computational approaches touches many areas of archaeological science. These are discussed in greater detail in the chapter to follow.

Chapter 3: Theory

3.1: Search and Rescue

The approach taken in this thesis is to treat the archaeological remains of the 1733 flotilla as a search and rescue problem. This requires the application of mathematical techniques to the study of the environmental context. The role of the environment in the development of the Spanish flotilla system—in fact, its significance to all Early Modern colonial endeavors—requires that it be given the most complete consideration achievable for the archaeological investigation. As Braudel (2009:203) said, "Spatial models are maps wherein social reality is projected and partially explained, models valid for all the temporalities… and for all social categories".

This thesis examines the Spanish treasure flotilla in the context of plural time, utilizing geophysical data from the longue durée (the ocean and climate of the Florida Keys), to interrogate the micro-historiá and archaeology of the 1733-shipwrecking event and its immediate aftermath. The flotilla exemplifies four Braudelian criteria: 1) it was a social system, reproducing itself in a given territory with the resources of that territory; 2) the system adapted over time; 3) this system initiated and carried out the succession of one community and culture by another; and 4) the mechanism of change relied upon hierarchy and domination (Villaseñor 2015:307). In the case of this thesis, the environmental context is broken into component mathematical forces (wind, ocean, and leeway vectors), in order to calculate the drift of materials from the shipwreck sites. The goal is to interpret the archaeological evidence with the support of a clear visualization of the probable drift trajectories, as this allows the interpreter to consider the concerns of survivors and salvors who recovered materials from the ships.

3.2: Statistical Archaeology

The application of principles and technology from the hard sciences to archaeological questions, as in this thesis, is not new. Archaeologists have experimented with numerical methods for analyzing archaeological data since the 1960s. Hodson et al. (1966) tested a variety of statistical techniques on an assemblage of Iron Age brooches to determine the value of these techniques for archaeological analysis. After describing the material in numerical terms, representing quantitative and qualitative characteristics, the archaeologists found that average-link cluster analysis and a multi-dimensional scaling procedure resulted in archaeologically significant classifications, useful for grouping and dating the brooches (Hodson et al. 1966:323-324). These and similar experiments of applying numerical methods to artifact-level data sets began to inform maritime site-formation process theories in the 1970s.

Keith Muckelroy was at the forefront of the application of process models to explain site formation, according to Harpster (2009). Muckelroy's application of cluster analysis to the *Kennemerland* shipwreck site enabled him to show, despite a lack of contextual hull remains, that similarities within clusters of material culture corresponded to the functions of those materials on board, and that only minimal post-wrecking depositional scrambling occurred on the site. However, more importantly, "Muckelroy demonstrated that it is possible to determine quantitatively, and not just intuitively, which artifact classes on a scattered wreck site are part of the cargo, or just personal items" (Harpster 2009:72). Some regarded this breakthrough as intuitive, but Muckelroy's insistence on applying the scientific method to the study of site formation processes

moved the study of shipwrecks in a forensic direction, and his framework informs this approach to shipwreck site formation and post-depositional salvage.

Muckelroy's quantitative approach enabled interpretation of the scattered material culture, but his efforts to reconstruct the ship from the shipwreck remains did not incorporate numerical environmental factors. Later archaeologists began converting environmental considerations into numerical measurements as part of the effort to understand site formation processes in the 1980s. In a 1981 survey of the US east coast by Science Applications, researchers identified links between environmental variables and the distributions of sites, and then expressed these correlations as models for management purposes. This macro-level examination of terrestrial site formation speaks directly to the motivations of humans in settling spaces along the coast. As a result of the study, the authors were even able to identify patters of settlement distribution in bathymetric data of the continental shelf and propose future research into shipwreck site formation. They advise research into "the distribution of shipwreck material and how artifact scatter patterns are affected by varying depositional environments… [to] determine to what extent environmental variables, such as water depth, bathymetry, currents and tidal action affect the archaeological data base" (Science Applications 1981:55). The study identifies sites that could be particularly useful for the conduct of these studies, including marine parks that encompass the 1733 shipwrecks: Biscayne National Monument, Key Largo Coral Reef Marine Sanctuary, Crocker Reef, Looe Key Marine Sanctuary, and Sand Key—most of which are now managed under the Florida Keys National Marine Sanctuary (Science Applications 1981:57).

Numerical modeling has also successfully informed the interpretation of ship construction techniques. For example, the study of wood thermodegradation (Pétrissans et al. 2013) quantifies the way heat-treating improves the durability of wood. Jonathan Adams (2013) observes that heat treatment utilized in the construction of an 11th-century vessel found in Utrecht, Holland, while this author has observed a similar technique applied in the construction of traditional dhows in the Tanzanian coastal village of Tongani (Cox unpublished field notes 2017). Mori et al. (2014:1) found the decomposition rates of rainforest woods "related positively" to wood density and concluded that ecologists could employ species-specific decomposition rates in the determination of ecosystem-level carbon dynamics. Archaeologists, therefore, might consider applying the same data in models of decomposition of wooden hull components in various environments, as has been proposed by Ward et al. (1999) for process-based modeling of shipwreck site formation. A final example of material studies, closely related to this, is the monitoring of wood transport during flash floods, by Virginia Ruiz-Villanueva et al. (2012). By numerically modeling a bridge clogging with wooden debris during a simulated flash flooding event and comparing it to an actual 1997 flood, the researchers showed the viability of such a simulation for predicting and simulating wood transport and hydrodynamics. A similar design approach, one that relies upon scientifically derived data, is applied in the development of this drift simulation.

Numerical methods are also useful in the analysis of large, or 'big' data sets. Kowalewski (2008) examines the role that cultural resource management databases can play in comprehending macro-scale patterns of human settlement. Kowalewski reviews computational methods for identifying patterns in the relations of people, places, and

activities, both to each other and to other features in the environment. For example, Kowalewski (2008:240) illustrates the ease with which market exchange extent can be studied by visualizing the geographic distribution of large bodies of ceramic data. He also notes the role large, region-scale data sets play in determining the level of human-induced erosion to the Mediterranean's environmental history (Kowalewski 2008:244). Finally, Kowalewski (2008:237) shares the application of k-means statistical measures to identifying clusters of settlements, and rank-size characterization to determine the hierarchical variation of Late Bronze Age city-states. These are just a few examples of the assistance computational methods afford archaeologists in the consideration of macro-level research questions.

3.3: Shipwreck Mathematics

While this study focuses on active, shallow-water sites, the interpretation of deeper shipwreck sites also benefits from the application of mathematical approaches. Church (2014) utilizes the "equation of site distribution methodology" to interpret the events leading to the sinking of several steel-hulled vessels from the WWII period. While the debris fields of such vessels are materially distinct from those of Early Modern wooden shipwrecks, this approach demonstrates the value of applying quantitative modeling methods to the reconstruction of shipwrecking events. Church suggests this approach could help locate sites, or find additional material from known sites:

> Using the same methodology, researchers could work forward to locate a sunken vessel if a location is known for the event that led to the vessels demise, or if only the wreck location is known, work backward to locate the additional elements of the site. In either case, finding all the major

> components of a site and being able to retrace the sequence of events leading to the initial site formation is key in accurately interpreting and in telling the complete story of each wrecking incident (Church 2014:39-40).

The application of modeling to so many areas of archaeological inquiry is a key sign that the approach has reached a critical juncture, in terms of its accessibility and value to the field. In discussing the history of computational modeling and the simulation of archaeological hypotheses, Lake outlines the takeover of inferential approaches by statistical and numerical methods, saying that, "simulation really has finally come of age as part of the archaeological toolkit" (Lake 2014:278).

The barriers to utilizing complex statistical approaches in archaeology have been greatly reduced in the past 20 years, by advances in computers and programming languages. Data have been gathered and research conducted that refine the scientist's ability to describe the physical world in probabilistic terms. These advancements are becoming more commonplace in the biological sciences and applied regularly in the fields of meteorology, chemistry, and oceanography. In hurricane forecasting, for example, error ranges for 72-hour hurricane track forecasts have been reduced by over 300 miles since the 1960s (Figure 12 and 13) (Cangialosi 2018). During the same period, computational models, observed datasets, and machined learning algorithms have optimized search and rescue planning (Ren et al. 2018). As a result, it is possible for archaeologists to rely upon methods from these fields to treat shipwreck sites as search and rescue or drift trajectory problems, in order to locate cultural material and better interpret wrecking events.

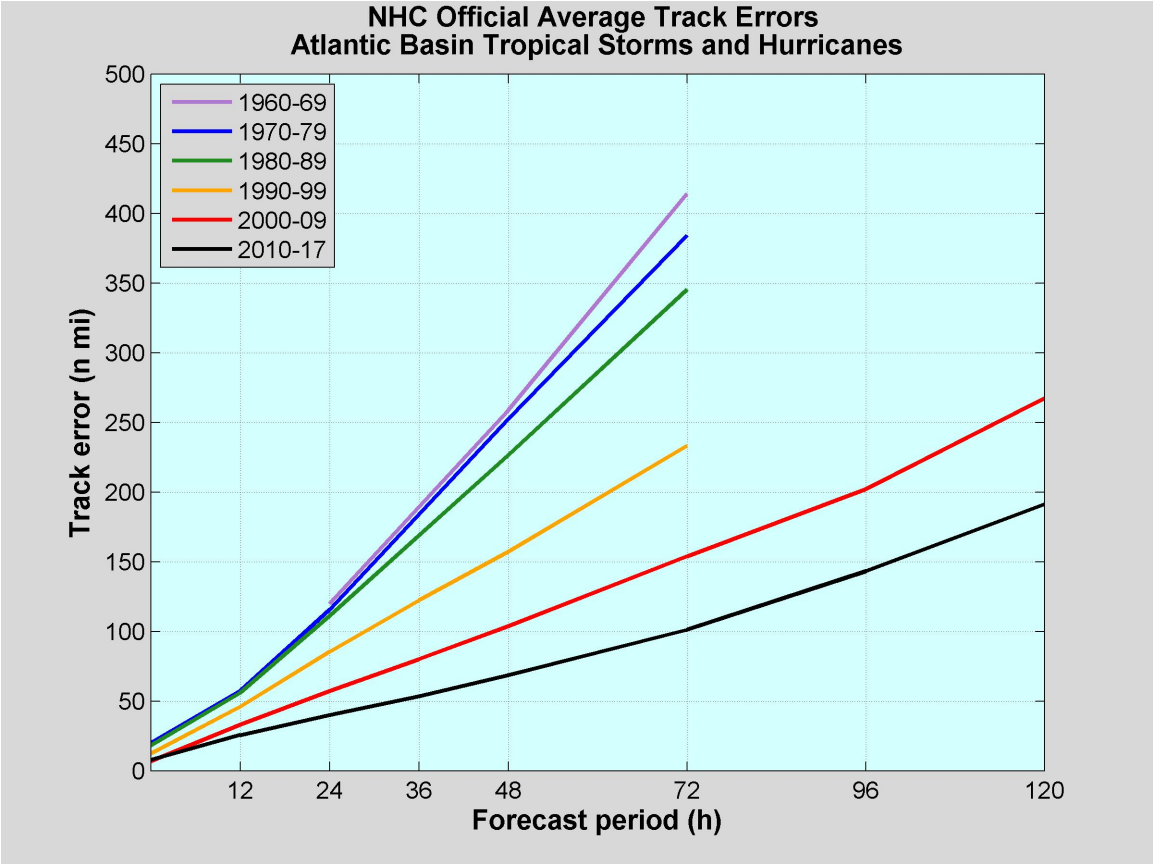

Figure 12: Average hurricane track errors in miles (Cangialosi 2018).

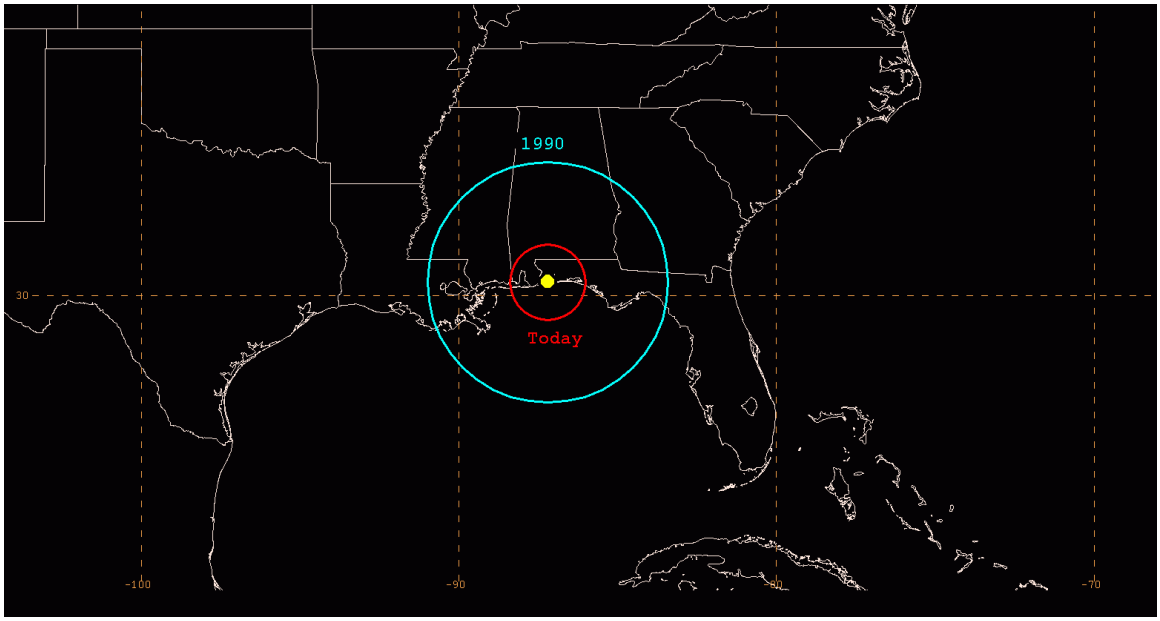

Figure 13: Average NHC 48-hour forecast track errors for a storm centered over Pensacola, Florida, in 1990 (blue) and today (red) (Cangialosi 2018).

3.4: Extending the 'Known'

Claims made about the past based on contemporary data are not without problems. Among the key theoretical challenges facing a modeling project such as this, is the difficulty inherent in validating the results with empirical tests. "It is significant that models are constructed in other scientific fields so as to predict data that have not yet been collected, rather than to account for observations already made" (Bevan and Lake 2013:155). The veracity of the meteorological and oceanographic data involved in the modeling technique applied here is not beyond question, but they comprise the same data that inform reliable forecasting and analyses in a variety of hard sciences. Even when the 'common sense' observations of a region's wind and current patterns closely correspond to the collected meteorological and oceanographic data these numerical data sets are ultimately more valuable for their ability to be included in complex environmental models. The methods applied in the development of this ocean drift model are a more relevant area of debate, and the assumptions underpinning the approach in this thesis are discussed in more detail in the methods chapter.

Muckelroy's efforts toward a taphonomy of shipwrecks, combined with Price's (2015) observations about historic and modern salvage, should give archaeologists the confidence to reconsider the limits of what a dynamic site can reveal about human behavior. Ward et al. (1999) make clear that various processes on shipwreck sites are increasingly accessible to the archaeologist for modeling and simulation. "Large structures coming to rest on the seabed will affect and be affected by the physical, chemical and biological environments" (Ward et al. 1999:569), and these processes can be quantitatively reproduced to interpret a shipwreck site. For the purpose of this study,

data on the physical processes figure as key inputs into the study of the wrecking event and depositional patters.

The work of Fernández-Montblanc et al. (2016:2) applied a quantitative process-based approach with search and rescue principles of material drift, to the study of archaeological shipwreck remains.

> The study of the depositional phase in wreckages or maritime accidents, aimed to estimate the trajectory of damaged vessels or the dispersion of different substances spilled during accidents, has attained considerable importance in environmental oceanography and search and rescue operations. However, the numerical modeling techniques employed in the abovementioned fields have not been applied to evaluate the dispersion of wreckage remains in an archaeological context.

The authors apply numerical modeling to investigate the dispersion of remains from the *Fougueux*, a French Temeraire-class ship of the line that sank in a storm following the Battle of Trafalgar. Their study follows three steps: 1) characterization of the oceanographic and meteorological conditions during the wrecking event; 2) implementation of a two-dimensional Lagrangian dispersion model (LDM) to assess high-probability areas where scattered material would be transported; and 3) an assessment of the computational scatter pattern in comparison to geophysical surveys.

The main inputs for their LDM include surface current velocity, wave characteristics, and 10-meter wind velocities. These inputs were derived from oceanographic and meteorological observations, based on the work of Wheeler (1985) in "The weather at the Battle of Trafalgar," which reconstructs the storm that followed the Battle of Trafalgar from English ships' logbooks. "The objective of the model is to simulate the trajectories of the floating pieces of the ship after the wreckage," which, in

addition to the oceanographic and meteorological forces, is "conditioned by ocean currents, wind, wave motion, and turbulence, as well as by the shape, the buoyancy, and the emerged/submerged ratio of the object" (Fernández-Montblanc et al. 2015:3). The authors note the complexity of drift simulations and the variable behavior of real floating objects among the key limitations, but demonstrate that, despite uncertainty regarding the size of the objects being detected and the error rates in their oceanographic and meteorological field data, they were able to establish strong correspondence between the archaeological remains identified in their geophysical survey and those of the *Fougueux*. For example, cannons found during the survey match French ordinances from the late-18th century, and the number of newly found pieces (42) equals the number missing from the previously identified shipwreck site—bringing the total of cannons across the assemblage to 74, the number said to be on board the ship during the battle (Fernández-Montblanc et al. 2015:13). Based on the mathematical links demonstrated in the dispersion model and the supporting archaeological evidence, the authors conclude that their method works successfully and may be applied to other cases.

The authors note that this methodology has several archaeological purposes. In addition to the delineation of probable search areas, which reduces survey costs, the method may also be useful for the identification of remains and the management of sites. The authors identify several key limitations in the application of their method. Foremost among these, is the necessity that climate patterns not be dramatically changed between the time of the wrecking event and the present. However, as discussed in Chapter 4: Methodology, NOAA's Florida Keys wind inputs closely correlate to the weather

observations of ships of the 1733 fleet, just as observations from Spanish watchtowers matched the weather inputs utilized by Fernández-Montblanc et al. (2016).

The work of Fernández-Montblanc et al. (2016) provides the main theoretical and methodological foundation for this thesis. Their team demonstrates the viability of Muckelroy's (1977) hypothesis: that site formation processes can be mathematically modeled to reconstruct shipwrecking events. The environment in which the *Fougeuex* broke up is more dynamic than that of the *Kennemerland*, characterized as a turbid, near-shore setting, which is more akin to that in which the 1733 fleet sank off the Florida Keys. The similarities in the conditions of the wrecking events, in that the 1733 fleet and the *Fougeuex* both sank in hurricanes, as well as the comparable limitations of relying on historical weather data, such that contemporary meteorological observations are incorporated into the drift simulation, make the approach of Fernández-Montblanc et al. (2016) a reasonable analogy for this research thesis. Despite the limitations, their research and survey team succeeded in uncovering new shipwreck remains. In this case, the aim is to verify this methodology through reliance on ambient weather data, hopefully revealing the utility of search and rescue principles in the interpretive process.

Chapter 4: Methodology

4.1: 2D Simulation

The approach taken in this thesis follows a typical data science workflow, comprising four components, or steps. These are: 1) data gathering and cleaning; 2) parameterization of assumptions; 3) computer simulation modeling drift trajectories; and 4) discussion of results. Ward et al. (1999) proposed that scattered shipwreck sites are commonly found in near-shore environments, where physical factors are continuously breaking down vessels. The 1733 shipwreck sites suffer an additional complication: the sustained scrambling of the sites by salvors and treasure hunters (Westrick and Cooks 2017). The aim of simulating environmental scatter processes is to identify the probable paths and extent of debris flow during salvage conditions, which are assumed to be the ambient conditions of the environment that prevailed when Spanish salvage teams were working at the sites from August to October 1733.

Certain human interventions in the site formation process leave a visible signature on a site (Price 2015:39). This methodology describes a simulation of environmental conditions at the 1733 sites in the Florida Keys. Historical documentation is used in combination with contemporary wind data and a computerized model to visualize the probable paths along which materials would drift, as a result of these environmental factors. The central hypothesis is that, when compared with baseline patterns of natural drift, material scatter can reveal signs of the type of human activity that impacted a wreck site.

4.2: Primary Sources

The use of historical accounts to ascertain past weather conditions is successfully accomplished in Wheeler's (1985) investigation of the storm that followed the Battle of Trafalgar in 1805. In this October storm, the *Fougeuex*—a French ship-of-the-line—foundered and sank within sight of the Spanish coastline north of Cadiz. Fernandez-Montblanc et al. (2016) combined the research of Wheeler (1985, 1987, 1995, 2001) and Aller-Hierro (2004) to identify analogous storms and use these in a computerized simulation to determine the highest-likelihood area where shipwreck scatter was deposited during the 1805 hurricane.

Wheeler (2001:362) describes mining ships' logs for "observations made twice daily (at 8 in the morning and 2 in the afternoon) of air pressure, temperature, wind direction, wind force and the state of the weather" in the Strait of Cadiz, and using these data to reconstruct the hurricane that struck the Spanish coast after the Battle of Trafalgar in 1805. Aller-Hierro (2004) compiled the *Documentary Corpus of the Battle of Trafalgar*, including in his compilation meteorological and oceanographic data recorded by military units, watchtowers, and ships logs. The observations are sufficiently consistent that, while qualitative, they enabled the meteorologists to render them numerically and reconstruct environmental conditions two centuries prior. With these data, Fernández-Montblanc et al. (2016) modeled the Napoleonic era hurricane and compared it to recent events, ultimately selecting a December 2009 storm for their simulation based on its similar sea level pressure and wind considerations. The researchers note that this approach does not indicate "complete correspondence" between the historic and contemporary storm events but is rather "a way to maximize the limited

information on the weather conditions existing during the wreckage" (Fernández-Montblanc et al. 2016:10). This approach enabled the team to limit their marine survey to an area with the highest likelihood of holding depositional remains of the *Fougeuex* and locate additional archaeological material (Figure 14). The success of their application is encouraging, and one research question of this thesis seeks to determine whether a similar approach can yield favorable results in the investigation of the 1733 storm and shipwreck events.

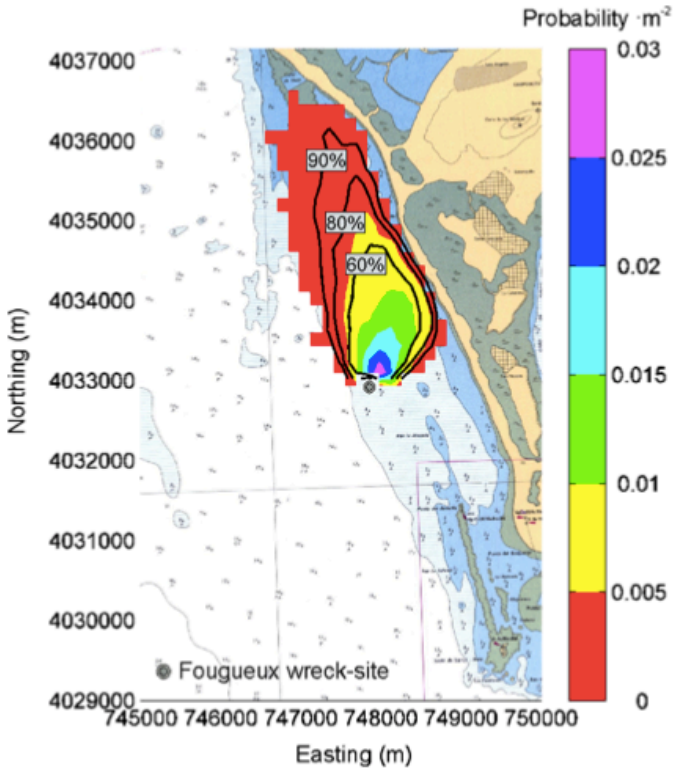

Figure 14: A likelihood distribution map of scattered archaeological remains from the *Fougueux* (Fernández-Montblanc et al. 2016:10). The color scale indicates the probability per unit area for remains, simulated with a Lagrangian dispersion model. The contour lines represent the probability in percentages.

The correspondence and logbook accounts of the 1733 hurricane offer the best means of deriving storm data contemporary to the wrecking event. Appendix A comprises a timetable of events reconstructed from the ships' log data, as translated by

Jack Haskins (Benson 2002: Appendix 1). Four accounts compiled from the documentary record concur on the timeline of events during the 1733 hurricane. The fleet departed Havana on 13 July and sailed on the region's prevailing easterly winds (Benson 2002:1). The logs record winds directly out of the east and from the east-northeast from the morning of 13 July until the evening of 14 July. At 18:00 that day, the wind direction shifted to the north for those ships in the Florida Straight, and a similar shift was noted a 20:00 in Havana (Benson 2002:7). By early morning of 15 July, the western edge of the hurricane was upon the flotilla and signals were made for the fleet to return to Havana. Through the day of 15 July, the flotilla attempted to sail east-southeast and put distance between the ships and the Florida Keys, before tacking west as the storm intensified. The effort to reach open sea was unsuccessful and by 22:30 on 15 July, the fleet had run aground on the shelf of the Florida Keys, with two vessels reporting the loss of their masts and rigging. The storm continued through the night and subsided by the morning of 16 July (Benson 2002: Appendix 1).

The ships' course reports, as well as wind and storm track accounts from the historic record, provide the best means of finding a more recent analogous storm for which wind, current, and wave data are available. English colonial records indicate that the 1733 hurricane struck the Caribbean island of Montserrat on 30 June (Robertson 1733), before proceeding to the Bahamas, Cuba, and Florida (Benson 2002: Appendix 1). Based upon these characteristics and the frequency of hurricanes in the Florida Keys, there are more than 20 hurricane or tropical storm events for which meteorological and oceanographic data are reasonable matches. From these, analogous storms include Hurricanes Donna (1960), Georges (1998), and Rita (2005), as well as six other unnamed

storms—including an 1899 hurricane that also began in July (NOAA 2018). Comprehensive storm modeling of the 1733 hurricane is beyond the scope of this study, but an understanding of the storm's track and timing sets the stage for the arrival of salvors on site. Identifying the effects of historic salvage activity is the primary focus of this study, and thus the process of inputting simulation data begins in the aftermath of the storm, when salvage efforts begin.

4.3: Documentary Records

The historical accounts of the storm and conditions in the Florida Keys in 1733, combined with NOAA wind and current observations, constitute the key data inputs for this simulation. The documentary records of the 1733 storm are limited but can still be formatted in a method that makes them usable for simulation. The wind directions recorded in the ships' logs and the overall track of the storm, can be reconstructed from the documentary evidence. Of the candidate storms, Hurricane Georges appears to be the closest match, based on these criteria. The International Best Track Archive for Climate Stewardship (IBTrACS) dataset, developed by the NOAA National Climatic Data Center, contains detailed wind, wave, and track data for hurricanes dating back to the mid-19th century. For the purposes of this simulation, accounts from the historical record of some vessels' dismasting are considered to offer a baseline minimum wind speed of 50 miles per hour. The barkentine *Orline St. John*, for instance, wrecked on the North Carolina coast in 1854 after dismasting in a "strong gale" (Heit 2012). The wind speeds involved in a gale of this type are typically 47-54mph, according to the National Weather Service. Hurricane Georges sustained winds over 50 mph as it traversed the Bahamas and Florida

Keys in 1998, and its longer track from Antigua to Alabama—in nearly a straight line—supported its candidacy over other, stronger storms.

4.4: Assumptions

Given similarities between the historic and modern storms, one assumption made in this study is that the ambient conditions are similarly analogous. There is evidence that this assumption is risky. C.E.P. Brooks' "The Climate of the First Half of the Eighteenth Century" (1930) explores variations between measurements of pressure, rainfall, temperature, and wind in Europe for the periods of 1701-1750 and 1881-1915. Wind is the most important data point for this thesis and Brooks observes the greatest variation in comparisons of winter readings. Specifically, Brooks notes shifts in the frequencies of winds from certain directions, with the largest variations observed in the winter months, but notable variations in the summer months as well. The dearth of weather data for the Spanish Caribbean is confirmed by Michael Chenoweth (2003:1), "The tropical regions of the Americas are almost completely devoid of daily weather records prior to 1800 and the few published records are usually very short summaries". Chenoweth (2003:75) examines Thomas Thistlewood's weather journals from July 1750 through November 1786—some 5000 pages of daily records—and concludes that "the middle and late eighteenth century was cooler and moister than in the twentieth century". This could have the impact of introducing appreciable error to this simulation, given the reliance on contemporary wind data. However, Wheeler (2008:24) asserts that the diversity exhibited by the climate of Europe in the 18th century undermines efforts to generalize linking climatic shifts with historical or cultural ones: "Case studies and examples warn against

offering generalizations concerning the interactions between these physical factors and social systems". Given the limited weather data available for the early 18th century and the close match between the Spanish wind records from 1733 and late-20th-century NOAA wind data for the Florida Keys, the approach applied here assumes climatic conditions on the sites are largely unchanged since the 18th century. The results of the simulator preliminarily demonstrate this assumption to be correct.

4.5: Climate Data

Meteorological and oceanographic datasets are the key inputs to the drift simulator. The simulator is designed to provide a rudimentary trajectory-modeling function derived from frequentist analysis of wind and ocean conditions near the 1733 shipwreck sites. As Thomas Lee and Ned Smith note in *Volume transport variability through the Florida Keys tidal channels*, "The curving shoreline causes regional differences in response to prevailing westward winds and Florida Current influences" (2002:1363). This simulator incorporates several datasets for the region to achieve highest probability accuracy with the lowest computational time.

The simulator requires user inputs to function: geographic boundaries of the area of interest, coordinates for the simulation's starting point(s), and forcing data (wind and current). One collection of wind bearing and wind speed data from the NDBC is used in this study, but more could be added to improve the accuracy and make a more robust model. The wind dataset comprises 25 years of observations from the NDBC's Molasses Reef MLRF1 climate buoy (Figure 15), south of Plantation Key. In addition to collecting wind bearing and wind speed data, the buoy also transmits a range of other sea surface

data (Appendix C). The data utilized in this study are manipulated using the Python programming language (van Rossum 2001), with specific reliance on the Numpy (Ascher et al. 2001), Pandas (McKinney 2010), and Matplotlib (Hunter 2007) libraries for computation, formatting, and visualization.

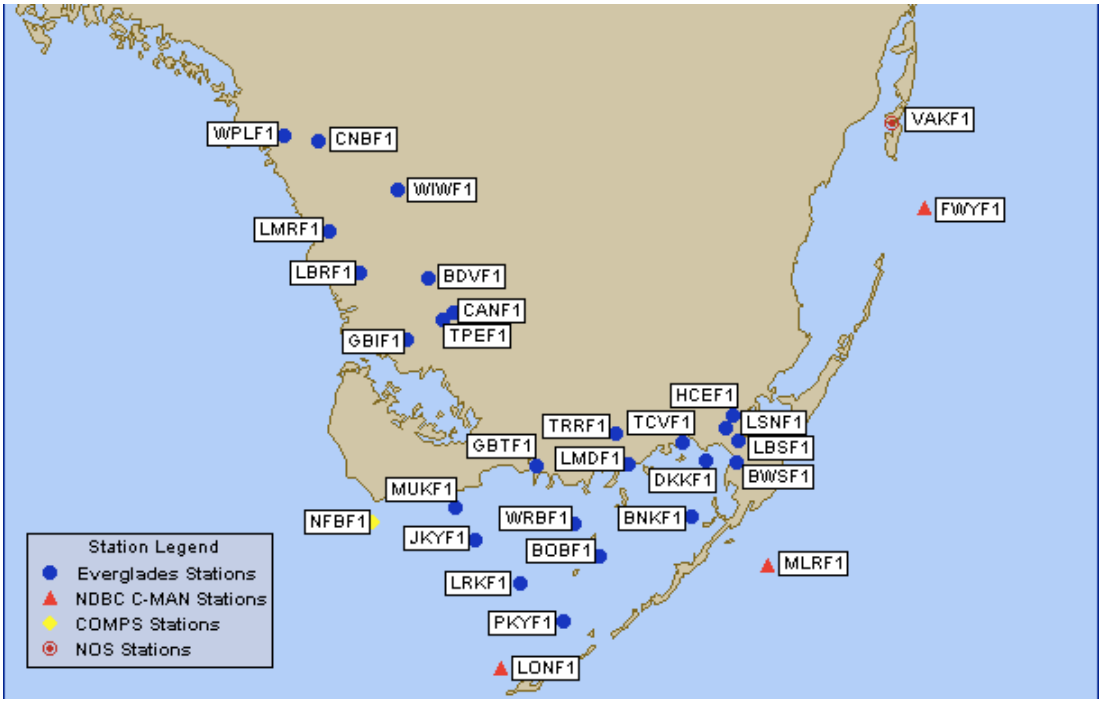

Figure 15: NDBC (2014) buoys deployed throughout the South Florida region.

4.6: Frequency algorithm

Prior to asserting probabilistic behavior of the weather in the South Florida region, it is necessary to demonstrate the non-random nature of the conditions in the area of study. To do so, the Python Pandas library (McKinney 2010) was utilized to analyze 23-years of NDBC data from the MLRF1 buoy. These outputs are compared to an identical analysis of a randomly generated dataset, created for this study. The Python Matplotlib Wind Rose functionality is used to visualize data, with mean wind bearing and wind speed plotted on a compass (Figure 16-19). For the randomized trial, 1,062,317 random wind readings—comparable to the number of readings in the MLRF1 dataset—were generated and analyzed (Table 2). In the case of the randomized trial, each bearing and speed are evenly distributed about the points of the compass (Figure 16). The same analysis of the MLRF1 dataset indicates the annual average wind directions and speeds are weighted toward the prevailing easterly source of the Florida Keys winds (Figure 17). Figure 18 shows the ambient conditions for 13 July at the MLRF1 buoy, and Figure 19 displays wind readings from the accounts of survivors of the 1733 hurricane, as logged immediately prior to the storm (13-14 July 1733). The Spanish logbooks available for the 1733 fleet make no mention of wind speed, only direction, so for the below illustration, speed readings of 5 meters per second, comparable to wind forces recorded by 18th-century ships in the North and Mid-Atlantic (Kelly and Ó Gráda 2014), are imputed.

Although the historical documentation of local conditions provides critical context for this research, the ships' logs and other accounts cannot be considered a complete dataset for a drift simulation. The data provided in these records do offer a baseline for comparing prevailing conditions to those exhibited prior to, during, and after the storm, and assist in recreating the course of the fleet throughout the events that led to its destruction. Still, the historical record offers only limited access to the state of the sunken vessels after the wrecking events, both in immediate terms (days and weeks) and over the longer term (decades and centuries).

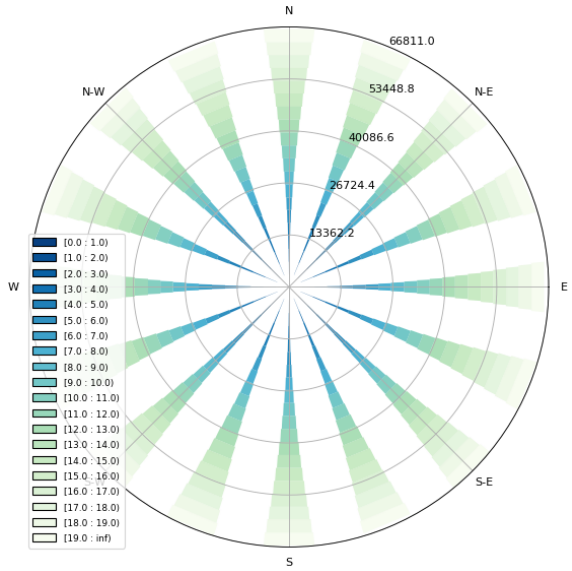

Figure 17: Randomly Distributed Wind Readings

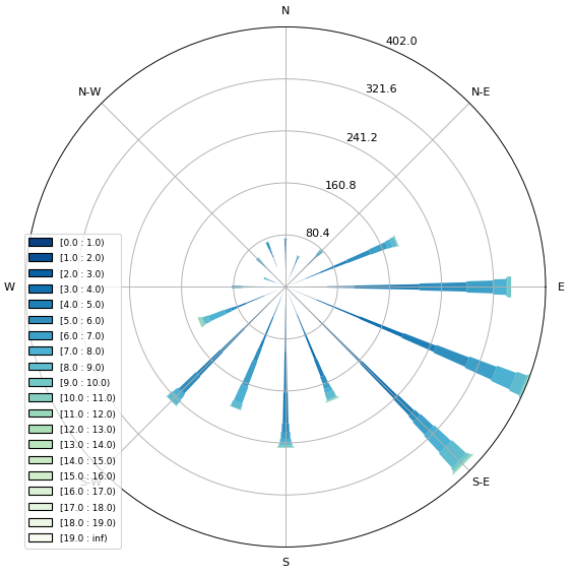

Figure 16: Ambient Wind at MLRF1 Buoy

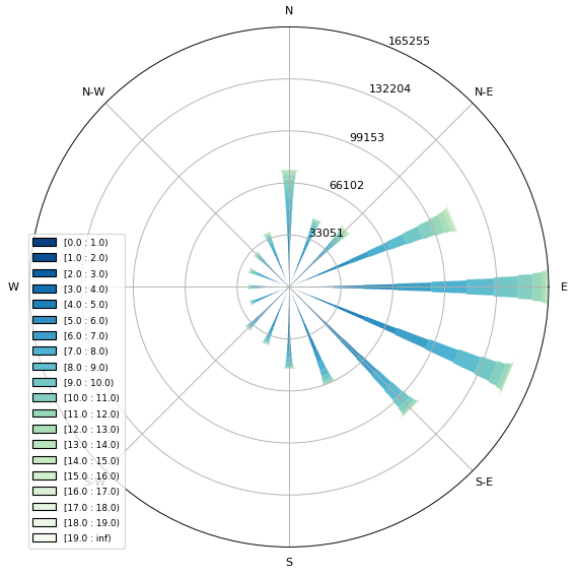

Figure 19: Mean Wind Readings for 13 July at MLRF1 Buoy

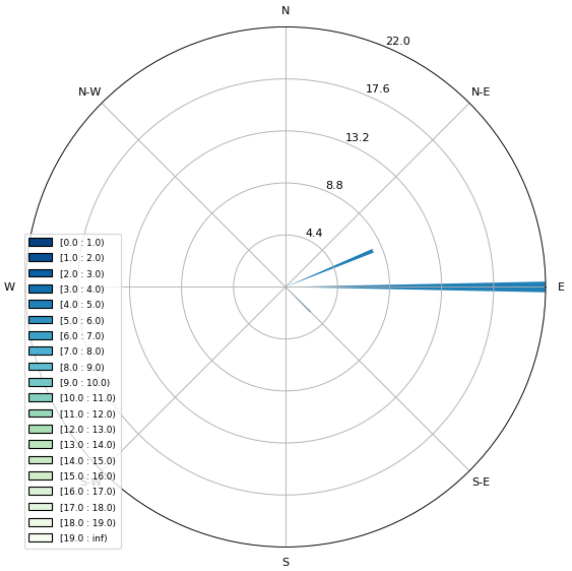

Figure 18: Plot of 1733 Fleet Wind Reports (Benson 2002:appendix 1; Cox 2019).

An example slice of the data, contained in Table 2 serves to further demonstrate the ambient wind conditions in the Florida keys. Some 75% of the annualized wind bearing readings at the MLRF1 buoy over a 23-year timespan were between 0° and 192°, confirmation of the easterly bias of the wind. Some 50% of the time, these readings were below 118°, and 25% of the time these readings are below 81°. This indicates that nearly one-quarter of the dataset is in 10% of the compass range between 81° and 118°. Similarly, it can be observed that 25% of the wind speed data is in the narrow 2.2 m/s band between 5.8 m/s and 8 m/s. As a result, an algorithm that weights directional and speed readings according to their frequencies is used to generate the forcing data necessary for the simulator.

Table 2: Ambient wind direction and speed at NOAA's Molasses Reef Buoy (NDBC 1971).

MLRF1 Buoy, 1992-2014	Wind direction	Wind speed
Count	1,061,883	1,062,317
Mean	143°	6 m/s
Minimum Reading	1°	0 m/s
25%	81°	3.8 m/s
50%	118°	5.8 m/s
75%	192°	8 m/s
Maximum Reading	360°	99 m/s

Ultimately, it is impossible to know the precise wind conditions during the 1733 salvage efforts, based on the limited historic records. However, this method offers a highest-likelihood approach with reasonable accuracy to determine forcing data for the simulation. The resulting data set represents the best-known wind forcing inputs for the simulation, and in future research can enable other statistical paths for analysis.

4.6: Module One, Debris Generator

The simulation is divided into four modules (Figure 20), intended to run in series. The purpose of separating the modules is to allow users to customize parameters and input their own data for computation and visualization. This section will describe each module and provide examples of customizable portions of the source code.

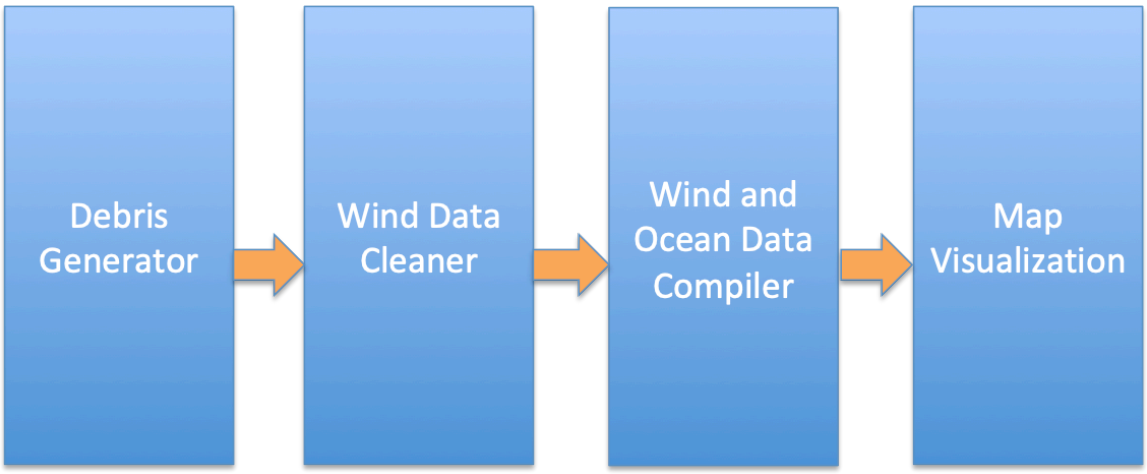

Figure 20: Simulation workflow comprising four modules

Debris_Generator.py (Appendix D) enables the user to create a variety of virtual debris objects for drift simulation. The script contains the Python class, "DebrisGenerator," with a customizable line (Table 3) where a user can define the number of drift objects to be created. The user can simply change the following line to produce the desired number of drift objects (default is '1'):

Table 3: Customizable line for creating user-defined number of drift objects in Module 1

```
84. debris = dg.generate(1)
```

The user can also make adjustments to codify the wood type, density, and object dimensions (Table 4). By default, the source code is set up to produce pine objects of randomly generated densities. A dictionary object, 'wood_types' is created that includes the most-common types of wood used in the construction of seventeenth- and eighteenth-century vessels.

Table 4: User may define wood type for simulation, relying upon this dictionary of wood types. Wood type is named, while the density in kg per cubic meter follows. In cases where the wood density varies for the type, a random density is selected within the range for that type.

```
18. wood_types = {'chestnut': 560,
19.             'elm': random.randint(550, 820),
20.             'pine': random.randint(350, 670),
21.             'oak': random.randint(740, 770)
22.             }
```

The digits that follow the wood type represent the density ranges of each variety. Pine, for example, ranges in density between 350 kg per cu meter and 670 kg per cu meter. By default, module one selects pine as the wood type for an object, returning a random density. Users who wish to test precise object densities can alter the 'wood_types' dictionary by removing the values following each key and assigning the desired density directly, for example, deleting 'random.randint(n,n)' and inputting the desired value, as in the case of 'chestnut'.

The debris generator relies on physical data about wood types used in the construction of Spanish colonial vessels. According to Rich et al. (2018:10), "The massive 30m-long ships built during the Age of Discovery were constructed of thousands of trees. Oak was still the primary ship timber, but pine, chestnut, elm, and others were used as well". Through experiment, scientists and engineers have calculated the physical factors of the wooden materials utilized in Early Modern ship construction, enabling

computational research into their behaviors in a variety of contexts. As a result, the study of physical and chemical site formation processes is approaching a stage where scholars can simulate a variety of factors affecting sites that go far beyond the scope of this thesis, but that are relevant to the archaeological investigation of shipwrecks. Site formation process studies can now rely upon this body of empirical, quantifiable data, to perform experiments that enable them to derive root physical causes for observed deposition. Furthermore, with the physical causes of a scatter pattern accounted for, cultural interpretations can be made within a framework, like that of Gibbs (2006), which ultimately seeks to explain more difficult to quantify cultural transformations of a site.

By ascribing quantities to the virtual objects, the debris generator defines them numerically so that their behavior can be virtually simulated. First, the module assigns dimensions to the drift object, followed by a wood type and density. From these qualities, other information about the drift object are derived, including its height above and below the waterline, mass, and immersion ratio. The wood type is chosen at random from Rich's (2018) list of known wood types used on Spanish Colonial vessels, with information about the wood types' densities taken from The Engineering Toolbox, an online repository of material science data (Table 5). The numerical information about the objects are then stored in a dictionary format in a text file, that can be read by the simulator module. The output of a single entry from Module One is shown in Table 6: a Pandas data frame storing the drift object, or objects, with associated parameters. By default, the source code creates objects of random dimensions totaling less than 1 cu meter. The code then calculates the object's volume, mass, reference areas above and below the water, the immersion ration, and density. Table 7 illustrates the output.

Table 5: Wood Types and Densities in kg/meter (Engineering Toolbox 2019)

Chestnut, sweet	560
Elm, American	570
Elm, English	550-600
Elm, Dutch	560
Elm, Wych	690
Elm, Rock	820
Pine, Pitch	670
Pine, Corsican	510
Pine, Radiata	480
Pine, Scots	510
Pine, white	350-500
Pine, yellow	420
Oak, American Red	740
Oak, American White	770
Oak, English Brown	740

Table 6: Example drift object

Start Time	Sun Jan 6 14:00:31 2019
Wood Type/Density	chestnut, 0.56
Dimensions	1.68, 2.46, 0.98
Volume	4.05014
Mass	2.268
Reference Areas	1.092, 0.9, 0.746, 1.318
Immersion Ratio	0.548179
Object Density	0.56

Table 7: Example output from Module One, structured as a data frame

.	1	
.	Start Time	Sun Jun 2 11:29:44 2019
.	Wood Type/Density	(pine, 476)
.	Dimensions	[1.74, 2.47, 0.43]
.	Volume	1.84805
.	Mass	879.674
.	Reference Areas	[0.574, 0.344, 0.404, 0.488]
.	Immersion Ratio	0.374944
.	Obj_Density	476

After the data frame has been generated, the user can assign it to a variable to be utilized in Module 3, in combination with the wind data that is prepared in Module 2, the wind data cleaning module.

4.7: Module Two, Wind Data Cleaning

The wind data cleaning module (Appendix E) processes data in a TXT file format from NOAA's National Data Buoy Center. The user need only include the script in a directory alongside the NDBC data they wish to process, stored in a subfolder entitled 'WindData'. The code is agnostic to any number of data files from the NDBC but must be acquired from the same buoy in order that the resulting calculations be correct. The raw forcing data is loaded into a Pandas data frame, cleaned, and then the calculations can be extracted for the user-defined month of the year. The user can define the month at the given line (Table 8).

Table 8: Line for user to define month for which data will be utilized in the simulation

138.	month = 8

Given the uncertain comparative value of data extracted some 300 years after the shipwrecking event, a calculation of central tendency—the circular mean—needs to be applied to the wind data. Stuart Grange (2014:1) describes the problem posed by data representing 360 degrees of freedom:

> …wind direction is usually reported as an angle in degrees, 0–360 (or –359) where 0 or 360 represents a wind blowing from a northerly direction. If the wind direction is blowing from the north and traverses the discontinuity at the beginning/end of the circular scale, and then the arithmetic mean is calculated, this will result in the average wind direction to be somewhere in the southern quadrant. This is clearly incorrect. To correctly deal with this scale discontinuity, trigonometric functions must be used to handle the angles.

In simpler terms, the average of two wind directions of bearing 1° and 360°—both northerly wind directions—is 180.5°, which is the bearing for a southerly wind. To correct for this inaccuracy, the Python Numpy library is called to apply the circular mean function to the bearing data, incorporating the component trigonometric functions Grange discusses above. This produces the correct average for the wind readings of 1° and 360°: 0.5°. This method of calculation is broadcast over the entire data frame for each 10-minute time step.

The data are time-delineated in 10-minute increments, reflecting the base structure of the NDBC's data (Table 9). Module Two slices and compiles these data into three-day data frames that are stored together in a dictionary object. The following example indicates the format and structure of simulation data that results from cleaning and calculating the circular mean for the first three hours of twenty-plus years of the NDBC's 1 October wind readings. The columns indicate the data index, day, hour, and

minute of the wind directions (WDIR) and wind speeds (WSPD) that are stored in a variable to be passed into the simulation.

Table 9: Example of data frame resulting from Module Two

	day	hour	minutes	WDIR	WSPD
0	1	0	0	75.571640	4.433333
1	1	0	10	59.767382	4.295238
2	1	0	20	71.499721	4.247619
3	1	0	30	64.803959	4.166667
4	1	0	40	88.381074	4.404762
5	1	0	50	107.265309	4.533333
6	1	1	0	90.748453	4.500000
7	1	1	10	82.792742	4.333333
8	1	1	20	83.300521	4.204762
9	1	1	30	92.877319	4.076190
10	1	1	40	92.723972	4.304762
11	1	1	50	91.046489	4.314286
12	1	2	0	95.011028	4.371429
13	1	2	10	91.600719	4.505000
14	1	2	20	91.181941	4.550000
15	1	2	30	83.032506	4.395000
16	1	2	40	91.519753	4.465000
17	1	2	50	102.035616	4.525000

With the dictionary of data frames defined to a variable, the user can invoke the third module. Module Three compiles the NDBC wind data with ocean current settings, calculating the leeward drift of the object, based on its parameters, and compiling this data into numerical formats that represent the distance and trajectory the object drifts for each 10-minute step. This data can then be passed to Module Four to simulate the object's drift path and map it visually.

4.8: Module Three, Leeway Field Calculator

The ocean drift simulator incorporates the leeway field method developed by Breivik et al. (2011), which derives the leeway direction and speed of an object from its

immersion ratio. Breivik et al. (2007, 2009, 2012a, and 2012b), utilized field experiments with a variety of drifting objects, upon which to base the development of robust search and rescue models. Their experiment examined the influence of downwind and crosswind components of leeway drift, as well as the probability that an object would jibe (change direction) in the water, due to the force of the wind shifting relative to the object, such that it strikes a new reference area. According the Breivik et al. (2011:1), "In general, an object's motion through the ambient water masses (referred to as its slip, windage, or leeway) is roughly inversely proportional to its immersion ratio".

In this third module (Appendix F), simple rectangular prisms are utilized as drift objects, like miniaturized shipping containers, with the immersion ratios derived from the division of the area of the object above the waterline by the sum of the object's total area. The probability of the object jibing is estimated at roughly 10% per hour—5% to the left and the right of the wind direction (Breivik et al. 2009)—while the divergence angle upon jibing is set as a constant 30 degrees of the wind direction, the maximum possible (Figure 21). The result is a partially stochastic model, that while simplistic and purely two dimensional, is consistent with the basic principles of search and rescue operations for objects adrift at sea.

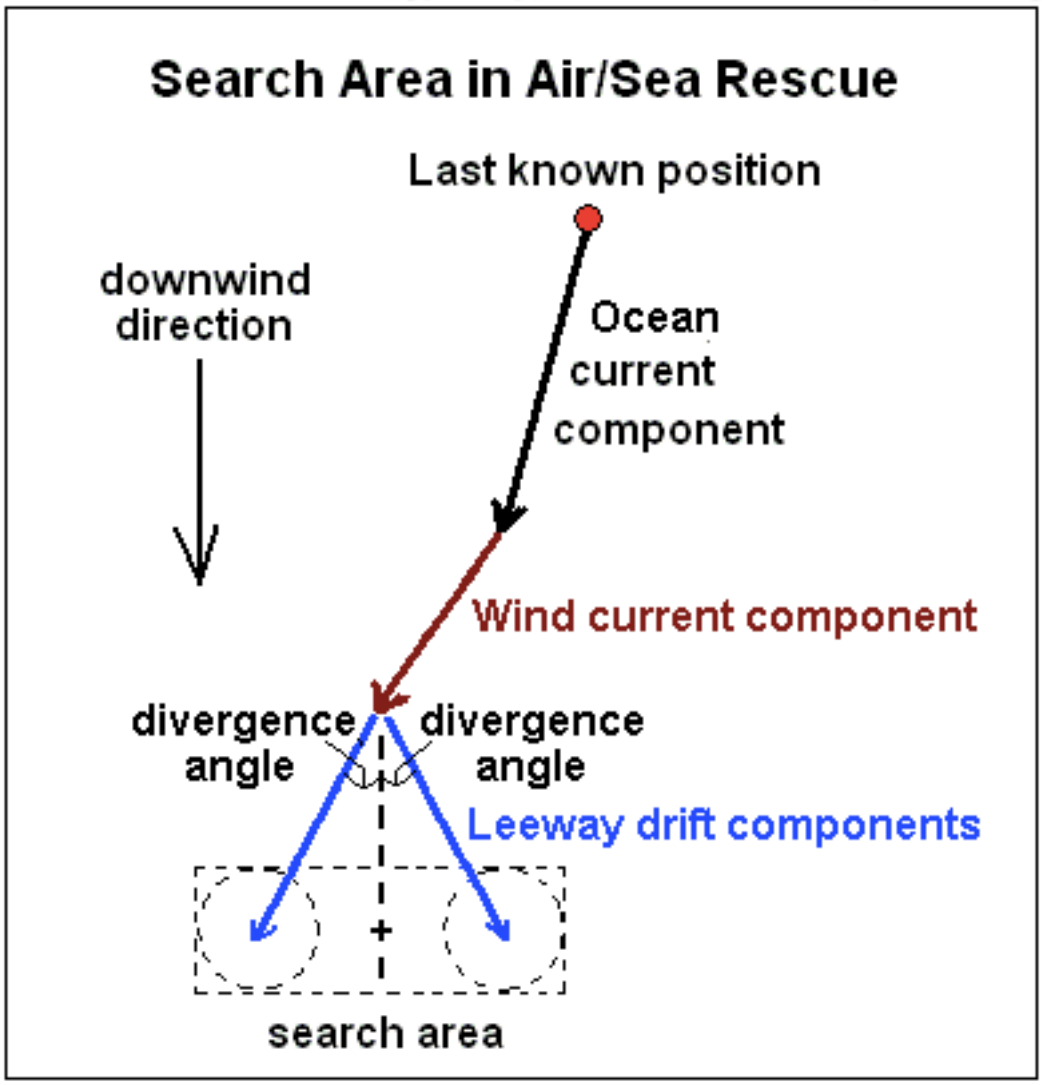

Figure 21: Process for determining the maximum search area for objects adrift at sea (Halpern 2012)

The leeway field calculator comprises a Python Class object that takes two parameters, the debris object and the wind conditions. With this data, the module calculates the leeward drift of the object, relative to the wind direction, supplies an ocean current direction and then sums these vectors before translating them into a final drift direction. Ocean current speeds and directions vary considerably in the Florida Keys, with variations resulting from tidal movement, depth of measurement, and temperature

(Lee and Williams 1999:1). For a more accurate model, archaeologists could rely upon the growing body of numerical data describing near-shore eddies and tidal activity near these or other shipwrecks, beyond the scope of this thesis.

For the purposes of this study, the annual mean current direction and speed were taken from scientific data gathered for the region. Lee and Williams (1991:36) observed the "strong downstream flow (eastward and northward) of the Florida Current tends to follow the continental slope and forms the offshore, open boundary of the coastal zone". Their data from the moored current station at Tennessee Reef indicates the mean current behavior at 7 meters of depth has a flow direction of 50.5° and variable flow speed between 6 cm/s and 8 cm/s (Lee and Williams 1991:43). These inputs were coded into the simulation's 'ocean_current' function (Table 10).

Table 10: Code defining ocean current direction and speed in Module Three, according to Lee and Williams 1991 (43)

```
35.  def ocean_current(self, lengh_of_wind_df):
36.      ocean_bearing = 50.5
37.      ocean_flow_rate = np.random.randint(6,8,size=(lengh_of_wind_df, 1))

38.      return ocean_bearing, (ocean_flow_rate / 100)
```

Module Three compiles the NDBC wind data with ocean current settings, calculating the leeward drift of the object, based on its parameters, and compiling this data into numerical formats that represent the distance and trajectory the object drifts for each 10-minute step. This data is stored in a dictionary object that is then passed to Module Four to simulate the object's drift path and map it visually.

The velocity and directional measurements for wind data are stored as a bearing and a speed, measured around 360° in meters per second. The ocean current data is set as

a range-bound constant of 39° to 50°, consistent with observations by Shay et al. (1998) and Georges et al. (1998), for the current near Florida Keys. For the simulator to function, it is necessary to reconcile these measures into the same format. The easterly wind common in the Florida Keys is typically described as having a bearing of roughly 90°, and the mean wind speed detected by the Molasses Reef buoy is 6 meters per second. In order that the wind and current vectors could be quickly summed, all measurements were converted into zonal and meridional vectors prior to vector summation in Module 3, with the resulting summed vectors being then converted back into bearing and velocity readings for the simulation of the dispersion cloud, which is visualized in the fourth and final module.

4.9: Module Four, Map Visualization

The fourth and final module (Appendix G) of the simulation calculates the locations of drift objects at each 10-minute interval in their course and plots these locations in a variety of map formats. The output from the third module is a dictionary object containing bearing and speed data for the drift object. In the fourth module, this dictionary is passed to the "distance_traveled" function to calculate the total distance the object travels, given its velocity over the 10-minute interval. This data is then compiled into a new dictionary object that stores 3-day slices of simulation data, starting on each day of the input month. Table 11 contains an example of the first five rows of the data output.

Table 11: Data output from Module Four. Each index represents a 10-minute step through the simulator, indicating the virtual drift object's bearing and speed, the distance covered during the step, and the final latitude and longitude for that step—representing the starting point for the next step in succession.

	Bearing	Speed	Float Distance	Latitude	Longitude
0	268.805482	0.111062	66.637470	24.924838	-80.515511
1	245.387987	0.098657	59.194041	24.924616	-80.515608
2	267.024496	0.093723	56.233811	24.924590	-80.515709
3	256.323467	0.086602	51.961384	24.924479	-80.515800
4	290.422450	0.114534	68.720158	24.924695	-80.515916

The "Bearing" column indicates the direction of an object's drift in a 10-minute period, while "Speed" indicates the velocity of the object in meters per second. "Float Distance" is the multiplication of "Speed" by 600 seconds in each 10-minute interval, and "Latitude" and "Longitude" are the ending coordinates of the object after traversing the distance along the bearing of the previous step. With the data in this numerical form, it is then possible to visualize in a variety of map formats.

The Python Matplotlib library is used to create the output maps. Matplotlib offers both variety and flexibility in its mapping displays that are useful for a project of this kind, but Python has several other mapping libraries that also provide these functionalities. For the purposes of this project, two specific types of map are utilized: a physical map (Figures 22 and 23) displaying the basic geography of the study region overlaid with plots of shipwreck scatter, and a density map (Figures 24 and 25) for visualizing the highest-likelihood areas where shipwreck components overlap at the same locations. With the ability to visualize climatic conditions and model material drift, it becomes possible to investigate discreet details of the site-formation process. For example, it is possible to compare simulated drift output with the scatter pattern of the

Capitana shipwreck site, as documented by Benson's team. It is additionally possible to model specific material behaviors and examine correspondence with actual scatter. Finally, the drift trajectory can be examined and compared to the conditions under which salvors and treasure hunters are presumed to be operating.

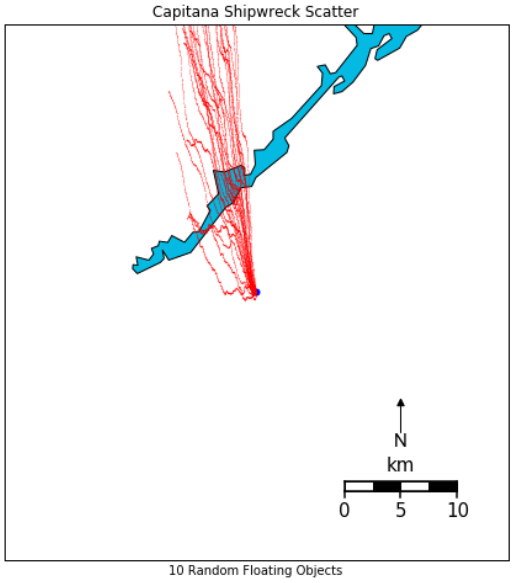

Figure 22: Shipwreck drift of 1m X 1m pine object from Capitana site. Scale: 40.3 km on east-west axis and 44.4 km north-south

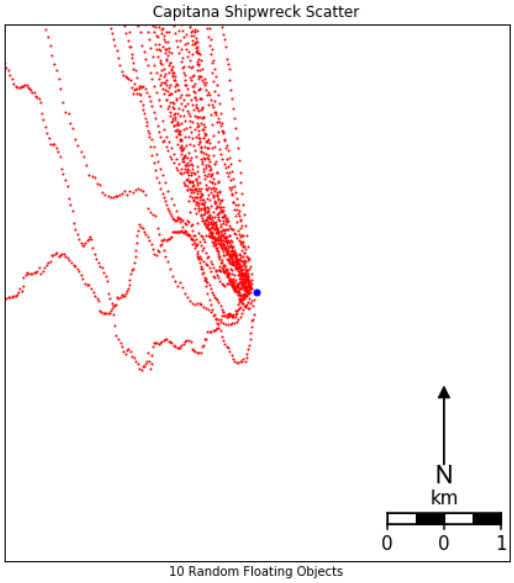

Figure 23: Close up view of figure 22. Scale: 40.3 km on east-west axis and 44.4 km north-south

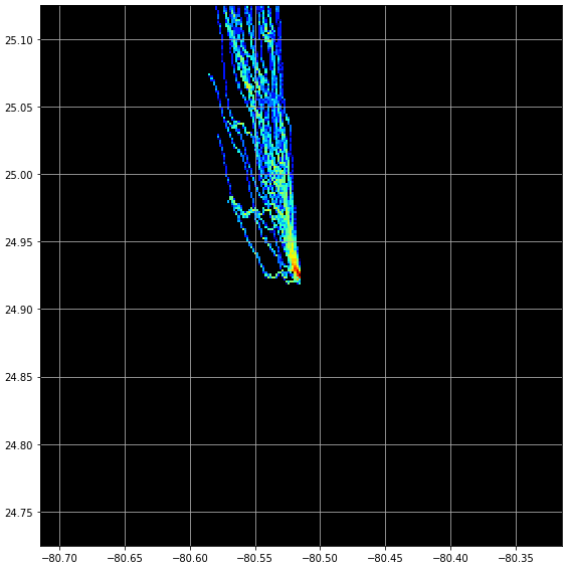

Figure 24: Density plot of Figure 22. Scale: 40.3 km on east-west axis and 44.4 km north-south

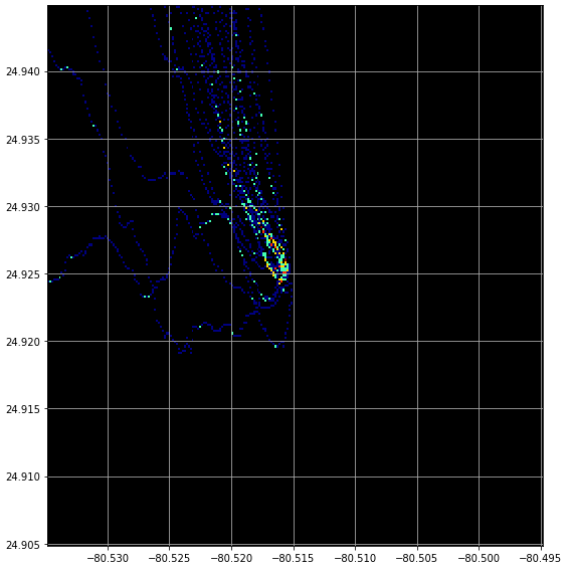

Figure 25: Density plot of Figure 23. Scale: 40.3 km on east-west axis and 44.4 km north-south

4.10: Limitations

Several important limitations should be kept in mind when considering the results of this simulation. The simulator is purpose-built for the Florida Keys, relying on current and wind data that can be imputed by the user to represent other regions. This flexibility in the code is not a guarantee of accuracy for other regions and researchers should take care to pair numerical observations with ground truths from the area being studied. In the case of this thesis, daily observations by the author of the prevailing easterly wind at the site of the *Pillar Dollar* Shipwreck, near Biscayne Bay, were instrumental in establishing the premise that meteorological data could help explain drift patterns for archaeological material. Such observations may not be readily available for other project areas. Additionally, as climate change alters atmospheric and oceanic behavior, the method of simulation described here will likely need to be updated to remove emerging patterns in prevailing conditions.

Weather data is not the only limiting factor in this study. Archaeological data collected from the 1733 shipwreck sites demonstrates impacts from salvors, who used invasive techniques to access the sites. The use of blowers and, in some cases, explosives, has scrambled the archaeological context. Furthermore, even when provenience has undergone a scrambling process, the extent to which archaeologists have recorded these sites is far smaller than the probable area across which material has scattered (Figure 22). As a result, study areas proposed in this thesis are much larger than those undertaken by past archaeologists, though the case of the *Fougueux* clearly demonstrates that the extent of shipwreck scatter can be far greater than ballast piles and trails may lead archaeologists to conclude. Future work at these sites can rely upon the site maps of

Benson (2002) and McKinnon (2006) as a useful baseline for designing surveys that reconsider the fullest possible extent of scattering at the sites, which can be measured on a scale of kilometers, as the simulation's output indicates, rather than tens or hundreds of meters around the shipwreck sites that has been surveyed.

4.10: Applications

Taken together, the four modules enable a researcher to simulate a variety of materials and conditions, with output indicating the probable two-dimensional drift of objects. The central hypothesis in this study is that shipwreck components will behave in a manner consistent with the environmental conditions and that modeling these conditions enables archaeologists to make plausible statements about depositional patterns. The climatic conditions in the Florida Keys are demonstrably non-random, offering researchers the opportunity to explore interpretive hypotheses with direct reference to the physical environment. Were conditions at the sites random, the drift trajectories of simulated objects would behave in random ways. However, even with variable wind conditions, the ambient trend at the sites of the 1733 shipwrecks is an easterly wind. When the wind vector is summed with the ocean vector and the drag forces acting upon a simple test object are calculated, the resulting output indicates a clear trend. Introducing randomly generated debris objects to the simulation is expected to broaden the range of potential drift trajectories, but not to the extent that the drift can be described as random. This relative predictability of varied objects can provide insight into the events—and even human contributions—to a shipwreck's scatter patterns, as will be discussed in Chapter Six: Results.

Chapter 5: Archaeology

5.1: A Treasure Fleet

The story of the 1733 shipwreck event and the recovery of precious metal remains sparked a culture of treasure salving in the Florida Keys that lives on to this day. The Spanish salvaged millions in gold, silver, and other cargo from the wrecks in the 18th century, and treasure-hunting divers pillaged much of the sites two centuries later. The result is an archeological record that is as scattered at the shipwreck level by human intervention and environmental conditions, which are also active at the regional level. Material culture from the sites has been subject to extensive human intervention and much of the known provenience of ship components and artifacts is thought to no longer be in situ (Benson 2002:18-19). The salvors themselves offer some of the scant accounts of shipwreck articulation and provide insight into possible changes that took place on the sites over the 20th century. For the purposes of this site-formation study, the key details offered by shipwreck salvors and archaeologists alike pertain to the position of materials across the seabed (Smith and Dunbar 1977; Benson 2002; McKinnon 2006).

In the context of *La Capitana El Rubi,* it appears scattered shipwreck components moved in a manner consistent with drift in the prevailing conditions. Wind-driven ocean surface currents moved material along a predominantly east-west trajectory. One possible explanation for this is that the material was scattered as a direct result of salvage activity, which likely took place in the ambient weather conditions, rather than during storm events. This is true for both the Spanish salvors and their modern counterparts. The prevailing easterly would have necessitated captains to decide where and how to anchor near the sites, with eyewitness accounts suggesting vessels moored as much as a mile

away (*New England Weekly Journal* 1733). The prevailing easterly and current would have pushed material hitting the water to the west of the sites, and indeed, that is the case with remains from *La Capitana* (Figure 26a and 26b). The vessels that contained the king's treasure—the core of the 1733 flotilla—are the focus of this discussion.

5.2: Grounded

Captain Don Nicolas de Arechavaleta made the first official report of the shipwrecks to Spanish colonial authorities in Havana. His crew had sighted 12 ships at the 'La Cabeza de los Martires', the southern edge of the Florida Keys. Shortly after filing this report, a rescue mission that had already begun preparations was launched, outfitted with divers and salvage equipment (Benson 2003:3). Surviving crew from the flotilla and rescue personnel began salvaging the site in just a week following the hurricane (Benson 2002: Appendix 1).

Spanish colonial administrators were primarily interested in recovering survivors and non-perishable material from the vessels, if not the vessels themselves. Chief among their concerns were the treasures being carried by the king's ships. Three ships of the crown—*Capitana El Rubi Segundo, Almiranta el Gallo Indiano,* and *Refuerza Nuestra Señora de Balvaneda*, called *El Infante*—carried between them 8,163,000 pesos (Benson 2002: Appendix 1). For colonial authorities, these ships were the focus of the initial salvage efforts, since they contained the most valuable cargo (both financially and politically). In the 20th century, the vessels were an attraction for modern treasure hunters and, eventually, archaeologists.

The important elements that make the Florida Keys a popular tourist destination—warm weather, clear waters, and predictable winds and currents—also made it a favorable location to conduct salvage operations. Approximately 70% of the benthic environment in the Florida Keys can be characterized by four types of materials: sea grasses on lime mud (27.5%); sea grasses on carbonate sand (18.7%); bare carbonate sand (17.3%); and bare lime mud or seagrass-covered muddy carbonate sand (9.6%) (Lidz et al. 2005). In the immediate aftermath of the hurricane, the ships sat in less than 10 meters of water, and historic and archaeological accounts suggest the environmental conditions at the sites have remained largely unchanged in the nearly three centuries since they wrecked (NDBC 1971; Benson 2002).

Archaeologists have focused on the 1733 shipwrecks since the 1970s, with Smith and Dunbar (1977) making key contributions to the study of eight merchant vessels that sank with the fleet. Logan (1977) and Skowronek (1984) concentrated their work on comparative analyses of material culture in the shipwreck corpus and terrestrial Spanish Colonial finds, while Benson (2002) organized an extensive in-situ investigation of *El Rubi*. Through the work of the Florida Bureau of Archaeological Reasearch (Scott-Ireton and Mattick 2006c) and McKinnon (2006), the sites were mapped for the creation of a shipwreck trail. More recently, Price (2015) examined the impact of treasure hunting activities on the site formation process at the *Pillar Dollar* shipwreck site; and Thomas (2017) studied culinary implements from the 1733 shipwrecks as part of her examination of shipwrecks from a 1715 hurricane in the same area. The material assemblage these ships carried is projected to the present day in the consistent and ongoing interest shown by archaeologists and the general public.

5.3: *La Capitana El Rubi*

The modern discovery of the flotilla's flagship *El Rubi*, in 1938, marks the beginning of a treasure salvage culture in the Florida Keys. Reggie Roberts, a commercial fisherman, reported seeing several sites to Arthur McKee, Homestead City Manager (Benson 2002:4). The pair reported a site in 18 to 20 feet of water, 3.5 miles from Tavernier Key (Scott-Ireton and Mattick 2006c). During a decade of work on the site, McKee recovered 20 cannons and over 1000 gold coins stamped with the date 1721, as well as small arms, jewelry, navigational instruments, and other ships' implements (Benson 2002:28). The interest inspired by the site contributed to the treasure hunting culture of eastern Florida that pervades to this day (Austin 2018). The state of Florida even enshrined historic salvage into law, following the 1966 passage of the National Historic Preservation Act. The 2012 Florida Statutes (Title VIII.267.031.5.n) still contains the authorization for the Division of Historic Resources to "issue permits for exploration and salvage of historic shipwreck sites by commercial salvors on state-owned sovereignty submerged lands".

The interest in the shipwrecks has come at a cost to the data and context they can provide. Price (2015:19) noted that salvage activity on sites in Florida greatly contributed to the destruction of important archaeological data. However, even before modern salvors reached the sites, the Spanish had worked to recover material in the 18th century. The Spanish report recovering thousands of chests of precious metals from the shipwrecks. Colonial records indicate that silver was the primary metal recovered, of which "one thousand nine hundred twenty-three boxes came from *Capitana*" (Benson 2002:

Appendix 1). Additionally, 48 boxes of fabricated silver and 550 slabs of copper were salvaged—42 shy of the total listed on the manifest (Benson 2002: Appendix 1).

At the original site, as found by Roberts and McKee (Benson 2002:4), the ballast pile was a discrete unit, concreted together an immovable. The ballast mound was measured as 125-feet long and 60-feet wide and piled some six feet from the bottom. This is an important detail and among the key changes at the site. Marx (1987:96) provides a comparative table of keel length and carrying capacity. By reconstructing a hypothetical ship within the constraints of the 125-by-60-foot ballast pile, a conservative estimate would place the keel length at about 100 feet, with a width on beam of around 40 feet. This would indicate *La Capitana El Rubi* was a galleon with over 1000 tons of carrying capacity—nearly double the 500-ton ship that would be expected for the period (Figure 9).

The Spanish recovery effort was sufficiently short of comprehensive that treasure salvors and tourists made finds on the site for decades in the mid-20th century (Scott-Ireton and Mattick 2006c:7). In the 1990s, a public-private partnership, comprising the Caribbean Shipwreck Research Institute, the National Center for Shipwreck Research, and the State of Florida, worked the site of *El Rubi* in order to test a model of for-profit archaeological science (Benson 2002:iv). In scouting for their recovery efforts, Benson's team found the site had scattered across a wide area, contrary to previous reports from the 1980s of a discrete ballast and timber assemblage beneath a moderate covering of sand. By the 1990s, the ballast and disarticulated timbers were scrambled beneath approximately 2.5 meters of sand (Benson 2002:11). With the use of prop blowers and baseline offset measurements, the team excavated 256,000 square meters and recovered

1600 artifacts (Scott-Ireton et al. 2006c:7). Ceramics comprised most of the recovered remains (Benson 2002:26). Benson's team tagged some 868 sherds, predominantly coarse earthenware of varied olive jar types consistent with transport amphora. These finds indicate that, in addition to the boxes for precious metals, there were meaningful quantities of dry- and wet-good storage vessels on board *El Rubi*.

Benson (2002: Table 1) characterizes the artifacts as secondary deposits, material scattered by the hydrological conditions and human intervention, which he says offer very limited contextual data, but do yield useful relative special relationships. The ceramic sherds comprise 187 olive jar pieces, other coarse earthenware, Guadalajara wares, and pieces of Chinese porcelain. Additionally, five sherds of hand-modeled Aboriginal wares were recovered (Benson 2002:30). The variety speaks both to the extent of the Spanish Caribbean trading empire and its diversity during the period. Benson's team also found bricks of red and gray/yellow varieties, glassware ranging from medicine vial components to onion bottles and case gin, and bones from a variety of creatures. Among the osteological finds are remains of a cougar, pig, chicken, cow, fish, shark, and turtle (Benson 2002:36).

When Benson's team arrived on site in1993, it was dramatically changed from earlier accounts. Smith et al. (1990) note that the large ballast pile was largely buried, but it is possible that prior to this analysis, or shortly after, the site was catastrophically disturbed. Scott-Ireton and Mattick (2006c) note in the NRHP report on *El Rubi* a variety of invasive techniques used by modern salvors to access materials at the site. They list such 'methods' as dynamite, in addition to the less destructive water jets and airlifts, which were used to remove sand and ballast to reach the bottom the wreck site. Benson

(2002:1) indicates he had some expectation, based on reports from other divers, that it would be more intact.

However, after mapping the site (Figure 26a & 26b), Benson (2002) notes the distribution of the shipwreck materials was consistent with dramatic human intervention. The concreted ballast stones were scattered beneath the sand, not concreted together as they had been before. The lightest-weight materials were spread furthest from the core ballast pile in a pattern consistent with the prevailing hydrological conditions. Still, Benson (2002) argues for a largely anthropogenic site-formation process, suggesting that the site was most likely disarticulated by modern salvors and singling out the destructiveness of salvage efforts in the 1980s.

> The conditions that contributed to the existence of secondary deposits were the original break-up of the vessel following their initial sinking along with 18th century salvaging by the Spanish, but modern recovery and salvage attempts are considered the major cause of the nature of the secondary deposit (Benson 2002:23).

Despite the damage to the site, it was nominated to the National Register of Historic Places in 2006 (Scott-Ireton and Mattick 2006c:15). It remains generally concealed, submerged in sand in the Florida Keys National Marine Sanctuary. Still, the National Register of Historic Places (Scott-Ireton and Mattick 2006c) nominating papers indicate that even Benson's team left an enduring mark on the site, in the form of blower depressions in the sand. The site's prominence as a destination for tourism is in notable decline, given its disarticulated and frequently covered state. Benson's maps of the site are particularly useful in the context of a drift trajectory study. Further discussion of *La Capitana* is in Chapter 6: Results.

Capitana (8MO146) | *El Rubi*

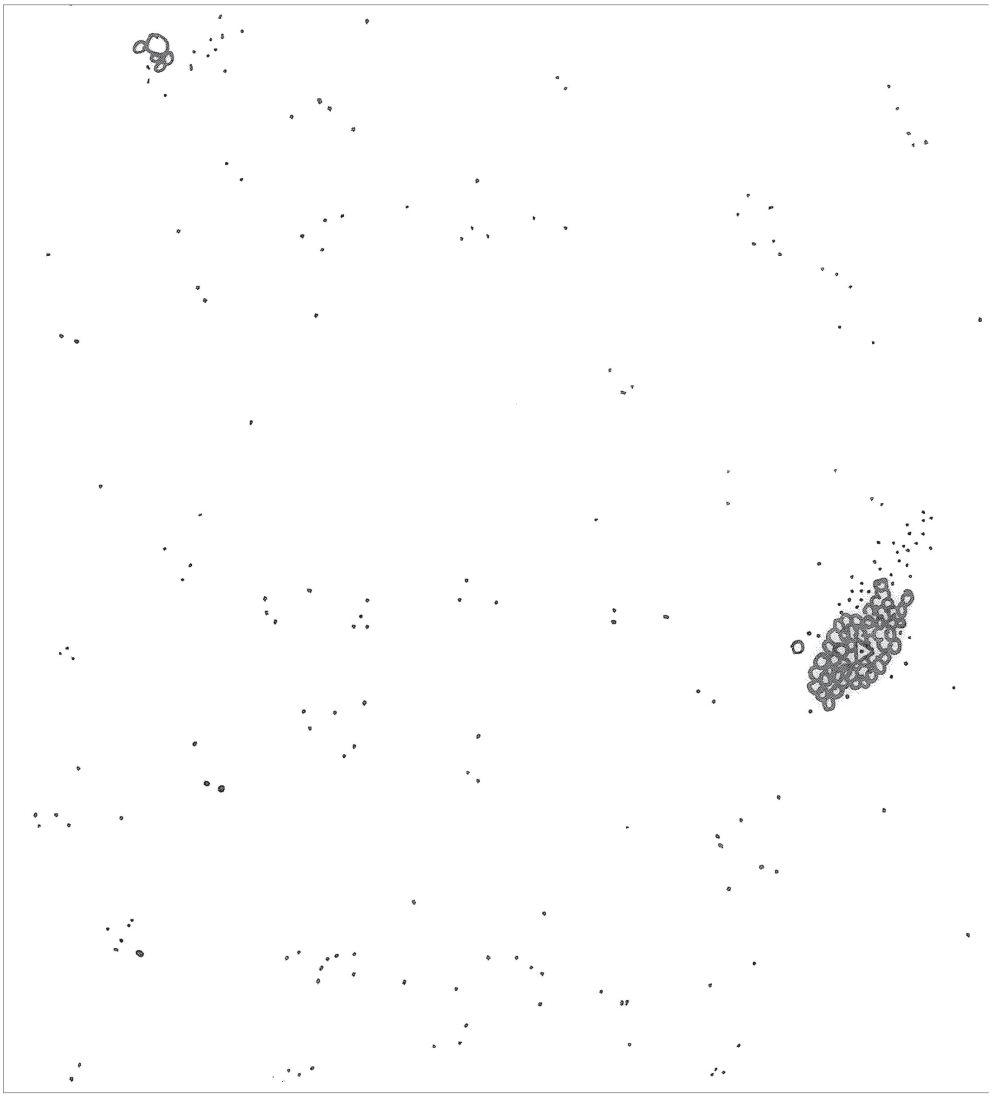

Figure 26a: Left (western) side of site map of La Capitana El Rubi (Scott-Ireton and Mattick 2006c:15).

April 15, 2005

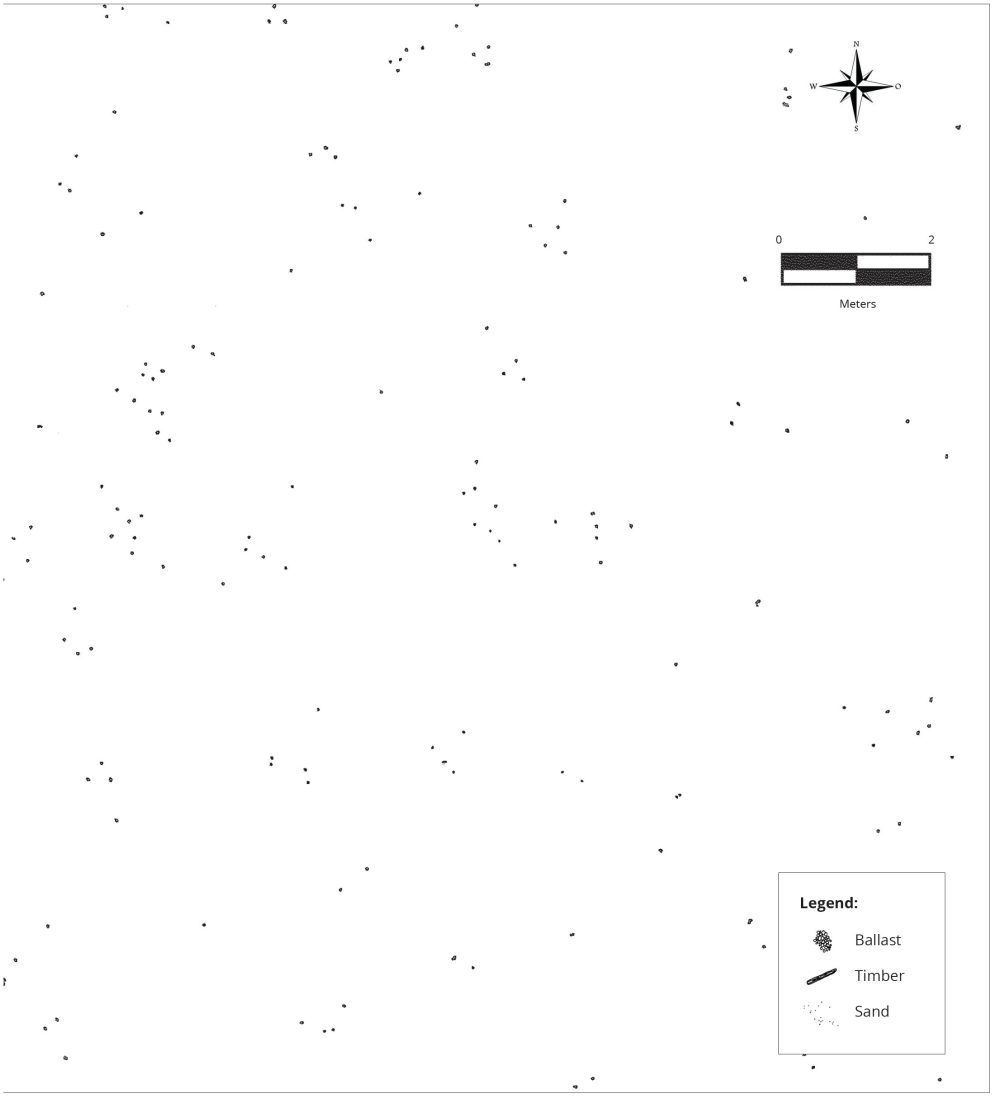

Figure 26b: Right (eastern) side of site map of *La Capitana El Rubi* (Scott-Ireton and Mattick 2006c:15; Yoonji Jung 2019).

5.4: Almiranta El Gallo Indiano

With its hold completely flooded *El Gallo Indiano*, vice-flagship of the 1733 flotilla, rode out the hurricane near the modern city of Layton, FL, bouncing with the waves in Channel #5 between Craig Key and Long Key (Benson 2002: Appendix 1). Nearly everyone on board survived, excepting a child, a soldier, and two sailors (Benson 2002:18). The ship was a considerable distance from *El Rubi* and following the passage of the storm its survivors established their own camp for concentrating their recovery and salvage operations (Benson 2002:21).

Dimensions for the 550-ton *Atocha*, built in roughly 1620, offer some insight into the advantages *el Indiano* had after it foundered in the channel. The *Atocha's* hold depth was almost 16 feet, drafting about 10 feet laden with cargo (Meide 2002:16). A similar or larger galleon in the channel could have been relatively dry on the upper decks, despite the grounding, with half its hull structure standing above the water line. The modern archaeological site of *el Indiano* is under 14 feet of water, and if similar conditions prevailed following the hurricane, the salvors would have been comparatively easier to that of other vessels. This bears out in the Spanish records of the recovered goods.

As of 15 July 1733, the ship's registered cargo included 5,654,979 pesos in silver coins, 3200 pesos in gold coins (Scott-Ireton et al. 2006a:8). In addition to the copper slabs Spanish salvors retrieved 1809 boxes of silver and 25 boxes of fabricated silver. While precious metals were the primary focus of the salvage effort, there was a wealth of other material on board the 60-gun *el Indiano* (Scott-Ireton and Mattick 2006a:8). The salvors recovered meaningful quantities of such perishable cargos as cochineal, chocolate, and indigo (Benson 2002: Appendix 1). Additionally, many of the

ship's fittings were salvaged. A sloop from the survivor camps returned to Havana with 10 cannons from the vice-flagship, "one of 18 pounds shot, and nine of 12," in addition to various other ships' hardware and equipment (Benson 2002:3). With so much of the ship accessible to colonial survivors and salvors, one can imagine that the galley, as well as the boson's, anchor, and sail lockers, were largely cleared out prior to abandoning the vessel.

The contemporary archaeological site (Figure 27) comprises a ballast mound, about which little appears to be known. The ballast mound is 42 meters by 30 meters, which along with surviving hull timbers is generally covered by sand and marine vegetation. When the sand is washed away, some 7.5 meters of the ship's keel can be exposed, and the hull elements comprising the keel, frames, keelson, ceiling and exterior planking, and fasters remain beneath the ballast. The impact of modern salvage efforts are characterized by scattered ballast stones that extend beyond the edge of the main mound. A 1977 survey by the State Bureau of Archaeology (Smith and Dunbar) also indicated the presence of concreted round shot among the debris (Scott-Ireton and Mattick 2006a:6). Among the few artifacts that have been documented are sherds of olive jars, the bases of onion bottles, and encrusted fasteners (Benson 2002; Scott-Ireton and Mattick 2006a). Given the northerly and southerly directions of the wind during the hurricane (Benson 2002: Appendix 1), it is not surprising that the ship is oriented in this direction, indicating that it may have been anchored to hold its position on the reef through the hurricane.

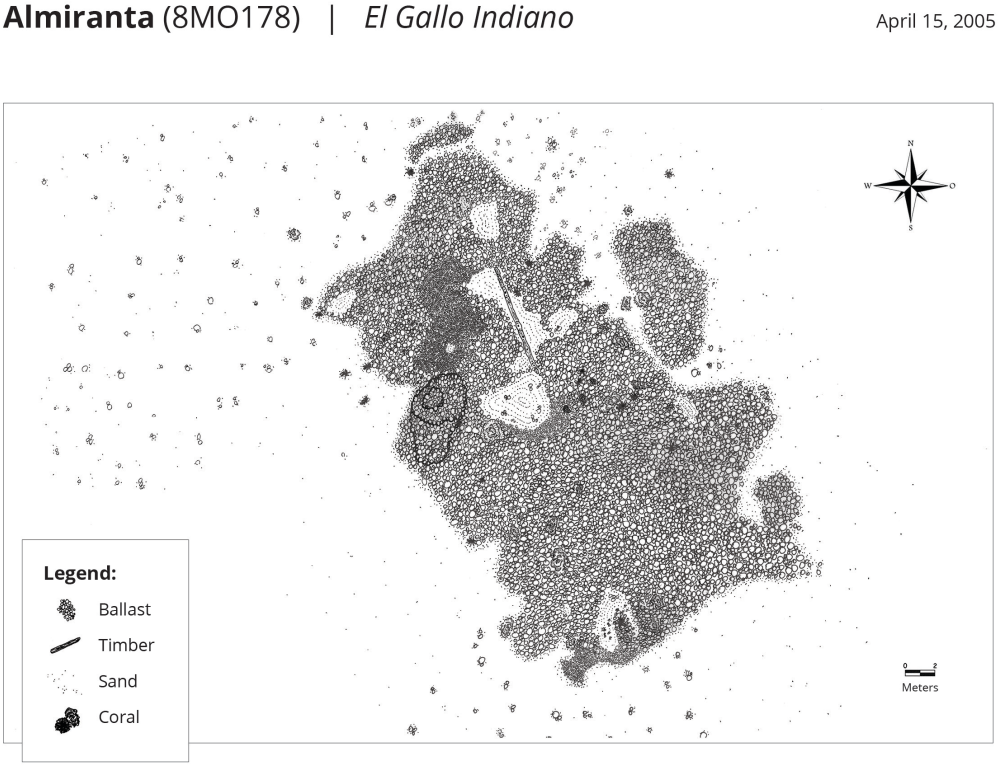

Figure 27: Site map of *Almiranta* (Scott-Ireton and Mattick 2006a:13; Yoonji Jung 2019)

5.4: Refuerzo El Infante

Reinforcing the fleet was *El Infante*, also known as *Nuestra Señora de Balvenda,* which survived the storm in similar fashion to *Almiranta*. The ship struck bottom in just 12 feet of water and rode out the hurricane without the risk of completely sinking (Smith et al. 1990:13). As the author of the ship's log (Benson 2002: Appendix 1) describes, *El Infante* had only survived by stripping the vessel of the overburden of the masts and rigging, which would have potentially rolled the vessel in the hurricane winds. The good fortune of wrecking in the shallows near Tavernier Key enabled most of the passengers and crew to survive the storm and eased their salvage efforts.

According to *El Infante's* National Register of Historic Places nomination form (Scott-Ireton and Mattick 2006b), the vessel was among the largest in the 1733 fleet—at 400 tons—and it carried some of the most precious cargo. "At Vera Cruz, *Infante* loaded brazilwood, cochineal, Guadelajara Ware, Chinese porcelain, leather hides, indigo, vanilla, and citrus, as well as 186 boxes silver coins (3000 *pesos* to the box = 558,000 *pesos*) for the King" (Scott-Ireton and Mattick 2006b:31). The same report indicates the ballast pile at the site is some 48 meters (roughly 160 feet) in diameter. However, applying the calculations of Marx (1987:96) to compare the vessel's length on keel to tonnage suggests it could be a much larger vessel, up to 1000 tons, given the extent of the ballast. In addition to the silver, the recovered materials from *El Infante* include much of the general cargo and ceramics.

Still, much was left behind for McKee and other salvors. Reports from modern salvage efforts at the site indicate recoveries of pillar dollars, porcelain, jewelry, ivory fans, and a silver helmet (Smith et al. 1990:13). The ballast has been disturbed by

treasure salving and the keelson, hull framing and futtocks, and some planking are exposed (Figure 28). According to Smith et al. (1990), the ballast and some timber remains were still intact when treasure salvage became a popular pastime in 1970s Florida. If this is the case, it would mean the modern salvage efforts are likely responsible for the destruction of the sites. Despite this, the material scattered from *La Capitana* appears to follow a distinctive pattern consistent with the prevailing conditions and simulated drift trajectory at the *el Infante* site may yield similar results. This could lead to an exoneration of the contemporary salvors, who are frequently faulted with the scrambling of the site (Benson 2002).

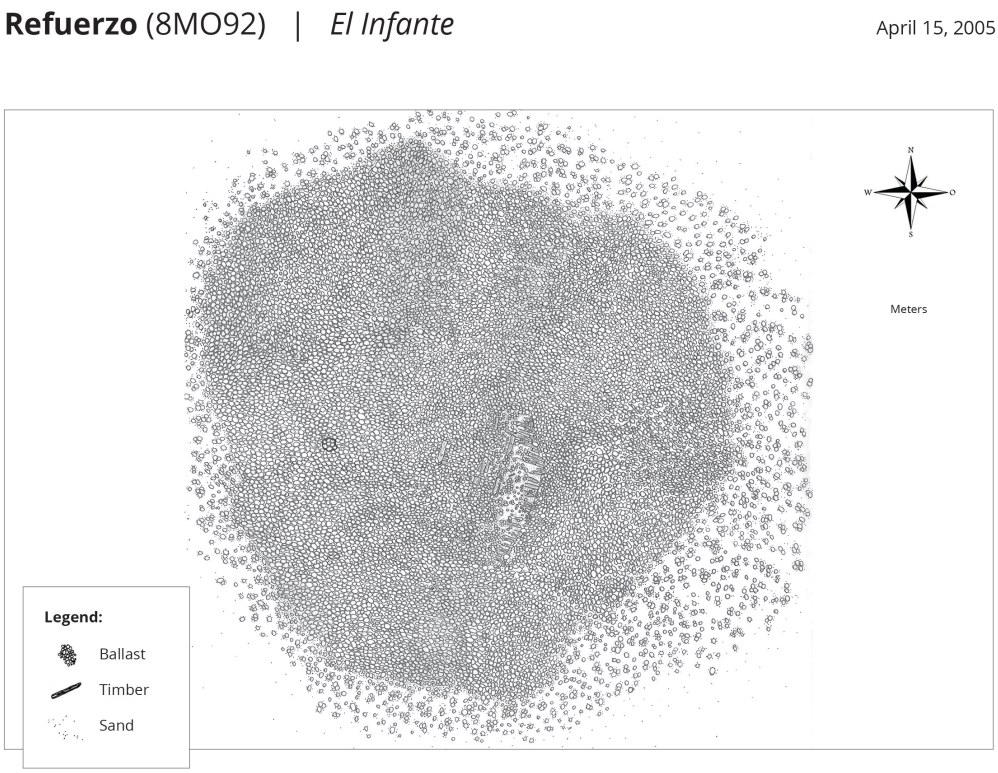

Figure 28: Site map of *La Refuerzo el Infante* (Scott-Ireton and Mattick 2006b:35; Yoonji Jung 2019)

5.5: Salvage at the Sites

Historic Spanish logbooks (Beson 2002: Appendix 1) and accounts from the modern salvors indicate the recovery of material from the 1733 shipwreck sites took place in the prevailing conditions of the Florida Keys. The Spanish began recovering material from the site within day of the hurricane's passing, seeking not only to secure salvage for the crown, but also for survival. This activity continued from mid-July through October 1733. The ships were accessible to anyone who could reach them and climb aboard, sitting upright as they were on the ocean floor in relatively shallow water. Thus, the disassembly of the shipwreck by salvors is assumed to have occurred in the ambient weather conditions and likely resulted in material drifting from the shipwreck as it was freed from fastenings, discarded, or burned. These destructive salvage methods may have been the underlying cause of the drift pattern observed by Benson's team at the site of *La Capitana*, though this is not their conclusion. For the remaining sites in the escort, the research has so closely focused on excavating in the presence of ballast, that drifting material has not been given archaeological consideration and *La Capitana* is the only shipwreck of the fleet for which there is provenience documentation meaningful to this simulation.

Benson's (2002) team notes the destructive intervention of 20th-century salvors as a primary scrambling mechanism at the site of *La Capitana*. This assessment is based on first-hand reports of an in-tact wreck site, for which there is no documentary evidence. Benson compares the scrambled site condition his team records in the 1990s with these early reports of an in-tact site. Gibbs (2006) believes such fragmentary accounts as these are an important data source to the study of a shipwreck's site formation process.

However, given the numerous shipwrecks in the Florida Keys region, some corroborating evidence of this would be useful. There is no reason to doubt the destructive potential of modern salvors' methods, which Price (2015) discusses in detail, but the evidence of modern salvage at *La Capitana* is indiscernible from material scatter in the ambient conditions, as discussed in Chapter 6: Results. Thus, it is impossible to conclude the impact of modern salvors on the site, or to distinguish it from the effects of their Early Modern counterparts, except through reliance on a single eyewitness account. As the drift simulation results discussed below indicate, this hypothesis could bear revisiting, as material from the 1733 shipwreck sites may have drifted much further than assumed by both archaeologists and salvors.

Chapter 6: Results

6.1: Vector Simulation

For over a century, archaeologists, anthropologists, ethnographers, and historians have relied on a broadly accepted approach to research: working from the known to the unknown (Thomas 1898:22; Meltzer 1985:249; Lyon 1996:56). Statistical models and environmental simulations enable archaeologists to both predict future events and explain the past in numerical terms, vastly extending the 'known' context of a site. The simulation utilized for this thesis is a limited example that relies on wind and ocean data, and the leeway field method for calculating drift trajectory. The results of the simulation correlate with the survey output from *La Capitana* (Benson 2002), indicating this method has explanatory relevance in the interpretation of shipwreck sites and predictive value for maritime survey planning. Future research combining additional data sources with more robust methods will even improve the reliability of computational models, but these results show that simplistic computational approaches can vastly extend the expected boundaries of a site, while limiting these boundaries to areas with the highest probability for locating archaeological targets.

The object simulated for Chapter 4: Methods, is a solid pine cube of 1 cu meter, an oversimplification of the debris encountered at shipwreck sites. Testing the model with simplistic shapes and material quantities enable the accuracy of its 2D physics engine to be validated. Four cubes are modeled, ranging in edge size from 0.1 meters to 1.5 meters (Figs 29-31). Following this test, iron and ice objects are also simulated to aid in validating the results (Figure 32 and 33). The behavior of ice has been modeled by Breivik et al. (2011) in testing the veracity of the leeway field method, while the choice

of examining iron objects is made to rule out the possibility that objects of dissimilar density behave the same as wooden shipwreck debris. Following these tests, trials were conducted on irregular shapes, such as those that could be found on Early Modern vessels: planking and a mast. These tests enable refinement of the object parameters in Module One to better reproduce the behavior of irregular prism objects.

For a full simulation, 10 objects like a mast and planking were randomly generated and run through the program. The output is layered in a density map to display the highest-likelihood area in which a survey for remains of *La Capitana el Rubi* shipwreck could be conducted, and these results are compared with the actual survey and the artifact provenience recorded by Benson (2002: Appendix 12) (Figure 41). From the entire 1733 fleet, only 14 sites have been documented and archaeological examinations have been limited to the immediate ballast piles. Benson and his team provide extensive provenience data from their work on *La Capitana* (Figures 41 and 42), making it the most relevant shipwreck from the group for this study.

6.2: Regular Cubes

Although cube-shaped crates are not a very likely shape for cargo containers in the Early Modern period, testing the drift simulation with cube shapes allows for the establishment of baseline behavior for drift objects in the Florida Straits. Four cubes (Table 5) of similar density and varied sizes were run through the ocean simulation, resulting in nearly identical drift patters (Fig 29-32) for each object under the same wind and current conditions, demonstrating that object shape is a more important factor in drift trajectory than object density, in the case of a 2D simulation.

Table 12: Virtual Cube Objects

	Cube Object 1	Cube Object 2	Cube Object 4	Cube Object 4
Wood Type	Pine	Pine	Pine	Pine
Dimensions	0.1 x 0.1 x 0.1	0.5 x 0.5 x 0.	1 x 1 x 1	51.5 x 1.5 x 1.5
Mass	0.397 kg	47.25 kg	352 kg	1302 kg

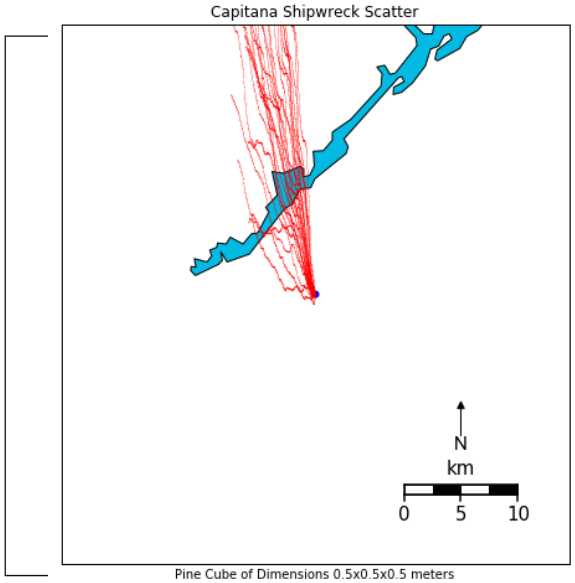

Figure 29: Simulated cube objects of 0.1x0.1x0.1 meter drifting from La Capitana site

Figure 30: Simulated cube objects of 0.5x0.5x0.5 meter drifting from La Capitana site

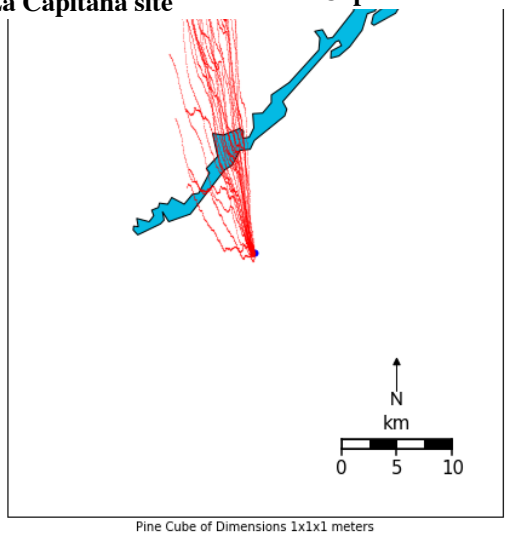

Figure 31: Simulated cube objects of 1x1x1 meter drifting from *La Capitana* site

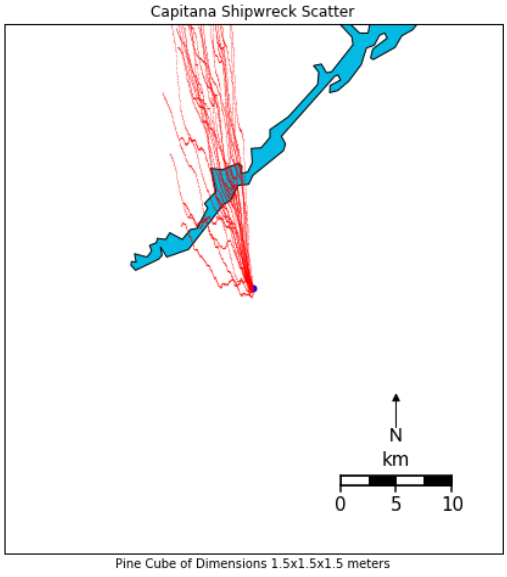

Figure 32: Simulated cube objects of 1.5x1.5x1.5 meter drifting from *La Capitana* site

Virtual ice and iron cube objects (Figures 33 and 34) offer a ground truth for the simulator's physics engine. The two-dimensional simulation of conditions treats ice as an object with greater density than the pine objects, and as a result it drifts in a manner more heavily influenced by the prevailing northerly current. The iron object exaggerates this effect, exhibiting limited drift from the wind, instead aligning more closely with the current force, though with each step of the simulation being shorter than for ice or pine objects of similar dimensions. A three-dimensional model could simulate the very short horizontal distance that high-density objects would float before sinking, but for the purposes of the pine objects in this simulation, two dimensional models suffice.

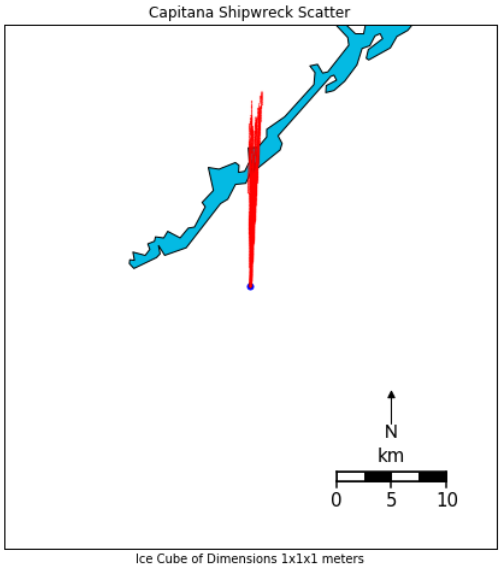

Figure 33: Simulated ice cube object of 1x1x1 meter drifting from La Capitana site

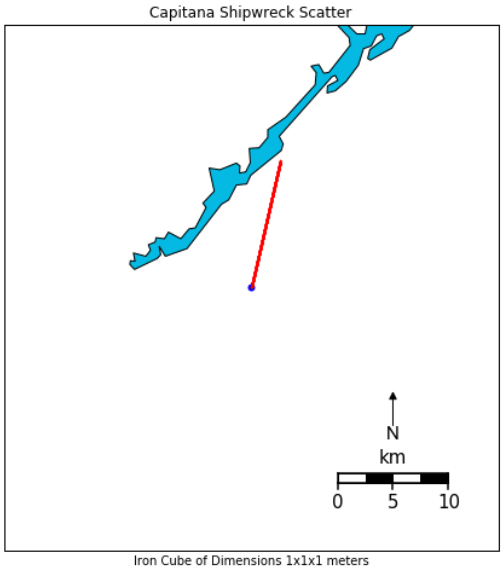

Figure 34: Simulated iron cube object of 1x1x1 meter drifting from La Capitana site

The strong north-west drift direction of the cube pine objects is readily discernable in Figure 29-32. At the *Rubi el Segundo* site (roughly 24.9 ° latitude), a degree of longitude is just over 100.2 km long. The maps above are scaled to 0.04° latitude by 0.04° longitude, making them roughly equivalent to a 4.4 km by 4 km square. Given the output of the simulation, the hope would be that a prudent surveyor could use the shipwreck site as an anchor at the southeast corner of a survey area and plan a 500-square-kilometer survey that would encompass the highest density of the simulated drift trajectories—the area where shipwreck remains are most likely to be found.

6.3: Shipwreck Components

The reliance on regular shapes in the examples above introduces a strong bias into the simulation's output and is not accurately reflective of the nature of actual shipwreck material, which can be characterized as irregular shapes. To broaden the highest-likelihood search area, the simulation was also run with irregular shapes generated from references of historical ship components. Table 13 contains details for a mast-like object and a plank-like structure, both rectangular prisms (Figure 35 and 36).

Table 13: Parameters for virtual planks and mast input into simulation

	Planks	Mast
Wood Type	Pine	Pine
Dimensions	5 x 0.2 x 1.5	30 x 0.5 x 0.5
Mass	559.5 kg	2895 kg

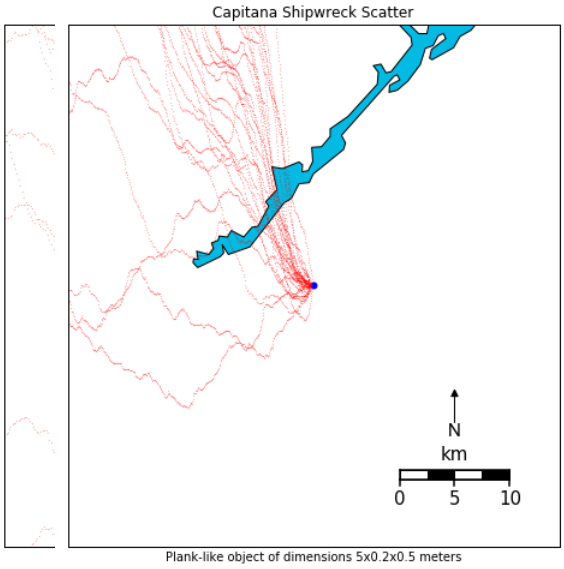

FigurFigure 36: Simulated plank object of 30x0.dimensions 5x0.2x0.5 drifting from La CapitCapitana site

The irregular plank shape and the mast both substantially depart from the drift trajectories of the cube objects. This variation is not random, showing a western drift trend from the shipwreck point of origin, with the objects tacking in both southern and northern directions along their courses, tacking in a manner consistent with the observed leeway of objects drifting in the wind (Breivik et al. 2011, 2012; and Allen et al. 2015). Additionally, the extent of the drift for both objects is much greater over a shorter period, resulting in a lower density of scatter, even compared to each other. Based on all the examples above, it becomes clear that a survey plan approximating 250 square kilometers would achieve the best results if the shipwreck were centered along the north-south axis of the eastern edge of the survey area. The examples serve to demonstrate that even superficial modeling of site formation processes yields a significant shift in the geographical focus of a survey plan. Archaeologists can use such an approach to work from the known toward highest-probable unknowns, rather than ascribing equal

probability to all regions surrounding a target—a critique of contemporary survey plans raised by Banning (2002).

6.4: Simulated Shipwreck

Rather than simulating specific debris shapes, the approach of randomly generating quantities of debris—within a range of archaeologically-relevant dimensions—enables a robust simulation of shipwreck dispersion. In this case, the simulated environment is the ambient conditions in the Florida Keys near the NDBC's MLRF1 buoy, south of Plantation Key. For the purpose of this simulation, the irregular debris objects are all rectangular prisms designed to resemble broken ship components, rather than cargos. The objects tested are each within the dimensions of 10 cm by 10 cm by 100 cm and 1 meter by 1 meter by 3 meters, and are solid pine throughout, with varying density between 350 kg and 400 kg per cubic meter (Appendix B). After the objects drift through the simulation, their combined outputs are layered and displayed in a density map (Fig 38).

The results (Figures 37-38) reveal a similar trend in the dispersion of objects as has already been indicated in individual tests—the strong north-western tendency of objects to drift. As the objects drifting over longer periods, they sometimes cross one another's paths. Figure 38 indicates a high density of material should be within a 250,000-square-meter zone, with the shipwreck ballast pile along the middle of its eastern edge. The greatest density of simulated material falls into a roughly 40,000-square-meter sector in the west, northwest, and northern vicinity of the ballast pile, with material also scattering southwest of the ballast pile. The ambient northeasterly ocean current provides

limited push against the prevailing easterly winds. As those winds shift, the objects tack and change directions, sometimes even drifting to the southwest, against the ocean current. While this is a simplistic simulation, relying on the limited ocean and wind vector data to propel the virtual objects, it demonstrates the dramatic effect the wind has on loose debris floating in the ocean, that the prevailing winds are a sufficient force to overcome an opposing ocean current. This simulation foreshadows more complex modeling, as the work of Graber et al. (1997) indicates ocean gyres in the region cause shoreward transport. A simulation pairing the same wind data with higher-accuracy ocean gyre data could allow drift trajectory projections of significantly greater detail, enabling probabilistic survey regions to be refined further. Still, these results on their own serve to eliminate the need for survey planning to the east of the example shipwreck target, barring additional data that increases the plausibility that remains may be located there.

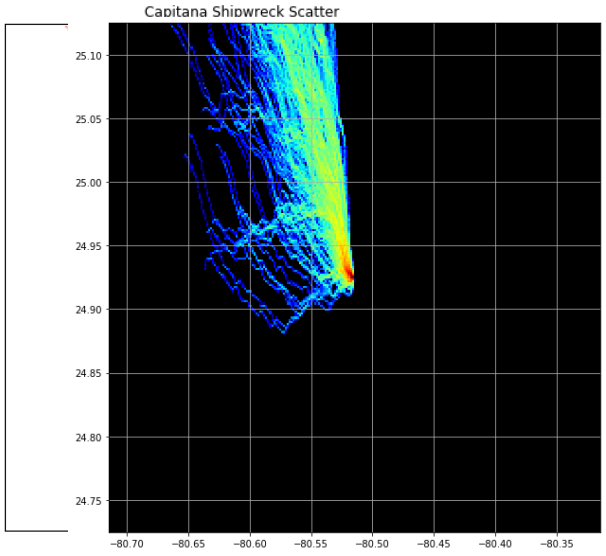

FigureFigure 38: Density map of Figure 37 rendered to virtualindicate areas of high probability (red) and low *Capita*probability (blue) for shipwreck scatter

Zooming in for a close-up, Figure 39 (roughly 4km X 4km) reveals additional details for a survey plan at *La Capitana* are revealed. With the site positioned in the center of the imaged area, the density map (Figure 40) indicates the quadrant bounded by the coordinate pairs 24.925, -80.515; and 24.930, -80.52—a roughly 1 square kilometer region immediately northwest of the site—is likely to contain most of the remains. While Benson's survey region (Figures 41 and 42) is slightly larger than this—about 1.12 square kilometers—his team located targets in an area consistent with this simulation.

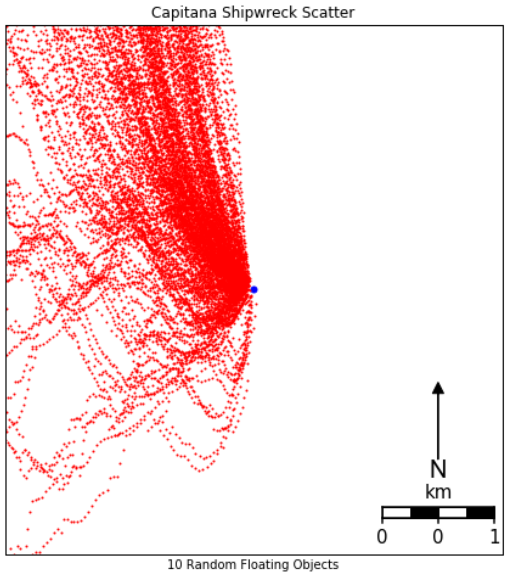

Figure 39: Close-up plot of material drifting from *La Capitana* shipwreck site

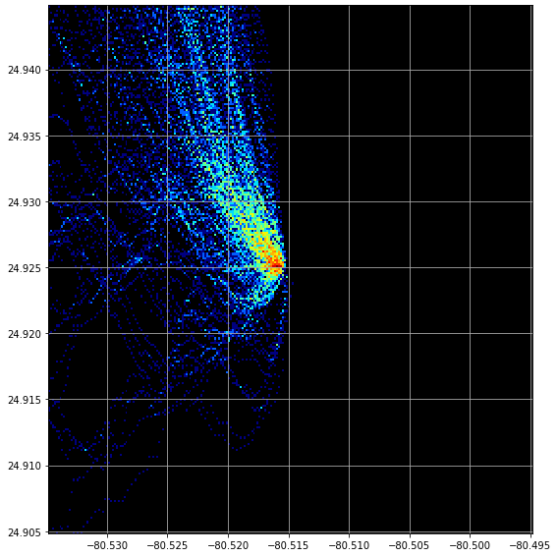

Figure 40: Density plot of Figure 29, indicating the highest-probability region for shipwreck remains is northwest or the site

6.5: Implications for Planning and Research

The simulation's three-day picture of the extent to which objects can drift (Figure 38) indicates surveyors should anticipate buoyant materials to scatter for kilometers, or even tens of kilometers from the site. However, denser shipwreck materials remain nearer the ballast pile in the first few hours of drifting, such that a systematic, small-scale survey should be expected locate such objects within a much smaller search area than the full 3-day drift extent, by tracing the simulated leeward drift of these objects. These simulated results are consistent with the actual artifact provenience reported by Benson (2002) (Figure 41 and 42) and serve as a limited validation of this methodology, particularly in light of the complete absence of material to the east of the shipwreck ballast pile, indicating the wind was likely an important factor in the deposition pattern. Benson's team started their survey operation with remote sensing data from the site (Figure 41), indicating anomalies in the sand. After orienting their search, the team used a prop-wash excavation method to clear sand from above the anomalous readings. Their search pattern uncovered no remains south of the ballast pile and remains to its east were within 25 meters of the pile's eastern edge. Most of the remains fall into the area that overlaps the modeled ambient conditions and drift trajectories—to the west and north of the main ballast pile. The trend among the excavation holes is that they are more likely to yield negative results further to the west, but artifacts were located as much as 300 meters west of the main ballast pile, a distance that indicates deposition through naturally occurring or anthropogenic-induced drift. The distance the objects traveled far exceeds the length of the ship's hull, so artifacts in that area could not have simply sunk in place as the hull collapsed. The scattering of artifacts in a manner consistent with drift on the

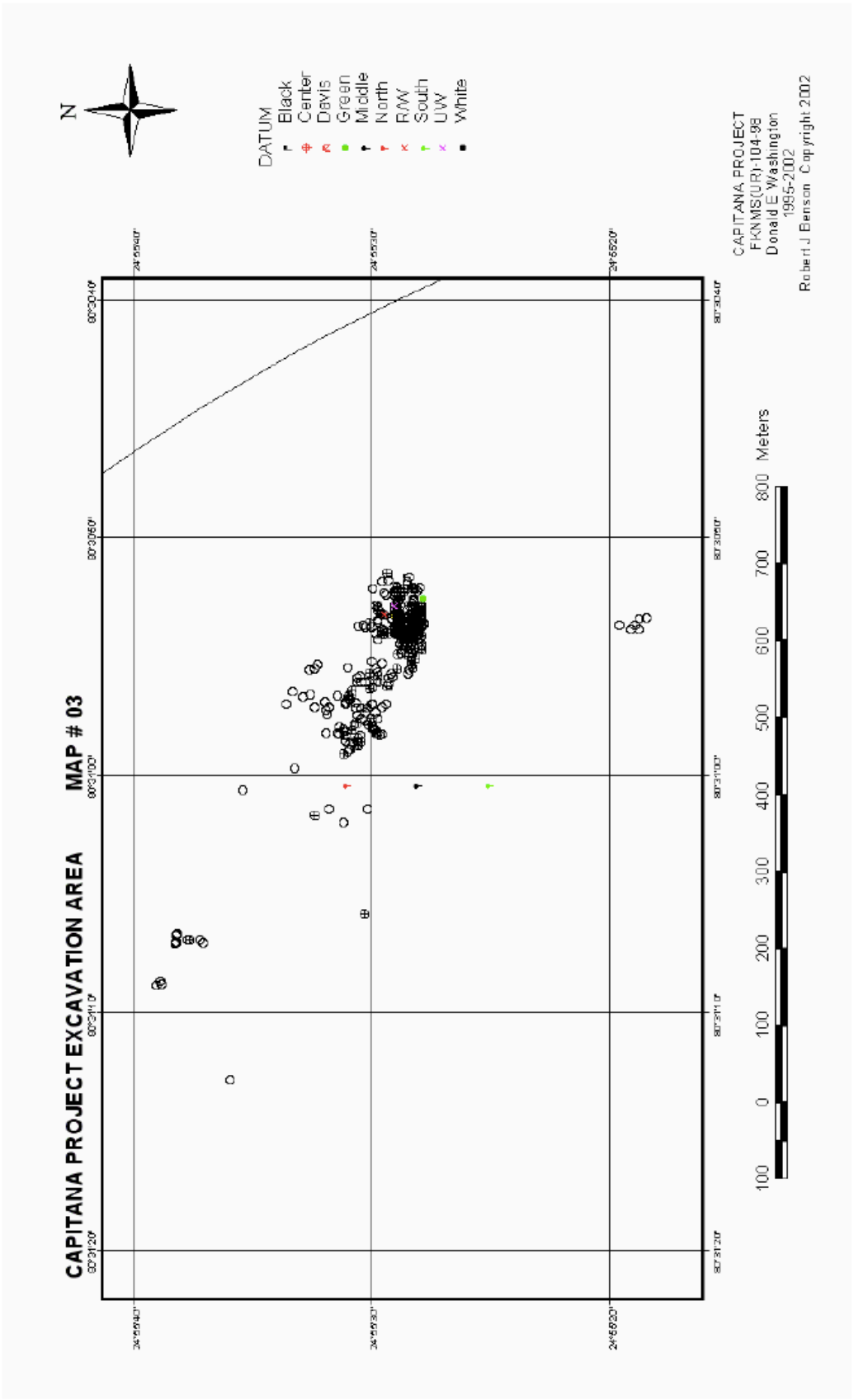
CAPITANA PROJECT EXCAVATION AREA
MAP # 03
N
DATUM
Black
Center
Davis
Green
Middle
North
R/W
South
UW
White
CAPITANA PROJECT
FKNMS(UR)-104-98
Donald E Washington
1995-2002
Robert J Benson Copyright 2002
100 0 100 200 300 400 500 600 700 800 Meters

pitana site.

La Capitana site.

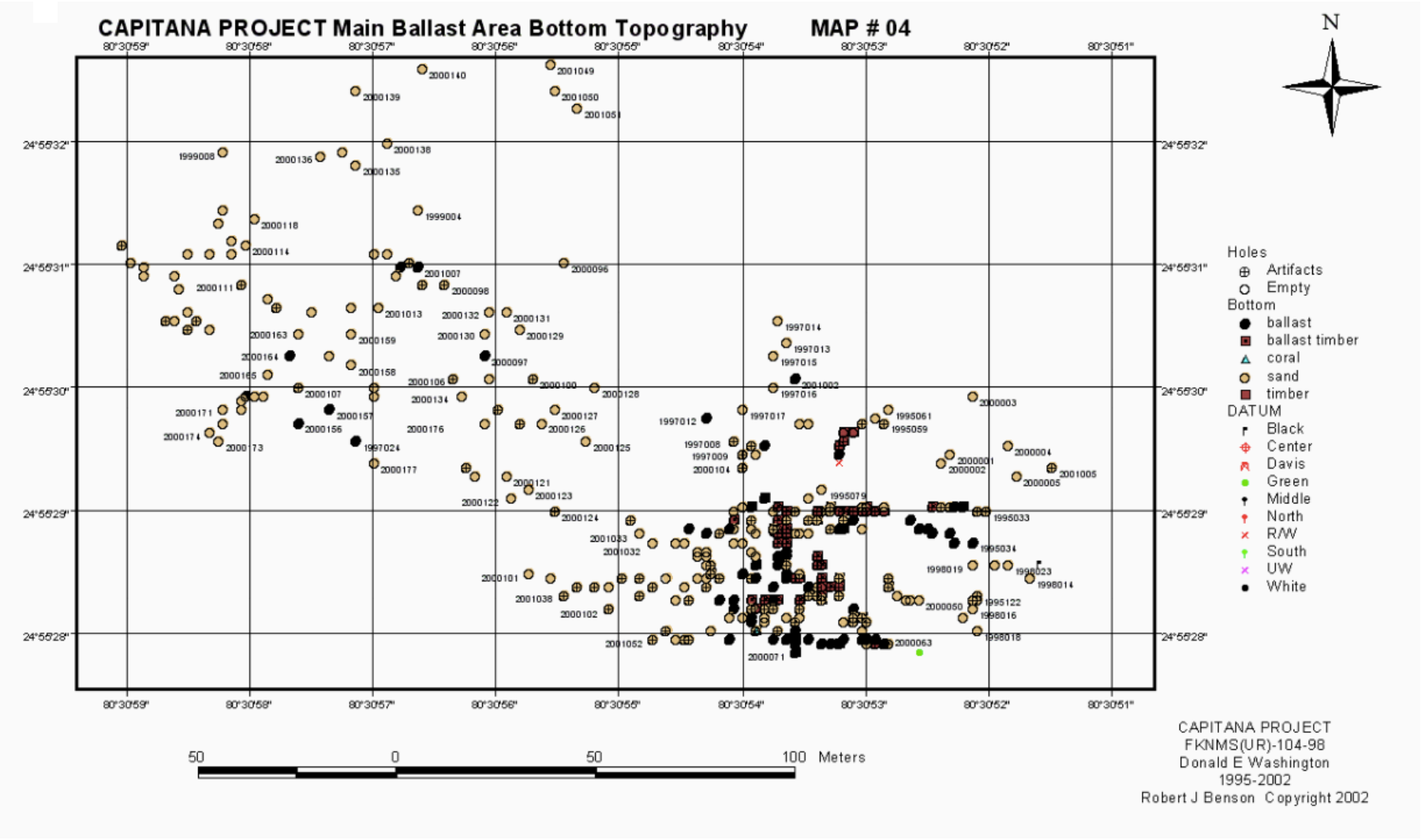

prevailing ambient wind and ocean conditions in relatively close proximity to the wreck site—proximity indicating mere hours of simulated drift time—suggests the scattering did not occur during the 1733 hurricane event, but later.

This study, taken alongside the interpretation of Fernández-Montblanc et al. (2016) of the *Fougeaux*, provides a second cases of the utility of results gained from simulating object drift using environmental data sets. In the case of the *Fougeaux*, historians reconstructed the storm and researchers paired these descriptions with modern wind and ocean datasets, in order to retrace the breakup of the ship near Cadiz, as described in the logs of Spanish watchtower personnel. With prior knowledge that the storm caused the ship to fracture, Fernández-Montblanc's team simulated the drift of shipwreck components and located previously unrecovered material within the highest-likelihood search area for remains. In this case, by relying on reports of Spanish salvage operations in the Florida Keys and modeling the ambient conditions in which those operations took place, the resulting simulated scatter pattern overlaps the survey results of the Benson et al. (2002) excavations in the 1990s. From the perspective of operations planning, these two studies suggest wind and ocean modeling can be a reliable determinant of high-probability survey areas and that surveys can be structured to maximize the potential to locate remains using computational simulations.

Among the implications for cultural resource management is a cost-benefit generality: if nothing more is known about the site, then using publicly available wind and ocean data to plan surveys can reduce time and effort, and maximize success in prospecting the debris field by limiting the survey's range to the areas with the highest probability of containing material, based on the region's ambient conditions. This method

departs from the more common planning approach, like that applied in *La Capitana* survey, that asserts equal likelihood of finding remains in all directions of a shipwreck site by placing the site in the center of the planned survey region. Non-random environmental conditions at shipwreck sites result in non-random distributions of material, and these distributions can be modeled and used for planning purposes.

In those cases where more information about a shipwreck site formation process is available through historic observations, search areas can be refined. As indicated in the cases of the *Fougeaux* and *La Capitana El Rubi*, prior knowledge that material scattered during a storm and during a salvage operation, respectively, enabled modelers to develop simulations that reflect these conditions and refine surveys to target areas with the highest likelihood of containing scattered remains.

In the case of *El Rubi*, the finding that scattered remains are consistent with the prevailing environmental conditions could potentially be a key signature of the salvage activities that impacted the site. Importantly, the opposite may be the case: that shipwreck components scattered in prevailing conditions are indistinguishable from those deposited by salvage operations. This strengthens the need for Gibbs' (2006) interpretive approach, because the forensic signatures revealed by the leeway drift simulation cannot conclusively be attributed to human salvage efforts.

If the salvage methods utilized by 18th- and 20th-century salvors deposited material in the water, the simulation indicates those materials could have drifted hundreds of meters from the ballast pile in a pattern consistent with the prevailing conditions. As a result, the salvage activity on *La Capitana el Rubi* cannot be conclusively interpreted from the available forensic evidence. Further modeling at a more granular level, built

around artifact typologies, is required to ascertain which group of salvors was more likely responsible for the scatter pattern Benson et al. (2002: Appendix 12) recorded. Certainly, given how closely the scatter of *La Capitana El Rubi* conforms to the ambient environmental conditions, scatter processes related to hurricane activity can be ruled out as causes for site distribution, as the hurricane winds were primarily northerly and southerly across the shipwreck in 1733. This study, therefore, cannot conclusively reframe the archaeological understanding of the site in favor of an interpretation that emphasizes formation processes due to shipwreck salvage over the natural environmental decay and scatter drifting from a hurricane or storm. The simulation enables archaeologists to rule out the 1733 hurricane as the primary cause of the shipwreck scatter, but offers limited interpretive utility beyond this. With the available scatter data, Spanish Colonial salvage efforts appear to have left no trace upon the site of *La Capitana el Rubi* that are verifiably distinct from the effects of the regional environment.

6.6: Conclusion

The success of two cases of shipwreck scatter simulation invites further research into the application of search and rescue principles to archaeological research designs and interpretive efforts. Computational tools have the potential to enable greater certainty about the causes of shipwreck scatter patterns. These tools can be applied with little prior understanding of a site, using publicly available environmental data and relatively simple two-dimensional computations. Refining the tools with historical information about the sites offers researchers an even more complete picture of the site. Given the fast pace with which computational speeds are improving, the future for such applications will

allow for more robust and fine-grained simulation of environmental conditions and site formation processes, even to the three-dimensional level, where sinking rates under drift and sediment deposition across a site can be modeled. Particle modeling of this kind is already being developed and an important area of future research will pair numerical environmental conditions with three-dimensional outputs from photogrammetric or side-scan sonar remote sensing techniques. Ultimately, advances in this area of research have the potential to enable archaeologists to revisit previously recorded sites with a higher probability of locating yet uncovered remains or remains overlooked by past archaeological and salvage endeavors.

References

Ascher, D., P.F. Dubois, K. Hinsen, J. Hugunin, and T. Oliphant
2001 *Numerical Python*. Report to Lawrence Livermore National Laboratory, Livermore, CA.

Allen, Arthur, Jens-Christian Roth, Christophe Maisondieu, Øyvind Breivik, and Bertrand Forest
2015 *Field Determination of the Leeway of Drifting Objects*. Report for the Norweigian Meteorological Institute, Oslo, Norway.

Aliaga, Eduardo Rubio
2015 La Flota De Indias: Formación Y Desarrollo A Lo Largo Del Siglo XVI. Master's thesis, Faculty of Philosophy and Letters, Lucentina University, Corodba, Spain.

Banning, E B.
2001 Archaeological Survey as Optimal Search. Paper presented at 29th Computer Applications and Quantitative Methods in Archaeology, Gotland, Sweden.
2002 *Archaeological Survey*. Kluwer Academic/Plenum Publishers. New York, NY.

Banning, E. B., A. L. Hawkins, and S. T. Stewart
2006 Detection Functions for Archaeological Survey. *American Antiquity* 71(4):723–42.
2011 Sweep Widths and the Detection of Artifacts in Archaeological Survey. *Journal of Archaeological Science* 38(12):3447–58.

Benson, Robert J (editor)
2002 The Capitana Project Final Excavation Report: The Shipwreck Believed to be La Capitana el Rubi. Report to the Caribbean Shipwreck Research Institute, Inc. Orlando, FL.

Bevan, Andrew, and Mark Lake
2013 *Computational Approaches to Archaeological Spaces*. Left Coast Press, Walnut Creek, CA.

Bethell, Leslie
1993 *Cuba: A Short History*. Cabridge University Press.

Boston Gazette
1733 A Description of the Late Storm or Hurricane on the 30th of June 1733, in the Island of St Cristophers in the West Indies. *Boston Gazette* 6 August 6. Boston, MA.

Boston Weekly News-Letter
1734 Extract of a Letter that came by Express from Mr. Keene, Dated at S. Ildefonso 10th of October. *The Boston Weekly News-Letter* 24 January. Boston, MA.

Braudel, Fernand, and Immanuel Wallerstein
2009 Review of *History and the Social Sciences: The Longue Durée*. Fernand Braudel Center 32(2):171–203.

Breivik, Øyvind, and Arthur A. Allen
2008 An Operational Search and Rescue Model for the Norwegian Sea and the North Sea. *Journal of Marine Systems* 69(1–2):99–113.

Breivik, Øyvind, Arthur A. Allen, Christophe Maisondieu, and Jens Christian Roth
2011 Wind-Induced Drift of Objects at Sea: The Leeway Field Method. *Applied Ocean Research* 33(2):100–109.

Breivik, Øyvind, Arthur A. Allen, Christophe Maisondieu, Jens-Christian Roth, and Bertrand Forest
2012 The Leeway of Shipping Containers at Different Immersion Levels. *Ocean Dynamics* 62(5):741–52.

Breivik, Øyvind, Arthur Addoms Allen, Christophe Maisondieu, and Michel Olagnon
2013 Advances in Search and Rescue at Sea. *Ocean Dynamics* 63(1):83–88.

Bromley, J.S.
1970 *The New Cambridge Modern History, Vol. 6: The Rise of Great Britain and Russia, 1688-1715*. Cambridge University Press, Cambridge, UK.

Brooks, C. E.
1930 The Climate of the First Half of the Eighteenth Century. *Quarterly Journal of the Royal Meteorological Society* 56:389-402.

Cangialosi, John
2018 The State of Hurricane Forecasting. Inside the Eye (blog). <https://noaanhc.wordpress.com/2018/03/09/the-state-of-hurricane-forecasting/>. Accessed on March 9, 2018.

Chenoweth, Michael
2006 A Reassessment of Historical Atlantic Basin Tropical Cyclone Activity, 1700–1855. *Climatic Change* 76(1–2):169–240.

Church, Robert A.
2014 Deep-Water Shipwreck Initial Site Formation: The Equation of Site Distribution. *Journal of Maritime Archaeology* 9(1):27–40.

Craven, John P.
1985 Technology and The Law of the Sea: The Effect Of Prediction And Misprediction. *Louisiana Law Review* 45(6):1143-1159.

2001 *The Silent War: The Cold War Battle Beneath the Sea*. Simon and Schuster, New York City, NY.
2002 What Every American Needs to Know about Our Nation and the Sea. *Marine Technology Society Journal* 36(2):66–69.

Denevan, William
1992 The Pristine Myth: The Landscape of the Americas in 1492. *Annals of the Association of American Geographers* 82(3): 369–385.

Eltis, David
2007 A Brief Overview of the Trans-Atlantic Slave Trade. Voyages: The Trans-Atlantic Slave Trade Database, Emory University, Oxford, GA <http://www.slavevoyages.org/voyage/essays>. Accessed on April 27, 2018.

Engineering ToolBox
2004 Density of Various Wood Species <https://www.engineeringtoolbox.com/wood-density-d_40.html>. Accessed October 19, 2019.

Fernández-Montblanc, T., A. Izquierdo, and M. Bethencourt
2016 Scattered Shipwreck Site Prospection: The Combined Use of Numerical Modeling and Documentary Research (Fougueux, 1805). *Archaeological and Anthropological Sciences* 10(1): 141–56.

Filstrup, Chris
2019 Research & Subject Guides: Latin American History: Archivo General de Indias, Stony Brook University, Stony Brook, NY <http://guides.library.stonybrook.edu/c.php?g=35538&p=225671>. Accessed October 7, 2019.

The Florida Senate
2012 Florida Statutes Chapter 267 Historical Resources. The State of Florida <https://www.flsenate.gov/Laws/Statutes/2012/Chapter267/All>. Accessed on October 19, 2019.

Fortes-Lima, Cesar, Jonas Bybjerg-Grauholm, Lilia Caridad Marin-Padrón, Enrique Javier Gomez-Cabezas, Marie Bækvad-Hansen, Christine Søholm Hansen, and Phuong Le, David Michael Hougaard, Paul Verdu, Ole Mors, Esteban J. Parra, and Beatriz Marcheco-Teruel
2018 Exploring Cuba's Population Structure and Demographic History Using Genome-Wide Data. *Scientific Reports* 8(1):11422.

Georges, T. M., J. A. Harlan, T. N. Lee, and R. R. Leben
1998 Observations of the Florida Current with Two Over-the-Horizon Radars. *Radio Science* 33(4):1227–39.

Gibbs, Martin
2006 Cultural Site Formation Processes in Maritime Archaeology: Disaster Response, Salvage and Muckelroy 30 Years on. *The International Journal of Nautical Archaeology* 35(1):4–19.

Gillings, Mark
2012 Landscape Phenomenology, GIS and the Role of Affordance. *Journal of Archaeological Method and Theory* 19(4):601–11.

Graber, Hans C., and Claire B. Limouzy-Paris
1997 Transport Patterns of Tropical Reef Fish Larvae by Spin-Off Eddies in the Straits of Florida. *Oceanography* 10(2):68-71.

Grange, Stuart K.
2014 Technical Note: Averaging Wind Speeds and Directions. <https://www.researchgate.net/publication/262766424_Technical_note_Averaging_wind_speeds_and_directions>. Accessed on October 19, 2019.

Gravette, Andrew
2000 *Architectural History of the Caribbean: An A-Z of Historic Buildings*. Ian Randal Publishers, Kingston, Jamaica.

Hackett, Bruce, Øyvind Breivik, and Cecilie Wettre
2006 Forecasting the Drift of Objects and Substances in the Ocean. In *Ocean Weather Forecasting: An Integrated View of Oceanography,* Eric P. Chassignet and Jacques Verron, editors, pp. 507–23. Springer, Dordrecht, The Netherlands.

Halpern, Samuel
2012 The Drift of Wreckage. Great Lakes Titanic Society <http://www.glts.org/articles/halpern/the_drift_of_wreckage.html>. Accessed October 7, 2019.

Harpster, Matthew
2009 Keith Muckelroy: Methods, Ideas and Maritime Archaeology. *Journal of Maritime Archaeology* 4(1):67–82.

Heit, Judy
2013 Not Just Another Day at Sea. Hatteras Island Vacation Blog. <https://hatterasblog.surforsound.com/all-posts/not-just-another-day-at-sea/>. Accessed October 7, 2019.

Hodson, F.R., P.H.A. Sneath, and J.E. Doran
1966 Some Experiments in the Numerical Analysis of Archaeological Data. *Biometrika* 53(3-4):311–324.

Hunter, John D.
2007 Matplotlib: A 2D Graphics Environment. *Computing in Science & Engineering* 9:90-95.

Judge, W. James, Daniel W. Martin, Lynne Sebastian
1989 *Quantifying the Present and Predicting the Past : Theory, Method, and Application of Archaeological Predictive Modeling*. Report for United States Bureau of Land Management, Denver, CO.

Kelly, Morgan, and Cormac Ó Gráda
2014 *Speed under Sail, 1750-1850*. School of Economics, University College Dublin, Ireland.

Kerr, Robert
2009 *The Metamorphosis of Cuban Architecture; Development, Decay and Opportunity*. University of Edinburgh, Edinburgh, Scotland.

Kowalewski, Stephen A.
2008 Regional Settlement Pattern Studies. *Journal of Archaeological Research* 16(3):225–85.

Lake, M. W.
2014 Trends in Archaeological Simulation. *Journal of Archaeological Method and Theory* 21(2):258–87.

Lidz, Barbara H, Christopher D Reich, and Eugene A. Shinn
2003 Regional Quaternary Submarine Geomorphology in the Florida Keys. *Geological Society of America Bulletin* 115(7):845-866.

Lee, Thomas N., Claes Rooth, Elizabeth Williams, Michael Mcgowan, Alina F. Szmantt, and M. E. Clarke
1992 Influence of Florida Current, Gyres and Wind-driven Circulation on Transport of Larvae and Recruitment in the Florida Keys Coral Reefs. *Continental Shelf Research* 12(7):971-1002.

Lee, Thomas N., and Elizabeth Williams
1999 Mean Distribution and Seasonal Variability of Coastal Currents and Temperature in the Florida Keys with Implications for Larval Recruitment. *Bulletin of Marine Science* 64(1):35–56.

Lee, Thomas N., and Ned Smith
2002 Volume Transport Variability Through the Florida Keys Tidal Channels. *Continental Shelf Research* 22:1361–1377.

Logan, Patricia
1977 The San Jose y Las Animas: An Analysis of the Ceramic Collection. Master's thesis, Department of History, East Carolina University, Greenville, NC.

Lyon, E. A.
1996 *A New Deal for Southeastern Archaeology*. The University of Alabama Press, Tuscaloosa, AL.

Maryland Gazette
1734 Foreign Affairs, London, 6 September. *Maryland Gazette*, 11 January. Annapolis, MD.

McKinnon, Jennifer
2006 Florida's Mystery Wreck. *International Journal of Nautical Archaeology* 35(2):187-194.
2007 Creating a Shipwreck Trail: Documenting the 1733 Spanish Plate Fleet Wrecks. In *Out of the Blue: Public Interpretation of Maritime Cultural Resources*. John H. Jameson, Jr. and Della A. Scott-Ireton, editors, pp. 85–94. Springer, New York, NY.

Meide, Chuck
2002 A Plague of Ships: Spanish Ships and Shipbuilding in the Atlantic Colonies, Sixteenth and Seventeenth Centuries. College of William and Mary.

Meltzer, David J.
1985 North American Archaeology and Archaeologists, 1879-1934. *American Antiquity* 50(2):249-60.

Mori, Sanae, Akira Itoh, Satoshi Nanami, Sylvester Tan, Lucy Chong, and Takuo Yamakura
2014 Effect of Wood Density and Water Permeability on Wood Decomposition Rates of 32 Bornean Rainforest Trees. *Journal of Plant Ecology* 7(4):356–63.

Murillo, Raphael
2013 Slavery and the Siege of Havana. *Berkeley Review of Latin American Studies* 20-21.

Muckelroy, Keith
1975 A Systematic Approach to The Investigation Of Scattered Wreck Sites. *The International Journal of Nautical Archaeology and Underwater Exploration* 4(2):173-190.
1976 The Integration of Historical and Archaeological Data Concerning an Historic Wreck Site: The 'Kennemerland'. *World Archaeology* 7(3):280-289.

National Data Buoy Center
1971 Meteorological and Oceanographic Data Collected from the National Data Buoy Center Coastal-marine Automated Network (C-MAN) and Moored (Weather) Buoys. Station MLRF1 - Molasses Reef, FL. National Oceanographic and Atmospheric Administration, National Ocean Service, US Department of Commerce <http://www.ndbc.noaa.gov/station_page.php?station=mlrf1> (accessed on Oct. 8 2019)

Office for Coastal Management
2018 Historic Hurricane Tracks. National Oceanographic and Atmospheric Administration, National Ocean Service, US Department of Commerce. <coast.noaa.gov/hurricanes/>. Accessed on 19 October 2019.

Pétrissans, A, R. Younsi, M. Chaouch, P. Gérardin, and M. Pétrissans
2014 Wood Thermodegradation: Experimental Analysis and Modeling of Mass Loss Kinetics. Maderas. *Ciencia y Tecnología* 16(2):133-148.

Phillips, Carla Rahn
1999 The Iberian Atlantic. *Itinerario: European Journal of Overseas History* 23(2):84-106.

Phillips, William D, and Carla Rahn Phillips
1977 Spanish Wool and Dutch Rebels: The Middelburg Incident of 1574. *The American Historical Review* 82(2):312-330.

Pike, Ruth
1965 The Sevillian Nobility and Trade with the New World in the Sixteenth Century. *Business History Review* 39(4):439–65.

Price, Melissa Rae
2015 Intellectual Treasure Hunting: Measuring Effects of Treasure Salvors on Spanish Colonial Shipwreck Sites. Master's thesis, Department of History, East Carolina University, Greenville, NC.

Puddifoot, Katherine
2018 Re-Evaluating the Credibility of Eyewitness Testimony: The Misinformation Effect and the Overcritical Juror. *Episteme* 42:1-25.

Ren, Lei, Zhan Hu, and Michael Hartnett
2018 Short-Term Forecasting of Coastal Surface Currents Using High Frequency Radar Data and Artificial Neural Networks. *Remote Sensing* 10(6):850.

Rich, Sara A., Nigel Nayling, Garry Momber, and Ana Crespo Solana

2018 *Shipwrecks and Provenance: In-Situ Timber Sampling Protocols with a Focus on Wrecks of the Iberian Shipbuilding Tradition*. Archaeopress Publishing, Oxford, UK.

Robertson, Robert
1733 *A Short Account of the Hurricane that Pass'd Thro' the English Leeward Caribbee Islands, on Saturday the 30th of June 1733*. London.

Rönnby, Johan, and J. Adams
2015 Interpreting Shipwrecks. Maritime Archaeological Approaches. *International Journal of Nautical Archaeology* 44(2):457–459.

Ruiz Villanueva, Virginia, Ernest Bladé Castellet, Andrés Díez-Herrero, José M. Bodoque, and Martí Sánchez-Juny
2014 Two-dimensional Modelling of Large Wood Transport During Flash Floods: Wood Clogging and Hydrodynamics. *Earth Surface Processes and Landforms* 39(4):438–49.

Schiffer, Michael B.
1987 *Formation Processes of the Archaeological Record*. University of New Mexico Press, Albuquerque, NM.

Science Applications, Inc.
1981 *A Cultural Resource Survey of the Continental Shelf from Cape Hatteras to Key West: Final Report Volume IV: Conclusions and Recommendations*. Report to Bureau of Land Management, New Orleans, LA.

Scott-Ireton, Della, and Barbara E. Mattick
2006a *National Register of Historic Places Registration Form for El Gallo Indiano Shipwreck Site*. Report to United States Department of the Interior-National Park Service, from Florida Division of Historical Resources, Bureau of Historic Preservation, Tallahassee, FL.
2006b *National Register of Historic Places Registration Form for El Infante Shipwreck Site*. Report to United States Department of the Interior-National Park Service, from Florida Division of Historical Resources, Bureau of Historic Preservation, Tallahassee, FL.
2006c *National Register of Historic Places Registration Form for El Rubi Shipwreck Site*. Report to United States Department of the Interior-National Park Service, from Florida Division of Historical Resources, Bureau of Historic Preservation, Tallahassee, FL.

Shay, Lynn K., Tom N. Lee, Elizabeth J. Williams, Hans C. Graber, and Claes G. H. Rooth
1998 Effects of Low-Frequency Current Variability on Near-Inertial Submesoscale Vortices. *Journal of Geophysical Research: Oceans* 103(C9):18691–714.

Skowronek, Russell

1984 Trade Patterns of Eighteenth-Century Frontier New Spain: The 1733 Flota and St. Augustine. *Volumes in Historical Archaeology 1*. Stanley South (Ed.) Columbia, SC.

Smallwood, Lawrence L.
1975 African Cultural Dimensions in Cuba. *Journal of Black Studies* 6(2):191–99.

Smith, Roger C., and James Dunbar
1977a *An Underwater Archaeological Survey of Eight Merchant Naos of the 1733 New Spain Fleet*. Report to the Florida Department of State, Division of Historical Resources, Bureau of Archaeological Research, Tallahassee, FL.
1977b *Survey of the Spanish Merchan Nao Nuestra Neora de Belem y San Juan Bautista (Tres Punetes)*. Report to the Florida Department of State, Division of Historical Resources, Bureau of Archaeological Research, Tallahassee, FL.

Smith, Roger C., Robert Finegold, and Eric Stephens
1990 Establishing an Underwater Archaeological Preserve in the Florida Keys: A Case Study. *The Journal of Preservation Technology* 22(3):11-18.

Stone, Lawrence D., Colleen M. Keller, Thomas M. Kratzke, and Johan P. Strumpfer
2014 Search for the Wreckage of Air France Flight AF 447. *Statistical Science* 29(1):69–80.

Stone, Lawrence D, Thomas M Kratzke, and John R Frost
2010 Search Modeling and Optimization in USCG's Search and Rescue Optimal Planning System (SAROPS). Paper presented at 13th Conference on Information Fusion, Cambridge, UK.

Tarver, H. Micheal, and Emily Slape
2016 *The Spanish Empire: A Historical Encyclopedia*. ABC-CLIO, Santa Barbara, CA.

Taylor, Paul S
1922 Spanish Seamen in the New World During the Colonial Period. *The Hispanic American Historical Review* 5(4):631.

Thomas, Cyrus
1898 *Introduction to the Study of North American Archaeology*. The Robert Clark Company, Cincinnati, OH.

Thomas, Olivia
2017 The Dish Ran Away with the Spoon: Revisiting Unprovenienced Foodways Artifacts from the Eighteenth-Century Spanish Fleet Shipwrecks. Master's Thesis, Department of History, East Carolina University, Greenville, NC.

Tracy, James D. (editor)
1990 *The Rise of Merchant Empires: Long-Distance Trade in the Early Modern World 1350-1750*. Cambridge University Press, New York, NY.

Verhagen, Philip, and Thomas G. Whitley
2012 Integrating Archaeological Theory and Predictive Modeling: A Live Report from the Scene. *Journal of Archaeological Method and Theory* 19(1):49–100.

Villaseñor, Alejandro Tortolero
2015 The Annales School and the Environmental History of Latin America. *Historia Caribe* X(26):301-340.

Ward, Ingrid, and Piers Larcombe
2003 A Process-Orientated Approach to Archaeological Site Formation: Application to Semi-Arid Northern Australia. *Journal of Archaeological Science* 30(10):1223–1236.

Ward, I.A.K., P. Larcombe, and P. Veth
1999 A New Process-Based Model for Wreck Site Formation. *Journal of Archaeological Science* 26(5):561–70.

The Weekly Rehearsal
1733 Boston, 13 August. *The Weekly Rehearsal*. Boston, Massachusetts

Weller, Robert M.
2001 *Galleon Alley: The 1733 Spanish Treasure Fleet*. Crossed Anchors Salvage, Lake Worth, FL.

Wheeler, Dennis
1985 The Weather at the Battle of Trafalgar. *Weather* 40:338–346.
1987 The Trafalgar Storm: 22–29 October 1805. *Meteorology Magazine* 116:197–205.
1995 A climatic Reconstruction of the Battle of Quiberon Bay, 20 November 1759. *Weather* 50:230–238.
2001 The Weather of the European Atlantic Seaboard During October 1805: An Exercise in Historical Climatology. *Climatic Change* 48(2-3):361-385.
2005 An Examination of the Accuracy and Consistency of Ships' Logbook Weather Observations and Records. *Climatic Change* 73(1–2):97–116.

Wheeler, Dennis, and Ricardo Garcia-Herrera
2008 Ships' Logbooks in Climatological Research Reflections and Prospects. *Trends and Directions in Climate Research*. Annals of the N.Y. Academy of Sciences 1146(1):1–15.

Appendix A: Timeline of the 1733 Fleet's Voyage from Havanna (Benson 2002: Appendix 1)

Date	Time	Author: Governor in Havana	Author: Francisco de Varas y Valdez	Author Unknown; Havana, 20/08/1733	Author Unknown; Ship's log for Infante	Numerical Wind Bearing
13/07/1733	7:00		7:30, SE Wind			135
13/07/1733	8:00					135
13/07/1733	9:00					135
13/07/1733	10:00				Havana, E Wind	90
13/07/1733	11:00				Ocean, ENE Wind, Course N	68
13/07/1733	12:00		ENE Wind, Course N		ENE Wind, Course N	68
13/07/1733	13:00		ENE Wind, Course N		ENE Wind, Course N	68
13/07/1733	14:00		ENE Wind, Course N		ENE Wind, Course N	68
13/07/1733	15:00		ENE Wind, Course SE		Course SE	68
13/07/1733	16:00		ENE Wind, Course SE		Course SE	68
13/07/1733	17:00		ENE Wind, Course SE		Course SE	68
13/07/1733	18:00		6:30, E Wind, Course N 1/4 NE		Course SE	90
13/07/1733	19:00		E Wind, Course N 1/4 NE		Course SE	90

13/07/1733	20:00		E Wind, Course N 1/4 NE		Course SE	90
13/07/1733	21:00		E Wind, Course N 1/4 NE		North of Jaruco, Course N	90
13/07/1733	22:00		E Wind, Course N 1/4 NE		Course N	90
13/07/1733	23:00		E Wind, Course N 1/4 NE		Course N	90
14/07/1733	0:00		E Wind, Course N 1/4 NE		Course N	90
14/07/1733	1:00		E Wind, Course N 1/4 NE		Course N	90
14/07/1733	2:00		E Wind, Course N 1/4 NE		Course N	90
14/07/1733	3:00		E Wind, Course N 1/4 NE		Course N	90
14/07/1733	4:00		E Wind, Course N 1/4 NE		Course N	90
14/07/1733	5:00		E Wind, Course N 1/4 NE		Course N	90
14/07/1733	6:00		E Wind, Course N 1/4 NE		Course N	90
14/07/1733	7:00		E Wind, Course N 1/4 NE		Course N	90
14/07/1733	8:00	E Wind	E Wind, Course N 1/4 NE		Course N	90

14/07/1733	9:00	E Wind	E Wind, Course N 1/4 NE		Course N	90
14/07/1733	10:00	E Wind	E Wind, Course N 1/4 NE		Vaca Key W, Course N	90
14/07/1733	11:00	E Wind	E Wind, Course N 1/4 NE		Course N	90
14/07/1733	12:00	E Wind	E Wind, Course SE		Vaca Key 3 Leagues, Course SE	90
14/07/1733	13:00	E Wind	E Wind, Course SE	Land Sighted, Key West, Currents NW	Couse SE	90
14/07/1733	14:00	E Wind	E Wind, Course SE	Land Sighted	Couse SE	90
14/07/1733	15:00	E Wind	ENE Wind, Course N	Land Sighted	Course N	68
14/07/1733	16:00	E Wind	ENE Wind, Course N		Course N	68
14/07/1733	17:00	E Wind	ENE Wind, Course N		Course N	68
14/07/1733	18:00	E Wind	Vaca Key NNW Wind, Course ESE		Vaca Key (N 1/4 NE), Course ESE	337
14/07/1733	19:00	E Wind	NN Wind (?), Course ESE		NNE Wind, Course ESE	1
14/07/1733	20:00	NN Wind	NN Wind (?), Course ESE		NNE Wind, Course ESE	1
14/07/1733	21:00	NN Wind	NN Wind (?), Course ESE		NNE Wind, Course ESE	1
14/07/1733	22:00	NN Wind	NN Wind (?), Course ESE	NN Wind	N Wind, Course E	1

14/07/1733	23:00	NN Wind	NN Wind (?), Course ESE	NN Wind	N Wind, Course E	1
15/07/1733	0:00	NN Wind	NN Wind (?), Course ESE	NN Wind	N Wind, Course E	1
15/07/1733	1:00	NN Wind	NN Wind (?), Course ESE	NN Wind	N Wind, Course E	1
15/07/1733	2:00	NN Wind	NN Wind (?), Course E	NN Wind	N Wind, Course E	1
15/07/1733	3:00	NN Wind	NN Wind (?), Course E	NN Wind	N Wind, Course E	1
15/07/1733	4:00	NN Wind	NN Wind (?), Course E	NN Wind	N Wind, Course E	1
15/07/1733	5:00	NN Wind	5:30, NN Wind, Course W	NN Wind	N Wind, Course E	1
15/07/1733	6:00		NN Wind, Course W	NN Wind, Course S	N Wind, Course W	1
15/07/1733	7:00	S Wind, Time unclear	NN Wind, Course W	NN Wind, Course S	Course SSW	1
15/07/1733	8:00		NN Wind, Course W	NN Wind, Course S	Course SSW	1
15/07/1733	9:00		Key Largo, Course S	NN Wind, Course S	Course SSW	1
15/07/1733	10:00		Course S, Starboard	NN Wind, Course S	Course SSW	1
15/07/1733	11:00		Course S, Starboard	NN Wind, Course S	Course SSW	1
15/07/1733	12:00		Course S, Starboard	NN Wind, Course S	Course SSW	1
15/07/1733	13:00		Course S, Starboard	NN Wind, Course S	Course SSW	1
15/07/1733	14:00		Course S, Starboard	NN Wind, Course S	Course SSW	1

15/07/1733	15:00		Course S, Starboard	NN Wind, Course S	Course SSW	1
15/07/1733	16:00		Course S, Starboard	NN Wind, Course S	Course SSW	1
15/07/1733	17:00		Course S, Starboard	NN Wind, Course S	Course SSW	1
15/07/1733	18:00		Course S, Starboard	Ships begin grounding...	S Wind, Course SSW	180
15/07/1733	19:00		Course S, Starboard		S Wind, Course SSW	180
15/07/1733	20:00		Course S, Starboard		20:30 Grounded	180
15/07/1733	21:00		Course S, Starboard		21:30 cutting masts	180
15/07/1733	22:00		Course S, Port		Masts cut away	180
15/07/1733	23:00		Drifting, Bow E			180
16/07/1733	0:00		Drifting, Bow E			180
16/07/1733	1:00		Drifting, Bow E, All masts lost, dumping cargo			180
16/07/1733	2:00					180
16/07/1733	3:00					180
16/07/1733	4:00					180
16/07/1733	5:00					
16/07/1733	6:00					
16/07/1733	7:00				Scouting for a landing	

Appendix B: Test Drift Simulation Objects

Start Time	Thu Oct 24 09:27:17 2019
Wood Type/Density	(pine, 376)
Dimensions	[0.7, 2.58, 2.24]
Volume	4.04544
Mass	1521.09
Reference Areas	[1.15, 0.57, 0.998, 0.656]
Immersion Ratio	0.33127
Obj_Density	376

Start Time	Thu Oct 24 09:27:17 2019
Wood Type/Density	(pine, 367)
Dimensions	[0.36, 2.37, 2.77]
Volume	2.36336
Mass	867.355
Reference Areas	[0.644, 0.303, 0.551, 0.354]
Immersion Ratio	0.319758
Obj_Density	367

Start Time	Thu Oct 24 09:27:17 2019
Wood Type/Density	(pine, 396)
Dimensions	[0.69, 0.86, 2.29]
Volume	1.35889
Mass	538.119
Reference Areas	[0.976, 0.227, 0.366, 0.605]
Immersion Ratio	0.188794
Obj_Density	396

Start Time	Thu Oct 24 09:27:17 2019
Wood Type/Density	(pine, 380)
Dimensions	[0.45, 1.19, 1.31]
Volume	0.701505
Mass	266.572
Reference Areas	[0.373, 0.197, 0.339, 0.216]
Immersion Ratio	0.345125
Obj_Density	380

Start Time	Thu Oct 24 09:27:17 2019
Wood Type/Density	(pine, 355)
Dimensions	[0.86, 0.44, 1.87]
Volume	0.707608
Mass	251.201
Reference Areas	[0.541, 0.13, 0.249, 0.282]
Immersion Ratio	0.193608

Obj_Density 355

Start Time Thu Oct 24 09:27:17 2019
Wood Type/Density (pine, 400)
Dimensions [0.82, 2.22, 1.54]
Volume 2.80342
Mass 1121.37
Reference Areas [1.117, 0.488, 0.775, 0.704]
Immersion Ratio 0.304092
Obj_Density 400

Start Time Thu Oct 24 09:27:17 2019
Wood Type/Density (pine, 386)
Dimensions [0.44, 0.84, 2.93]
Volume 1.08293
Mass 418.01
Reference Areas [0.808, 0.138, 0.232, 0.481]
Immersion Ratio 0.145673
Obj_Density 386

Start Time Thu Oct 24 09:27:17 2019
Wood Type/Density (pine, 395)
Dimensions [0.97, 2.95, 3.0]
Volume 8.5845
Mass 3390.88
Reference Areas [1.799, 1.092, 1.769, 1.111]
Immersion Ratio 0.377684
Obj_Density 395

Start Time Thu Oct 24 09:27:17 2019
Wood Type/Density (pine, 355)
Dimensions [0.89, 0.35, 2.91]
Volume 0.906465
Mass 321.795
Reference Areas [0.669, 0.107, 0.205, 0.349]
Immersion Ratio 0.137684
Obj_Density 355

Start Time Thu Oct 24 09:27:17 2019
Wood Type/Density (pine, 394)
Dimensions [0.55, 0.71, 1.73]
Volume 0.675565
Mass 266.173
Reference Areas [0.589, 0.149, 0.242, 0.362]
Immersion Ratio 0.201445
Obj_Density 394

Appendix C: National Data Buoy Center MLRF1 Readings

YY	MM	DD	hh	mm	DIR	SPD	GDR	GSP	GMN
92	12	31	23	10	81	9.2	999	99.0	99
92	12	31	23	20	78	9.3	999	99.0	99
92	12	31	23	30	83	9.3	999	99.0	99
92	12	31	23	40	79	9.2	999	99.0	99
92	12	31	23	50	76	9.4	999	99.0	99
93	1	1	0	0	79	9.3	81	10.8	54
93	1	1	0	10	79	9.0	999	99.0	99
93	1	1	0	20	83	8.3	999	99.0	99
93	1	1	0	30	78	8.3	999	99.0	99
93	1	1	0	40	78	8.5	999	99.0	99
93	1	1	0	50	77	8.2	999	99.0	99
93	1	1	1	0	78	8.4	82	10.1	8
93	1	1	1	10	77	8.8	999	99.0	99
93	1	1	1	20	75	8.7	999	99.0	99
93	1	1	1	30	80	8.5	999	99.0	99
93	1	1	1	40	81	8.0	999	99.0	99
93	1	1	1	50	84	7.6	999	99.0	99
93	1	1	2	0	87	7.9	76	9.9	1
93	1	1	2	10	86	7.7	999	99.0	99
93	1	1	2	20	82	8.0	999	99.0	99
93	1	1	2	30	79	8.3	999	99.0	99
93	1	1	2	40	82	8.8	999	99.0	99
93	1	1	2	50	87	9.2	999	99.0	99
93	1	1	3	0	91	9.1	88	10.1	51
93	1	1	3	10	93	8.6	999	99.0	99
93	1	1	3	20	93	8.4	999	99.0	99
93	1	1	3	30	92	7.8	999	99.0	99
93	1	1	3	40	87	7.2	999	99.0	99
93	1	1	3	50	80	7.3	999	99.0	99
93	1	1	4	0	83	7.6	91	9.5	10

Appendix D: Module 1, Debris Generator

```
import pandas as pd
import random
import time

class DebrisGenerator:
    """
        Create debris objects of variable dimensions to feed into the simulation
    """

    def select_wood_type(self):
        '''
            Generate a random wood type and associated density (in kg/m**3), 1
            kg/m3 = 0.001 g/cm3
            Returns: wood type, density
        '''
        wood_types = {'chestnut': 560,
                      'elm': random.randint(550, 820),
                      'pine': random.randint(350, 400),
                      'oak': random.randint(740, 770),
                      'iron': 7874,
                      'ice': 916.7
                      } # 670 is the upper range for pine, but for testing, is
                          capped lower
        # To select random wood types, uncomment the following line, and comment out the three that below it:
        #wood_type, density = random.choice(list(wood_types.items()))

        # 'Pine' is the given wood type below, the third(2) index in the wood_
          types list.
        type(list(wood_types.keys()))
        wood_type = list(wood_types.keys())[2] # Changing this digit between
          0 and 3 will select the corresponding wood type from the list above.
        density = wood_types['pine']

        return wood_type, density

    def generate(self, number_of_objects):
        '''
            Create debris objects of variable dimensions to feed into the
                simulation.
            Returns: debris object dict
        '''
        object_dict = {}
        i = 1
        while i <= number_of_objects:
            # Generate data for the object
            random_obj_dims = [random.randint(10, 100) / 100,
                               random.randint(10, 300) / 100,
                               random.randint(100, 300) / 100] # Divided by
                                                   100 to express in meters
            drift_obj = random_obj_dims
            start_time = time.asctime()
            wood_type = self.select_wood_type()
            obj_density = wood_type[1]
            length = max(drift_obj)
            width = sorted(drift_obj)[1]
```

```
            height = min(drift  obj)
            volume = length * width * height
            mass = round(volume * obj_density, 3)
            height_below_water = (obj_density / 1035) * height # 1035 is the
                                        mass density of salt water
            ref_area1_air = (height - height_below_water) * length
            ref_area1_water = height_below_water * width
            ref_area2_air = (height - height_below_water) * width
            ref  area2  water = height  below  water * length

            reference_areas = [round(ref_area1_air, 3),
                               round(ref_area1_water, 3),
                               round(ref  area2  air, 3),
                               round(ref_area2_water, 3)
                               ]
            # Physical parameters of object in (and out of) water
            area  over  water = ref  area1  air
            area_under_water = ref_area1_water
            immersion_ratio = area_under_water /
                (area_over_water + area_under_water)
            # Create the dictionary key and entries
            key = i
            # Define the qualities that are stored within the object dictionary
            object_dict[key] = start_time, wood_type, drift_obj, volume, mass, \
               reference  areas, immersion  ratio, obj  density
            i += 1
        return object_dict

dg = DebrisGenerator()
debris = dg.generate(10)

"""
The following is simply a formatting convention for sharing the data in a more
visually appealing format; debris_df is never used.
'''
debris_df = pd.DataFrame.from_dict(debris)
debris  df = debris  df.rename(index={0: 'Start Time',
                                      1: "Wood Type/Density",
                                      2: "Dimensions",
                                      3: "Volume",
                                      4: "Mass",
                                      5: "Reference Areas",
                                      6: "Immersion Ratio",
                                      7: "Obj_Density"
                                      })
```

Appendix E: Module 2, Wind Data Cleaner

```
import os
import numpy as np
import pandas as pd
from scipy.stats import circmean


class FormatWindInDictionary:
    """
        Organize and clean NOAA wind data to be used in the simulation.
        Returns: Pandas dataframe of wind data
    """

    def __init__(self, wind_folder_name=None):
        self.wind_folder_name = wind_folder_name

    def get_filenames(self):
        """
            Returns: all txt files in wind_folder_name subdir of wherever file
                    is located
        """
        f_dir = os.path.join(os.path.dirname(__file__), self.wind_folder_name)
        fns = [os.path.join(f_dir, t) for t in os.listdir(f_dir) if
               os.path.isfile(os.path.join(f_dir, t)) and t.endswith(".txt")]
        if len(fns) > 0:
            return fns
        else:
            print('No txt files in current directory.')
            return False

    def create_dataframe(self):
        """
            Returns: dataframe with extra filename column
        """
        fns = self.get_filenames()
        if fns:
            dfs = [pd.read_table(f, delimiter=' ') for f in fns]
        if dfs:
            for dataframe, filename in zip(dfs, fns):
                dataframe['filename'] = filename
                df = pd.concat(dfs, axis=0, ignore_index=True, sort=False)
            return df
        else:
            return False

    def clean_data(self, dataframe):
        """
            The data sets have been combined and are next cleaned.
            Extraneous data are removed and columns renamed.
            Returns: standardized dataframe
        '''
        # Rename columns
        year_cols = dataframe.filter(like='YY').columns
        dataframe['year'] = dataframe[year_cols].sum(1)
        wind_direction_columns = dataframe.filter(like='DIR').columns
        dataframe['direction'] = dataframe[wind_direction_columns].sum(1)
```

```
        wind_speed_columns = dataframe.filter(like='SPD').columns
        dataframe['speed'] = dataframe[wind_speed_columns].sum(1)
        dataframe.rename(columns={'MM': 'month', 'DD': 'day',
                                  'hh': 'hour', 'mm': 'minutes'}, inplace=True)

        # Drop columns
        poison_columns = ['GDR', 'GMN', 'GSP', 'GST', 'GTIME',
                          wind_speed_columns[0], wind_direction_columns[0]]
        dataframe.drop(poison_columns, inplace=True, axis=1)

        # Specify new column names
        dataframe = dataframe[['year', 'month', 'day', 'hour',
                               'minutes', 'direction', 'speed', 'filename']]
        dataframe = dataframe.drop_duplicates()

        # Add 1900 to year column to make all years four digits
        mask = dataframe['year'] <= 99
        dataframe.loc[mask, 'year'] = dataframe.loc[mask, 'year'] + 1900

        # Clean out direction = 999.0 and speed = 99.0
        dataframe = dataframe.loc[dataframe.direction != 999]
        dataframe = dataframe.loc[dataframe.speed != 99]
        return dataframe

    def circular_mean(self, df):
        """
        Broadcasting Scipy's circmean function on a datafram with
        aggfunc does not allow space for the 'high' and 'low' parameters,
        necessary for accurate calculation. This solves that.
        Return: Dataframe with Scipy's circmean function applied to all
                bearing data.
        '''
        return circmean(df, high=df.max(), low=df.min())


    def three_day_slice(self, df):
        """
        Receive a dataframe of wind data and return
        3-day slices of the dataframe in a dict.

        '''
        days = df.day.unique()
        a_dict = {}
        for day in days:
            trimmed_df = df.loc[(day <= df['day']) & (df['day'] < (day + 3))]
            a_dict[day] = trimmed_df.dropna()
        del a_dict[30], a_dict[31]
        return a_dict

    def mean_df_to_dict(self, mean_df):
        """
            Stacks the dataframes horozontally into a dictionary
            (making 3D array, with each dictionary key as a 'day')
            Returns dictionary.
        '''
        the_wind = mean_df.copy()
        the_wind.rename(index=str, columns={"direction": "WDIR", "speed": "WSPD"}, inplace=True)
        the_wind = the_wind.reset_index()
        the_wind['day'] = pd.to_numeric(the_wind.day)
        the_wind['hour'] = pd.to_numeric(the_wind.hour)
        the_wind['minutes'] = pd.to_numeric(the_wind.minutes)
```

```
        wind_dictionary = self.three_day_slice(the_wind)
        dict_of_wind_dfs = {k: pd.DataFrame(v) for k,v in /
                            wind_dictionary.items()}
        return dict_of_wind_dfs

class RunProcess:
    fw = FormatWindInDictionary(wind_folder_name='WindData')
    df = fw.create_dataframe()
    clean_df = fw.clean_data(df)
    #months = [i for i in range(1, 13)]
    month = 8
    month_df = clean_df.loc[clean_df['month'] == month]
    mean_month = month_df.pivot_table(values=['direction', 'speed'],
                                      index=['day', 'hour', 'minutes'],
                                      aggfunc = {'direction': /
                                                 fw.circular_mean, /
                                                 'speed': np.mean})
    data = fw.mean_df_to_dict(mean_month)
wind_dict = RunProcess
winds = wind_dict.data
# Wind speed (WSPD) is in meters/second
```

Appendix F: Module 3, Leeway Field Calculator

```
1.  import pandas as pd
2.  import numpy as np #  Numpy is used for its 'where' method.
3.
4.  class CompileWindOceanLee:
5.      """
6.          Take the wind data, generates constant ocean current, and computes
7.          leeway drift, then compile into dataframe.
8.          Returns datafame.
9.      '''
10.     def __init__(self):
11.         print("CompileWindOceanLee is defined")
12.
13.     def leeway_drift(self, leeway_to_wind_ratio, wind_condition_df):
14.         """ (float)(dataframe)-> (float)
15.         Calculates the leeway drift distance in meters of an object for a
16.         10-minute slice of a wind dataframe.
17.         Returns a float
18.         '''
19.         leeway_speed = (leeway_to_wind_ratio * wind_condition_df['WSPD']) # in
20.                                         meters/s # 600 second in 10 minutes
21.         wind_condition_df['LSPD'] = pd.Series(leeway_speed, \
22.                                 index=wind_condition_df.index)
23.         return wind_condition_df
24.
25.     def ocean_current(self, length_of_wind_df):
26.         """
27.         Ocean Bearing taken from Thomas N. Lee And Elizabeth Williams
28.         '''
29.         ocean_bearing = 50.5 #***#np.random.randint(39,51,size= /
30.                                             (length_of_wind_df, 1))
31.         ocean_flow_rate = np.random.randint(6,8,size=(length_of_wind_df, 1))
32.         return ocean_bearing, (ocean_flow_rate / 100) # in meters/sec
33.
34.     def apply_mask(self, df):
35.         """
36.         Applies a mask to the elements of a datafram, in the assigned ratio.
37.         Here, masks are applied to 10% of the dataframe:
38.         5% for a left drift, 5% for a right drift.
39.         '''
40.         mask_left = (np.random.choice([True, False], size=df['WTRAV'].values.shape, p=[.05, .95]))
41.         mask_left_verified = df[mask_left]
42.         mask_right = (np.random.choice([True, False], size=df['WTRAV'].values.shape, p=[.05, .95]))
43.         mask_right_verified = df[mask_right]
44.         df.loc[mask_left, 'WCUR'] = mask_left_verified['WTRAV'] - 30
45.         df.loc[mask_right, 'WCUR'] = mask_right_verified['WTRAV'] + 30
46.         return df
47.
48.     def left_or_right(self, df):
49.         '''
50.         WCUR column will, 10% of the time, be 30 degrees more/less than WTRAV
51.         '''
52.         self.apply_mask(df)
53.         df['WCUR'] = df.apply(lambda df: df['WTRAV'] * 1 if np.isnan(df['WCUR']) else df['WCUR'], axis=1)
54.         df['WCUR'] = np.where(df['WCUR'] < 0, df['WCUR'] +360, df['WCUR'])
55.         return df
```

```
56.
57.     def load_drift_conditions(self, immersion_ratio, wind_condition_df):
58.         density_air = 1.29 #kg m−3
59.         density_water = 1025 #kg m−3
60.         drag_coefficient_air = 0.8
61.         drag_coefficient_water = 1.2
62.         leeway_to_wind_ratio = np.sqrt(((density_air * drag_coefficient_air) \
63.                                 / (density_water * drag_coefficient_water)) \
64.                                 * ((1 - immersion_ratio) / immersion_ratio)) \
65.                                 # debris_dict[obj][6] is the immersion ratio,
66.                                 # using string key causes type error
67.         #print('leeway to wind ratio: ', leeway_to_wind_ratio)
68.         wind_drift = self.leeway_drift(leeway_to_wind_ratio, wind_condition_df)
69.
70.         #print(wind_drift.head().to_string())
71.         # Combine the wind_DF with the ocean array as two new columns.
72.         drift_conditions = wind_drift.copy()
73.         ocean_conditions = self.ocean_current(len(drift_conditions))
74.         drift_conditions['ODIR'] = ocean_conditions[0]
75.         drift_conditions['OSPD'] = ocean_conditions[1]
76.         # Use wind direction to determine the wind current
77.         # Step 1: invert wind dirction to its direction of travel
78.         mask1 = (drift_conditions['WDIR'] <= 180)
79.         mask1_verified = drift_conditions[mask1]
80.         mask2 = (drift_conditions['WDIR'] > 180)
81.         mask2_verified = drift_conditions[mask2]
82.         drift_conditions.loc[mask1, 'WTRAV'] = mask1_verified['WDIR'] + 180
83.         drift_conditions.loc[mask2, 'WTRAV'] = mask2_verified['WDIR'] - 180
84.         #print(drift_conditions.head().to_string())
85.         # Step 2: WDIR +- 30 degrees, via left_or_right function
86.         the_drift = self.left_or_right(drift_conditions)
87.         #print(drift_conditions.head().to_string())
88.         wind_ocean_lee = the_drift.drop(columns=['WTRAV'])
89.
90.         return wind_ocean_lee
91.
92. class CombineVectors:
93.     """
94.         Takes the wind, ocean, and leeway forces in bearing/speed format in a
95.         dictionary and converts them to vectors.
96.         Returns dictionary containing dataframes.
97.     '''
98.     def __init__(self):
99.         print("CombineVectors is defined")
100.
101.     def vector_math(self, data_df):
102.         x_Lee = data_df['LSPD'] * np.sin(np.deg2rad(data_df['LDIR']))
103.         y_Lee = data_df['LSPD'] * np.cos(np.deg2rad(data_df['LDIR']))
104.         x_Ocn = data_df['OSPD'] * np.sin(np.deg2rad(data_df['ODIR']))
105.         y_Ocn = data_df['OSPD'] * np.cos(np.deg2rad(data_df['ODIR']))
106.         wind_df = pd.concat([x_Lee, y_Lee, x_Ocn, y_Ocn], axis=1)
107.         wind_df.rename(index=str, columns={0:'Lee_x', 1:'Lee_y', 2: \
108.                     'Oc_x', 3:'Oc_y'}, inplace=True)
109.         return wind_df
110.
111. class RunProcess:
112.     """
113.         Debris and wind are the result of running Debris_Generator
114.     and DataframeDict_Generator, and are stored as variables.
115.     '''
116.
```

```
    def compile  conditions(self, debris, winds):
        wol = CompileWindOceanLee()
        WOL_data = {}
        for debris_obj in debris:
            immersion  ratio = debris[debris  obj][6]
            new_wind = {}
            for i in range(1, len(winds) + 1):
                new_wind[i] = wol.load_drift_conditions(immersion_ratio,
                                                        winds[i])
                new_wind[i] = new_wind[i][['WDIR', 'WSPD', 'WCUR', \
                                           'LSPD', 'ODIR', 'OSPD']]
                new_wind[i].rename(index=str, columns={'WCUR': 'LDIR'},
                                   inplace=True)
            data_deck = new_wind
            WOL_data.update({'Obj' + str(debris_obj) : data_deck})
        return WOL_data

"""
Debris and wind are already in memory,
the result of Debris_Generator and DataframeDict_Generator.
Vdrift = Vcurr + LeewayDrift
'''
process = RunProcess()
WOL_data = process.compile_conditions(debris, winds)

vectors = CombineVectors()




bearing_speed_data = {}
obj_keys = list(WOL_data.keys())
bearing  speed  data = dict.fromkeys(set(obj  keys))
obj_vectors = {}


# vectorize  conditions
for obj in WOL_data:
    sim_keys = list(range(1, 30))
    bearing_speed_data[obj] = dict.fromkeys(set(sim_keys))
    for i in range(1, len(WOL  data[obj]) + 1):
        temp_vectors = vectors.vector_math(WOL_data[obj][i])
        temp_vectors['x_sum'] = temp_vectors.iloc[:, 0::2].sum(axis=1)
        temp_vectors['y_sum'] = temp_vectors.iloc[:, 1::2].sum(axis=1)
        temp  summed  vectors = temp  vectors.copy()
        temp_summed_vectors.drop(columns=['Lee_x','Lee_y',
                                 'Oc_x','Oc_y'], inplace=True)
        discontinuity_bearing = np.rad2deg(np.arctan2(temp_summed_vectors['y_sum'], temp_summed_vectors['x_s
    um']))
        obj_bearing = (90 - discontinuity_bearing) % 360
        obj_speed = np.sqrt((temp_summed_vectors['x_sum']**2) + (temp_summed_vectors['y_sum']**2))
        obj_vectors.update({i: pd.DataFrame()})
        obj  vectors[i]['Bearing'] = obj  bearing.copy()
        obj  vectors[i]['Speed'] = obj  speed.copy()
        bearing_speed_data[obj].update({i: obj_vectors[i]})
```

Appendix G: Module 4, Map Visualization

```
1.  #!/usr/bin/env python3
2.  # -*- coding: utf-8 -*-
3.  """
4.  Created on Mon Feb 25 20:27:05 2019
5.
6.  @author: sccx
7.  """
8.  import numpy as np
9.  from mpl_toolkits.basemap import Basemap
10. import matplotlib.pyplot as plt
11. import copy
12. from matplotlib.colors import LogNorm
13. import pandas as pd
14.
15.
16. def first_step(bearing_speed_df, ship_lat, ship_lon):
17.     R = 6371000
18.     brng = np.deg2rad(bearing_speed_df['Bearing'][0])
19.     start_lat = np.deg2rad(ship_lat)
20.     start_lon = np.deg2rad(ship_lon)
21.     distance = bearing_speed_df['Float Distance'][0]
22.     lat2 = np.arcsin(np.sin(start_lat)*np.cos(distance/R) +
23.                 np.cos(start_lat)*np.sin(distance/R)*np.cos(brng))
24.     lon2 = start_lon + np.arctan2(np.sin(brng) * np.sin(distance/R) * np.cos(start_lat), np.cos(distance/R) - np.sin(st
    art_lat) * np.sin(lat2))
25.     bearing_speed_df['Latitude'][0], bearing_speed_df['Longitude'][0] = np.rad2deg(lat2), np.rad2deg(lon2)
26.     return bearing_speed_df
27.
28. def distance_traveled(bearing_speed_df):
29.     """
30.     Calculate the distance the object floats each step,
31.     using the speed,time, and drag.
32.     Returns column of float distances to the drift_vectors dataframe.
33.     '''
34.     speeds = bearing_speed_df['Speed']
35.     travel_time = 600 # seconds
36.     float_distance = speeds * travel_time
37.     return float_distance
38.
39.
40. def circle_distance(bearing_speed_df):
41.     """
42.         Receives dataframe of float distances and calculates latitude and longitude points traveled.
43.         Returns dataframe.
44.     '''
45.     for i in range(1, len(bearing_speed_df)):
46.         R = 6371000 # Circumference in meters
47.         latitude = np.deg2rad(bearing_speed_df['Latitude'][i-1])
48.         longitude = np.deg2rad(bearing_speed_df['Longitude'][i-1])
49.         distance = bearing_speed_df['Float Distance'][i] / R
50.         bearing = np.deg2rad(bearing_speed_df['Bearing'][i])
51.         next_lat = np.arcsin(np.sin(latitude)*np.cos(distance) +
52.                     np.cos(latitude)*np.sin(distance)*np.cos(bearing))
53.         next_lon = longitude + np.arctan2(np.sin(bearing) * np.sin(distance) * np.cos(longitude),
54.                             np.cos(distance) - np.sin(latitude) * np.sin(next_lat))
```

```
        bearing_speed_df['Latitude'][i] = np.rad2deg(next_lat)
        bearing_speed_df['Longitude'][i] = np.rad2deg(next_lon)
    return bearing_speed_df

#Capitana
ship_lat = 24.92485
ship_lon = -80.51485

# Scale of the map boxes: 0.4 x 0.4 and 0.04 x 0.04 degrees latitude and longitude
# Equal to approximately 44.4 km x 40.3 km and 4444 meters x 4030.5 meters, respectively

geo_points = np.empty(2)
coordinates = dict.fromkeys(set(obj_keys))


for obj in bearing_speed_data:
    coordinates[obj] = {}
    for key in bearing_speed_data[obj]:
        drift_distance = distance_traveled(bearing_speed_data[obj][key])
        bearing_speed_data[obj][key]['Float Distance'] = drift_distance
        bearing_speed_data[obj][key]['Latitude'], bearing_speed_data[obj][key]['Longitude'] = np.nan, np.nan
        bearing_speed_data[obj][key] = first_step(bearing_speed_data[obj][key], ship_lat, ship_lon)
        coordinates[obj].update({key: pd.DataFrame()})
        coordinates[obj][key] = circle_distance(bearing_speed_data[obj][key])
        bearing_speed_data[obj].update({key: coordinates[obj][key]})
        lats1 = pd.DataFrame(coordinates[obj][key]['Latitude'])
        lons1 = pd.DataFrame(coordinates[obj][key]['Longitude'])
        new_coordinates = pd.concat([lats1, lons1], axis=1)
        geo_points = np.vstack((geo_points, new_coordinates))

# Density mapping function adapted from:
# https://www.julienphalip.com/blog/drawing-geographical-density-maps-with-matplotlib/

def density_map1(latitudes, longitudes, center, bins=250, radius=0.2):
    cmap = copy.copy(plt.cm.jet)
    cmap.set_bad((0,0,0))  # Fill background with black

    # Center the map around the provided center coordinates
    histogram_range = [
        [center[1] - radius, center[1] + radius],
        [center[0] - radius, center[0] + radius]]

    fig = plt.figure(figsize=(8,8))
    plt.hist2d(longitudes, latitudes, bins=bins, norm=LogNorm(),
               cmap=cmap, range=histogram_range)

    # Remove all axes and annotations to keep the map clean and simple
    plt.grid(True)
    plt.axis(True)
    fig.axes[0].get_xaxis().set_visible(True)
    fig.axes[0].get_yaxis().set_visible(True)
    plt.tight_layout()
    plt.show()


def density_map2(latitudes, longitudes, center, bins=250, radius=0.02):
    cmap = copy.copy(plt.cm.jet)
    cmap.set_bad((0,0,0))  # Fill background with black

    # Center the map around the provided center coordinates
```

```
    histogram_range = [
        [center[1] - radius, center[1] + radius],
        [center[0] - radius, center[0] + radius]
    ]

    fig = plt.figure(figsize=(8,8))
    plt.hist2d(longitudes, latitudes, bins=bins, norm=LogNorm(),
               cmap=cmap, range=histogram_range)

    # Remove all axes and annotations to keep the map clean and simple
    plt.grid(True)
    plt.axis(True)
    fig.axes[0].get_xaxis().set_visible(True)
    fig.axes[0].get_yaxis().set_visible(True)
    plt.tight_layout()
    plt.show()


def phys_map1(lat1, lon1, coordinates):
    north_lat = lat1 + 0.2
    south_lat = lat1 - 0.2
    east_lon = lon1 + 0.2
    west_lon = lon1 - 0.2
    fig = plt.figure(figsize=(8,8))
    fig.set_canvas(plt.gcf().canvas)
    m = Basemap(projection='mill',llcrnrlat=south_lat, urcrnrlat=north_lat,
llcrnrlon=west_lon,urcrnrlon=east_lon,resolution='h')
    m.drawcoastlines()
    m.drawcountries()
    m.drawstates()
    m.fillcontinents(color='#04BAE3',lake_color='#FFFFFF')
    m.drawmapboundary(fill_color='#FFFFFF')
        x,y = m(lon1,lat1)
    m.plot(x,y,'bo',markersize=5)
    x,y = m(coordinates[:,1],coordinates[:,0])
    m.plot(x,y, 'ro', markersize=.1)
    plt.title("Capitana Shipwreck Scatter")
    plt.xlabel('10 Random Floating Objects')
    # Map scale
    atLon = -80.4 # Longitude position for scale
    atLat = 24.78 # Latitude position for scale
    forLength = 10 # length in km
    m.drawmapscale(atLon, atLat, atLon, atLat, length=forLength, barstyle='fancy', fontsize=15)
    # End scale
    # North Arrow
    atLon = -80.4  # Longitude position for north arrow
    atLat = 24.82 # Latitude position for north arrow
    forLength = .02 # length in degrees
    x, y = m(atLon, atLat)
    x2, y2 = m(atLon, atLat + forLength)
    plt.arrow(x, y, 0, y2 - y, fc="k", ec="k",
          head_width=600, head_length=600)
    plt.text(x, y, "N", verticalalignment="top", horizontalalignment="center", fontsize=15, family='Arial')
    # End arrow
    plt.show()
    #fig.savefig(file + '_large' + '.jpeg', format='jpeg')

def phys_map2(lat1, lon1, coordinates):
    north_lat = lat1 + 0.02
    south_lat = lat1 - 0.02
```

```
    east  lon = lon1 + 0.02
    west_lon = lon1 - 0.02
    fig = plt.figure(figsize=(8,8))
    fig.set_canvas(plt.gcf().canvas)
    m = Basemap(projection='mill',llcrnrlat=south  lat, urcrnrlat=north  lat,
llcrnrlon=west_lon,urcrnrlon=east_lon,resolution='h')
    m.drawcoastlines()
    m.drawcountries()
    m.drawstates()
    m.fillcontinents(color='#04BAE3',lake_color='#FFFFFF')
    m.drawmapboundary(fill_color='#FFFFFF')
    x,y = m(lon1,lat1)
    m.plot(x,y, 'bo', markersize=5)
    x,y = m(coordinates[:,1],coordinates[:,0
    m.plot(x,y, 'ro', markersize=1)
    plt.title("Capitana Shipwreck Scatter")
    plt.xlabel('10 Random Floating Objects')
    # Map scale
    atLon = -80.5 # Longitude position for scale
    atLat = 24.908 # Latitude position for scale
    forLength = 1 # length in km
    m.drawmapscale(atLon, atLat, atLon, atLat, length=forLength, barstyle='fancy', fontsize=15)
    # End scale
    # North Arrow
    atLon = -80.5  # Longitude position for north arrow
    atLat = 24.912 # Latitude position for north arrow
    forLength = .005 # length in degrees
    x, y = m(atLon, atLat)
    x2, y2 = m(atLon, atLat + forLength)
    plt.arrow(x, y, 0, y2 - y, fc="k", ec="k",
          head_width=100, head_length=100)
    plt.text(x, y, "N", verticalalignment="top", horizontalalignment="center", fontsize=20, family='Arial')
    # End arrow
    plt.show()

# Coordinates of Capitana's center
capitana = [ship  lat, ship  lon]
# Separate latitude and longitude values from our list of coordinates
latitudes = geo_points[:,0]
longitudes = geo_points[:,1]
# Render the map
density_map1(latitudes, longitudes, center=capitana)
density_map2(latitudes, longitudes, center=capitana)
phys_map1(ship_lat, ship_lon, geo_points)
phys_map2(ship_lat, ship_lon, geo_points)
```